TECHNICAL REPORT NO. 1

SPONSORED BY THE OFFICE OF NAVAL RESEARCH

Contract No. ~~N3014~~-67-A-0117-0012, NR 036-093
N00014

CORROSION FATIGUE OF METALS AND ALLOYS

D. J. Duquette

Materials Division

Rensselaer Polytechnic Institute

Troy, New York 12181

May 10, 1972

Security Classification

DOCUMENT CONTROL DATA - R&D

(Security classification of title, body of abstract and indexing annotation must be entered when the overall report is classified)

1. ORIGINATING ACTIVITY (Corporate author) Rensselaer Polytechnic Institute Materials Division Troy, New York 12181	2a. REPORT SECURITY CLASSIFICATION Unclassified 2b. GROUP

3. REPORT TITLE

CORROSION FATIGUE OF METALS AND ALLOYS

4. DESCRIPTIVE NOTES (Type of report and inclusive dates)

Technical Report

5. AUTHOR(S) (Last name, first name, initial)

Duquette, David J.

6. REPORT DATE	7a. TOTAL NO. OF PAGES	7b. NO. OF REFS
May 10, 1972	118	196

8a. CONTRACT OR GRANT NO.	9a. ORIGINATOR'S REPORT NUMBER(S)
N0014-67-A-0117-0012, NR036-093 b. PROJECT NO.	Technical Report No. 1
c.	9b. OTHER REPORT NO(S) (Any other numbers that may be assigned this report)
d.	

10. AVAILABILITY/LIMITATION NOTICES

Reproduction in whole or in part is permitted for any purpose of the United States Government.

11. SUPPLEMENTARY NOTES	12 SPONSORING MILITARY ACTIVITY
	Office of Naval Research

13. ABSTRACT

The combined influence of cyclic stresses and aggressive environments is known to adversely affect the useful mechanical properties of metals and alloys. Fatigue crack propagation is accelerated by gaseous environments at low temperatures but at high temperatures either initiation or growth may be accelerated or decelerated by exposure to aggressive gas phases. Corrosive aqueous environments, on the other hand, almost invariably degrade the mechanical properties of metals and alloys.

This review presents a detailed summary of the current understanding of the phenomenon of corrosion fatigue in gaseous and in aqueous environments. The effects of gaseous environments at low and at elevated temperatures and the mechanisms which govern fatigue crack initiation and propagation in the presence and in the absence of reaction films are discussed. The effects of aggressive aqueous solutions on fatigue crack initiation and propagation in ferrous and non ferrous alloys, and the effectiveness of protective measures are treated in detail and a critical review of previously proposed and currently accepted models is presented.

DD FORM 1 JAN 64 1473

Unclassified

Security Classification

Security Classification

14 KEY WORDS	LINK A		LINK B		LINK C	
	ROLE	WT	ROLE	WT	ROLE	WT
fatigue corrosion fatigue gaseous environments aqueous environments cyclic deformation						

INSTRUCTIONS

1. ORIGINATING ACTIVITY: Enter the name and address of the contractor, subcontractor, grantee, Department of Defense activity or other organization *(corporate author)* issuing the report.

2a. REPORT SECURITY CLASSIFICATION: Enter the overall security classification of the report. Indicate whether "Restricted Data" is included. Marking is to be in accordance with appropriate security regulations.

2b. GROUP: Automatic downgrading is specified in DoD Directive 5200.10 and Armed Forces Industrial Manual. Enter the group number. Also, when applicable, show that optional markings have been used for Group 3 and Group 4 as authorized.

3. REPORT TITLE: Enter the complete report title in all capital letters. Titles in all cases should be unclassified. If a meaningful title cannot be selected without classification, show title classification in all capitals in parenthesis immediately following the title.

4. DESCRIPTIVE NOTES: If appropriate, enter the type of report, e.g., interim, progress, summary, annual, or final. Give the inclusive dates when a specific reporting period is covered.

5. AUTHOR(S): Enter the name(s) of author(s) as shown on or in the report. Enter last name, first name, middle initial. If military, show rank and branch of service. The name of the principal author is an absolute minimum requirement.

6. REPORT DATE: Enter the date of the report as day, month, year; or month, year. If more than one date appears on the report, use date of publication.

7a. TOTAL NUMBER OF PAGES: The total page count should follow normal pagination procedures, i.e., enter the number of pages containing information.

7b. NUMBER OF REFERENCES: Enter the total number of references cited in the report.

8a. CONTRACT OR GRANT NUMBER: If appropriate, enter the applicable number of the contract or grant under which the report was written.

8b, 8c, & 8d. PROJECT NUMBER: Enter the appropriate military department identification, such as project number, subproject number, system numbers, task number, etc.

9a. ORIGINATOR'S REPORT NUMBER(S): Enter the official report number by which the document will be identified and controlled by the originating activity. This number must be unique to this report.

9b. OTHER REPORT NUMBER(S): If the report has been assigned any other report numbers *(either by the originator or by the sponsor)*, also enter this number(s).

10. AVAILABILITY/LIMITATION NOTICES: Enter any limitations on further dissemination of the report, other than those imposed by security classification, using standard statements such as:

(1) "Qualified requesters may obtain copies of this report from DDC."

(2) "Foreign announcement and dissemination of this report by DDC is not authorized."

(3) "U. S. Government agencies may obtain copies of this report directly from DDC. Other qualified DDC users shall request through

_____."

(4) "U. S. military agencies may obtain copies of this report directly from DDC. Other qualified users shall request through

_____."

(5) "All distribution of this report is controlled. Qualified DDC users shall request through

_____."

If the report has been furnished to the Office of Technical Services, Department of Commerce, for sale to the public, indicate this fact and enter the price, if known.

11. SUPPLEMENTARY NOTES: Use for additional explanatory notes.

12. SPONSORING MILITARY ACTIVITY: Enter the name of the departmental project office or laboratory sponsoring *(paying for)* the research and development. Include address.

13. ABSTRACT: Enter an abstract giving a brief and factual summary of the document indicative of the report, even though it may also appear elsewhere in the body of the technical report. If additional space is required, a continuation sheet shall be attached.

It is highly desirable that the abstract of classified reports be unclassified. Each paragraph of the abstract shall end with an indication of the military security classification of the information in the paragraph, represented as *(TS), (S), (C), or (U)*.

There is no limitation on the length of the abstract. However, the suggested length is from 150 to 225 words.

14. KEY WORDS: Key words are technically meaningful terms or short phrases that characterize a report and may be used as index entries for cataloging the report. Key words must be selected so that no security classification is required. Identifiers, such as equipment model designation, trade name, military project code name, geographic location, may be used as key words but will be followed by an indication of technical context. The assignment of links, rules, and weights is optional.

DD FORM 1 JAN 64 1473 (BACK)

Security Classification

CORROSION FATIGUE OF METALS AND ALLOYS

D. J. Duquette
Materials Division
Rensselaer Polytechnic Institute
Troy, New York 12181

Abstract

The combined influence of cyclic stresses and aggressive environments is known to adversely affect the useful mechanical properties of metals and alloys. Fatigue crack propagation is accelerated by gaseous environments at low temperatures but at high temperatures either initiation or growth may be accelerated or decelerated by exposure to aggressive gas phases. Corrosive aqueous environments, on the other hand, almost invariably degrade the mechanical properties of metals and alloys.

This review presents a detailed summary of the current understanding of the phenomenon of corrosion fatigue in gaseous and in aqueous environments. The effects of gaseous environments at low and at elevated temperatures and the mechanisms which govern fatigue crack initiation and propagation in the presence and in the absence of reaction films are discussed. The effects of aggressive aqueous solutions on fatigue crack initiation and propagation in ferrous and non ferrous alloys, and the effectiveness of protective measures are treated in detail and a critical review of previously proposed and currently accepted models is presented.

1. Introduction

Corrosion fatigue may be defined as the combined action of an aggressive environment and a cyclic stress leading to premature failure of metals by cracking. In this definition, the word "combined" must be emphasized, since it has been shown by many investigators that neither cyclic stresses nor environmental attack applied separately produces the same damaging results as conjoint action. That is, a pre-corroded specimen does not necessarily show appreciable reduction in fatigue life, nor does pre-fatiguing in air increase the corrosion rate of metals. The majority of observed fatigue failures are, in fact, corrosion fatigue failures since only fatigue occurring in an absolute vacuum could be termed as pure "fatigue". For example, it has been shown that for many metals, air contributes quite strongly to increases in fatigue crack propagation.

A number of reviews have been written since the first reported observations of corrosion fatigue by Haigh in 1917[1] some of which have dealt with only specific aspects of the problem such as the effect of gaseous environments on fatigue crack propagation[2]. For instance, particular attention may be focused on the extensive review of Gough in 1932[3] and of Gilbert in 1956[4]. Accordingly, the aim of this review will be to underline certain key issues in the early work on corrosion fatigue and to emphasize recent data and theories of the mechanisms of corrosion fatigue. Thus, it should not be regarded as an exhaustive study of the subject but one underlining the critical

processes which govern corrosion fatigue mechanisms and attempts to point out areas where more work is needed before this complicated phenomenon can be completely understood. In particular, the effects of gaseous and aqueous environments on ultimate corrosion fatigue failure, and the success of protective measures will be reviewed; an attempt will be made to correlate both initiation and propagation processes.

Gaseous Environments

A. Low Temperatures

In general, oxygen is known to accelerate fatigue crack propagation and, accordingly, to reduce fatigue life. For example, Gough and Sopwith, in an extensive series of experiments conducted on a variety of engineering alloys, noted that a partial vacuum of only 10^{-3}mm Hg resulted in appreciable increases in fatigue lives and endurance limites for carbon steels, brasses, copper, while 30% copper-nickel alloys and nickel chromium steels showed little improvement[5] (Table 1). Later experiments on copper and 70-30 brass in laboratory air, partial vacuum, humidified and dry air, and humidified and dry nitrogen led these investigators to suggest that a joint effect of oxygen and water vapor is primarily responsible for the reduction of fatigue life, although oxygen alone also leads to some reduction especially in the case of brass[6] (Fig. 1, 2). Experiments on lead[7] (Fig. 3) and Armco iron[7] (Fig. 4) also showed marked changes in fatigue behavior with vacuum tested materials exhibiting extended fatigue lives.

The effect of atmospheric oxygen on fatigue crack initiation and growth in copper, aluminum, and gold has also been investigated by Wadsworth and co-workers [3-10], who noted that oxygen and water vapor reduce fatigue life in copper and aluminum but has no effect on gold, that alternate static exposure to air and dynamic exposure to vacuum does not affect fatigue life, and that the S-N curves diverge as applied stresses are reduced (Fig. 5). Based on these experiments, these investigators concluded that: 1) fatigue cracks form early; the majority of life being concerned with crack propagation, (environment having little or no effect on nucleation and initial growth); 2) oxygen and water vapor are the primary damaging constituents in air (water vapor alone being effective in aluminum); and 3) oxygen must be a gas i.e., pre-oxidation or intermittent exposure is not effective. Similar results were also obtained for an iron 0.5% carbon alloy tested in air and in vacuum, with the significant result that air also lowers the observed fatigue limit as well as fatigue life above the fatigue limit [9]. This result was linked with the appearance of non-propagating microcracks below the fatigue limit; air apparently reducing the stress required to affect propagation. Vacuum has also been shown to delay crack propagation in Ni [11], in nickel base superalloys [12,13] in Cu-Al alloys at room temperature and at 77°K [14] and in polycrystalline Pb [15-21].

For most materials, environment appears to be most effective early in the crack growth process, with little or no effect at high

crack growth rates. Additionally, the majority of S-N curves diverge at decreasing stresses, the increase in fatigue life due to vacuum becoming greater at lower stresses. In contrast to this behavior, however, aluminum and aluminum alloys have been shown to exhibit conflicting results. For example, a 2017-T4 alloy tested in air and at 2×10^{-10} torr [22] and a 2024-T3 alloy tested in air and at 10^{-10} torr [23] in rotating bending exhibit convergence of S-N curves at low stresses, the effect of environment apparently becoming less important at decreasing stresses (Fig. 6). Pure aluminum [24] and an 1100 aluminum alloy [25] compared in air and at 10^{-6} and 10^{-7} torr respectively, on the other hand, show the more commonly observed divergence and Meyn has shown that crack propagation is more sensitive to environment at low strain amplitudes in a 2024 alloy [26]. This conflict may be related to the presence of water vapor at the "softer" vacuum levels, since it has been shown that the fatigue of aluminum is highly sensitive to the presence of this gaseous species. For example, Broom and Nicholson have shown that water vapor is the only atmospheric constituent necessary to induce enhanced propagation rates in aluminum and aluminum alloys [27]; a hypothesis which was supported by the work of Bradshaw and Wheeler [28].

The Mechanism of Gaseous Environmental Fatigue

Previously proposed mechanisms for the effect of gaseous environments on fatigue behavior can be divided into four principal categories:

1) interference with a reverse slip process, 2) prevention of slip band crack rewelding, 3) surface energy reduction due to gas phase adsorption, and 4) accelerated corrosion at a growing fatigue crack tip.

Thompson et al, suggested that gas phase interaction with fatigue deformation processes was connected with the transition from slip bands to Stage I cracking[10]. According to this model, slip bands become regions of high dissolved oxygen concentration; increased thermal effects and vacancy generation associated with slip reversal effectively "pulling" oxygen into the developing slip band (Fig. 7). Dissolved oxygen then expedites crack growth by preventing reclosing or rewelding of the crack surfaces.

Later results by the same investigators, particularly on gold where no effect of gaseous environments is noted, led to the conclusion that this mechanism was probably not correct and to the suggestion that the observed increased crack propagation rates were due to the joint action of accelerated atmospheric attack at the base of a growing crack; the gas phase chemisorption either preventing rewelding of newly generated crack surfaces[9] or interfering with slip reversibility[8].

Laird and Smith, conducting experiments on aluminum, copper and nickel noted that the atmospheric effect decreases with crack length and concluded that a rewelding mechanism could not be valid, since the higher local stresses and increased cold work associated with longer cracks should intensify a rewelding process[29]. Additionally, a mechanism based on chemisorbed films preventing crack reclosing or

rewelding was not supported, since the physisorbed film present on gold should be as effective in increasing crack propagation rates as chemisorbed films. Based on their observations, these authors concluded that the effect of oxygen in increasing crack growth rates must be due solely to chemical attack of the metal at the crack tip. A similar conclusion was also reached by Jacisin who noted that dry nitrogen was as effective as ultra-high vacuum in preventing accelerated crack growth in a 2017-T4 aluminum alloy[22]. The implication was that neither interference with bulk rewelding or gas phase adsorption could be responsible for accelerated crack growth, but that a chemical reaction of metal with an aggressive environment must take place.

Bulk oxide interference with slip processes has also been suggested to explain the effect of gaseous environmental fatigue. Fujita, for example, suggested that a thin adherent oxide, rapidly formed on newly emerging slip steps and at the crack tip, reduces the degree of reversibility thus accelerating crack growth[30]. Pelloux has also noted that aluminum alloys tested in vacuum do not show the striations associated with Stage II crack growth normally observed when specimens are cyclically stressed in air (Fig. 8) and proposed that completely reversible slip must occur in vacuum[31]. In air, on the other hand, the fracture surface oxidizes, striations are developed due to irreversible slip and crack growth is accelerated (Fig. 9). Heyn has also observed the absence of striations and slip markings in high strength aluminum alloys tested in vacuum[25].

Grosskreutz has shown that the slip character of aluminum is markedly altered in vacuum and has associated this observation with changes in properties of the oxide film formed on aluminum. At 10^{-9} torr, formation of slip bands was markedly suppressed when compared to slip band formation in air (Fig. 10)[32,33]. Numerous dislocation dipoles were observed in the near surface region and the effect of atmosphere was associated with oxidation of emerging surface slip steps leading to a local "work-hardening" of surface dislocation sources thus reducing or preventing slip band reversibility and accordingly leading to delayed crack initiation in vacuum. An extension of this model was also used to explain accelerated crack growth. Later experiments to further understand this effect, however, showed that the mechanical properties of the oxide film are markedly increased in vacuum, the Young's modulus of the thin oxide film being increased by a factor of 4[34]. Thus the stronger pre-existing film observed in vacuum is responsible for the reduction of surface slip and, conversely, the weaker film in air is easily ruptured by emerging slip steps and crack initiation and propagation are accordingly accelerated. The change in modulus and strength of the oxide film was associated with absorbed water vapor from the ambient environment, aluminum oxide being highly hydroscopic.

A similar mechanism based on a strong oxide film to explain accelerated crack initiation and growth in an aluminum alloy has been postulated by Shen et al[24]. Noting that the number of cycles to

failure in an 1100 aluminum alloy was independent of partial pressure of oxygen above 3 x 10^{-3} torr and below 10^{-2} torr, these investigators suggested that surface regions are strengthened by oxide films. Specifically, surface films prevent dislocation escape through the alloy free surface and accordingly lead to large accumulations of dislocation debris in near surface regions. The formation of cavities and voids (as suggested by Wood et al. to explain fatigue crack growth [35]) is thus enhanced and crack propagation rates increase. At low pressures, oxidation of newly created surfaces is slower, dislocation escape from the surface is more common, and cavity formation and void linkage delayed (Fig. 11).

The incidence of a small range of critical partial pressure of oxygen appears to be characteristic of gaseous environmental fatigue; "s" shaped curves of cycles to failure being reported by a number of investigators (Fig. 12) [2,20,24,36]. Generally these curves are explained by equating the arrival of a gaseous species at a growing crack tip and the reaction rate of the gas with the metal. A number of models have been proposed based on kinetic gas theory with varying results. For example, Bradshaw and Wheeler [28], Hordon [25] and Snowden [37] all equated the rate of a surface coverage at the crack tip with the rate of new surface generation to arrive at a critical pressure for the effect of adsorbed gases.

Hordon's equation, expressed as a critical pressure, reduces to:

$$P_c = \frac{3}{8}\left(\frac{l}{r}\right)^2 \frac{(MT)^{\frac{1}{2}}}{(3.5 \times 10^{22})(A)(t)} \qquad (1)$$

where P_c = critical pressure

$\frac{l}{r}$ = ratio of crack length to width

A = cross sectional area of impinging molecules

M = molecular weight of adsorbate

T = absolute temperature.

Results using this type of formulation have not been entirely successful, with discrepancies as large as 10^3 torr in critical pressure being observed and being attributed either to capillary attenuation factors [25,37] or to a requirement for multilayer adsorbed gas coverage.

Achter and co-workers, on the other hand, has been able to resolve some of the noted discrepancies without recourse to either of these factors by taking into account the observed crack propagation rate, the fact that fatigue cracks are usually only exposed to the environment for part of each cycle, and the argument that the crack propagates in discrete increments of the order of a lattice constant, each increment being saturated with adsorbate before the next is produced [38]. The time of exposure for each increment is:

$$f = \frac{\gamma}{2\frac{da}{dN}f} \text{ sec.} \qquad (2)$$

where γ is the interatomic spacing

$\frac{da}{dN}$ is the observed crack propagation rate, and

f is the frequency of applied stress.

For metals, χ is the order of 3Å and the density of sites on the metal surface is $\approx 1.4 \times 10^{15} cm^{-2}$.

The impingement rate from kinetic gas theory is

$$\nu = \frac{3.5 \times 10^{22} p}{1.4 \times 10^{15} (MT)^{\frac{1}{2}}} \text{ sec.}^{-1} \qquad (3)$$

where p = gas pressure

M = molecular weight of adsorbate

T = absolute temperature.

Accordingly the time required for saturation is:

$$t = \frac{1.4 \times 10^{15} (MT)^{\frac{1}{2}}}{3.5 \times 10^{22} p} \qquad (4)$$

and, equating (2) and (4)

$$P_c = 2.0 \times 10^2 \left(\frac{da}{dN}\right) (f) \text{ torr} \qquad (5)$$

Using this formulation Achter was able to reduce the discrepancy for the work of Bradshaw and Wheeler in aluminum alloys and for his own work on stainless steels at 500°C to a factor ranging from 5-10.

The physical process of chemisorption involves an exchange or sharing of bonding electrons between a substrate and an adsorbate and hence, by definition, lowers the surface energy of the substrate. This behavior has been used to explain environmental cracking phenomena under a variety of conditions, and has recently been used to explain the effect of oxygen to accelerate fatigue crack propagation rates[12]. In gaseous environments one or more aggressive species in the atmosphere is thought to chemisorb at a growing crack tip,

lowering the bond energy of the metal atoms and thus accelerating propagation.

Although the majority of metals and alloys considered in environmental studies fail predominantly by Stage II fatigue cracking (cracking normal to the stress axis) with a large degree of associated plasticity, some authors have suggested that the Stage I mode of cracking (along slip bands) is more sensitive to environmental effects [10,29]. Since Stage I cracks extend only a few microns or a grain diameter from the surface in most materials, this conclusion has been difficult to support. However, it has recently been shown that extensive Stage I fractures occur in high-strength nickel alloy single crystals because of the highly planar nature of plastic deformation in that class of alloys and, significantly, single crystals of these alloys show marked differences in fatigue life and fracture surface appearance when crystals tested in air are compared with crystals tested in moderate vacuo of $\approx 10^{-5}$ torr [12] (Fig. 13, 14).

Although fcc materials do not usually fail by cleavage and the tensile ductility of nickel base superalloys single crystals exceeds 15% at room temperature, localized cleavage occurs at the crack tip in the low stress range tests in air while ductile (dimpled) rupture occurs in vacuum. One approach to understanding this behavior is that of the Kelly, Cottrell, Tyson criterion for whether cracking in crystalline materials will occur in a ductile or a brittle manner [39]. These authors have proposed that cleavage will occur if the ratio, R,

of the normal stress to the applied shear stress at the crack tip, σ/τ, is greater than the ratio of the theoretical fracture stress to the theoretical shear stress, σ_{th}/τ_{th}, for a perfect crystal of the material. In general, $R > \sigma_{th}/\tau_{th}$ for bcc metals, alkali halides, diamond and $R < \sigma_{th}/\tau_{th}$ for fcc metals, which is in agreement with the relative tendency for these materials to cleave. Westwood et al have shown that cleavage of aluminum in the presence of liquid gallium can be explained by a lowering of σ_{th} by adsorption[40]. The build-up of edge dislocation dipoles observed in the case of the superalloy single crystals can be viewed as increasing σ and the lowering of the surface energy by oxygen adsorption as reducing σ_{th}, both effects tending to make $R > \sigma_{th}/\tau_{th}$ and thus promoting local cleavage. In vacuum tests at low stress ranges, σ_{th} is not affected by adsorption, and Stage I fracture occurs with more local plastic deformation as evidenced by the dimples on the fracture surface and the slower rate of crack growth.

In dealing with cleavage under conditions of limited plastic deformation, the Griffith-Orowan equation:

$$\sigma_f = C \sqrt{\frac{E(\gamma_s + \gamma_p)}{(1-\nu^2)\pi L}} \qquad (6)$$

has been successfully applied, where σ_f is the fracture stress under plane strain conditions, C is a constant dependent on the orientation of the crack with respect to the tensile axis and the location of the crack at the surface or in the interior. E is Young's modulus, γ_s is

the energy expended in plastic deformation during the formation of new crack surface, ν is Poisson's ratio and L is the crack length. Using this criterion, cracking will start if

$$\sigma_f > C \sqrt{\frac{E(\gamma_s + \gamma_p)}{(1-\nu^2)\pi L}} \qquad (7)$$

and will be catastrophic because γ_p is reduced and L is increased as the crack grows.

Since Stage I fracture in nickel-base superalloys and in other alloy systems involves a localized cyclic cleavage, it is possible to extend the Griffith-Orowan criterion to this situation. In addition to the applied stress, σ_a, there is a local stress σ_p near the crack tip resulting from an appropriate distribution of dislocations or other defects in the plastic zone. The magnitude of σ_p will decrease with distance from the crack tip in accordance with a reduced dislocation density in going from the crack tip to the edge of the plastic zone. In order to consider the effect of this stress in a modified Griffith-Orowan criterion, we define an equivalent stress, σ_e, applied at infinity that gives the <u>same strain energy release during crack growth</u> as that provided by σ_p near the crack tip. The relevant equation may then be expressed as follows:

$$\sigma_f = \sigma_a + \sigma_e = C \sqrt{\frac{E(\gamma_s - \gamma_{ads} + \gamma_p)}{(1-\nu^2)\pi L}} \qquad (8)$$

where $-\gamma_{ads}$ is the lowering of surface energy due to gas adsorption.

the energy expended in plastic deformation during the formation of new crack surface, ν is Poisson's ratio and L is the crack length. Using this criterion, cracking will start if

$$\sigma_f > C \sqrt{\frac{E(\gamma_s + \gamma_p)}{(1-\nu^2)\pi L}} \qquad (7)$$

and will be catastrophic because γ_p is reduced and L is increased as the crack grows.

Since Stage I fracture in nickel-base superalloys and in other alloy systems involves a localized cyclic cleavage, it is possible to extend the Griffith-Orowan criterion to this situation. In addition to the applied stress, σ_a, there is a local stress σ_p near the crack tip resulting from an appropriate distribution of dislocations or other defects in the plastic zone. The magnitude of σ_p will decrease with distance from the crack tip in accordance with a reduced dislocation density in going from the crack tip to the edge of the plastic zone. In order to consider the effect of this stress in a modified Griffith-Orowan criterion, we define an equivalent stress, σ_e, applied at infinity that gives the <u>same strain energy release during crack growth</u> as that provided by σ_p near the crack tip. The relevant equation may then be expressed as follows:

$$\sigma_f = \sigma_a + \sigma_e = C \sqrt{\frac{E(\gamma_s - \gamma_{ads} + \gamma_p)}{(1-\nu^2)\ L}} \qquad (8)$$

where $-\gamma_{ads}$ is the lowering of surface energy due to gas adsorption.

Crack propagation will occur so long as

$$\sigma_a + \sigma_e > C\sqrt{\frac{E(\gamma_s - \gamma_{ads} + \gamma_p)}{(1-\nu^2)\pi L}} \qquad (9)$$

For the majority of high cycle fatigue experiments, σ_a may be considered fixed by the maximum stress in the cycle and σ_p is a local enhancement of stress at the crack tip. For nickel base alloys this stress enhancement has been attributed to an array of dislocation dipoles in the crack plane[12]. As a first approximation $\sigma_a + \sigma_e$ may be considered constant in each cycle prior to crack extension. Once a crack begins to propagate, it runs into a region of lower σ_p (and σ_e) as a result of the gradient in defect structure with distance from the crack tip and thus comes to a stop in each cycle.

When σ_a is low, $\gamma_p \to 0$ and γ_{ads} can be a significant fraction of $\gamma_s + \gamma_p$. Thus, the difference in magnitude between the left and right-hand sides of Eq. 8 will be greater in air than in vacuum and as a result, a crack in air will grow further in each cycle.

This model may be used to consider both Stage I and Stage II fracture in other materials where localized cleavage occurs at the crack tip. Slip plane fractures that are highly reflective and exhibit fracture steps and river lines have also been observed in a number of Al alloys that exhibit planar slip[41,42]. In addition cyclic cleavage fractures that occur in the Stage II mode have been described in some bcc alloys[43-45]. In support of this model, it is

interesting to note that nickel base superalloy single crystals cycled at ultrasonic frequencies also show increased fatigue lines and dimpled fracture surfaces [46]. At these test frequencies where failure occurs in a matter of minutes, oxygen presumably adsorbs at a lower rate than the crack growth rate and the fatigue crack accordingly propagates in a virtual vacuum.

Although this model appears to be sound for cases where limited ductility is observed such as is presumably the case for Stage I microcracks in the majority of materials and for both Stage I and Stage II cracks in high strength precipitation hardened alloys, it seems unlikely that it would be valid for Stage II cracks in more ductile materials. The criticism of a surface energy reduction mechanism in these cases generally hinges on the fact that the strain energy associated with large plastic zones in the vicinity of growing cracks should be orders of magnitude greater than the amount of energy reduction attributed to surface adsorption. This criticism would appear to be well founded and, based on the conflicting observations of a number of investigators, it must be concluded that no general mechanism to explain the effect of environment on Stage II crack propagation in ductile metals and alloys can yet be accepted unequivocally. Perhaps, the most promising models are those which suggest an interference with slip reversibility due to a thin corrosion product interaction with emerging slip bands such as those proposed by Wadsworth and co-workers [8-10] and apparently supported by

the work of Pelloux [31]. Perhaps extensive fractographic studies of noble metals (such as gold) tested in air and in vacuum and of more reactive alloys in air and in carefully controlled inert atmospheres would be helpful in resolving some of the current controversies.

B. Elevated Temperatures

An understanding of the effects of environment at elevated temperatures is dependent on an understanding of the various modes of crack initiation and propagation that can occur. While researchers have noted a transition from transgranular to intergranular fracture as the temperature is increased or the frequency reduced at elevated temperatures, little has been done to separate the effects of elevated temperature testing variables on the modes of crack initiation and crack propagation. In recent work on both polycrystalline and single crystal nickel-base superalloys, the creep component associated with elevated temperature deformation is also thought to be a factor. (In a constant stress test this can be determined by measuring the specimen elongation in each cycle.) For a given alloy, the creep component in each cycle increases with increased temperature, mean stress, hold times and with reduced frequency. Where there is no creep component or it is small, the normal low temperature behavior is observed. Crack initiation and propagation are transgranular, with the propagation mode showing the normal Stage I to Stage II transition. Exceptions to this may arise if grain boundaries contain brittle phases that are a source of

intergranular initiation. The first observed effect of an increased creep component is usually a transition from transgranular to intergranular initiation. The propagation stage may be left unchanged. With a further increase in the creep component, intergranular deformation undergoes a change from the planar to the wavy mode. Where deformation at the crack tip is wavy, then only Stage II cracking will occur[47]. Finally, when sufficient creep occurs in each cycle, both the initiation and propagation stages become intergranular. As an example, the effect of temperature on the mode of cracking at the surface of polycrystalline Udimet 700 is shown in Fig. 15[43]. Slip band cracking is evident at 70°F and grain boundary cracking at 1700°F. These changes in the modes of crack initiation and propagation are significant because (1) the rate of intergranular crack initiation and propagation is faster than when cracking is transgranular[49,50] and (2) the environment can also affect these transitions and therefore the fatigue life.

In a single crystal, surface oxidation occurs at a reasonably uniform rate over the entire surface, except where phases or non-metallic inclusions that are less oxidation resistant than the matrix intersect the surface. The rate of penetration of the oxide in these phases can be many times greater than that in the surrounding matrix. In polycrystals of most structural alloys, grain boundaries are surfaces along which these precipitates or non-metallic inclusions are preferentially concentrated. As a result, oxide penetration along a

grain boundary intersecting the surface is deeper than in the matrix. Since in most cases the oxide is brittle and often poorly bonded to the surrounding metal, a fatigue crack can easily form in the oxide or at the oxide-metal interface (Fig. 15). Paskiet, Boone and Sullivan[50] have shown that pre-oxidation of a specimen at 1800°F followed by fatigue testing at 1400°F produces many surface intergranular cracks; whereas, testing of specimens without prior oxidation produces a single intergranular crack. Thus, pre-oxidized or preferentially-oxidized phases or grain boundaries serve as incipient cracks. Another example of the effect of oxidation on fatigue crack initiation was demonstrated by Hodgson. This investigator showed that, for stainless steels at high temperatures and high strain rates, air formed oxide induces notches which result in nucleation of new surface grains and result in grain boundary initiation[54] (Fig. 16).

Just as grain boundary oxidation affects the rate of intergranular crack initiation, it may also control the rate of grain boundary crack propagation. The microstructure of the grain boundary ahead of a crack is changed by oxidation[51-54]. Not only is oxide formed near the crack tip, but for a distance ahead of the crack, the region is depleted of oxide-forming elements. Fig. 17 shows the oxide just ahead of a crack in a nickel-base superalloy[55] (dark phases). At further distances from the crack, the region is denuded of the strengthening γ' precipitate (light etching area) because aluminum and titanium diffuse out of the region to form oxide. As a result of

oxidation, the crack in the next period will propagate into a region having changed chemical and mechanical properties. Thus, there are a number of possible influences of oxygen on the rate of intergranular crack growth. If the rate of crack growth in the absence of oxygen (i.e., in a vacuum test) is greater than the size of the zone affected by oxidation, then the crack propagation rate will be relatively unchanged by oxidation. This case would be found at relatively high strain ranges and frequencies or at low temperatures. On the other hand, at low strain ranges, low frequencies and high temperatures, the increment of crack growth in each cycle may be controlled by the size of the oxygen-affected zone at the crack tip. This may be viewed as a stress corrosion phenomenon[53].

Comparisons of the fatigue lives in air and vacuum at elevated temperatures have been conducted for nickel-base and cobalt-base alloys as well as stainless steel. In all of these materials, over most of the life range, the fatigue life in vacuum is greater than that in air (Fig. 18)[56]. The lives in air and vacuum converge at low stress ranges and it appears that, in some materials at very long lives, there is a cross over point beyond which the lives in air are greater than that in vacuum[36,56]. Danek, Smith and Achter[36] and Achter[57] have explained these results on the basis of two competing effects. At high stresses and short lives, oxygen adsorption at the crack tip accelerates the rate of crack growth in air. At low stresses and long times, a thicker oxide forms which is thought to strengthen the metal.

An alternate explanation for these results that is consistent with

the previous discussion is possible. At high stresses and short lives, crack initiation and, in some cases, crack propagation are intergranular because of the high creep component in the cycle. For tests run in air, oxidation of grain boundary phases accelerates the rates of intergranular crack initiation and propagation and reduces the fatigue life. As the stress is lowered, the creep component in the cycle is reduced, which favors a transgranular mode of cracking. Since the fatigue life is longer, oxide can form on the surfaces of Stage II cracks and retard the rate of Stage II crack growth.

The degree of oxidation and the creep component in the cycle depend on the alloy system, environment, temperature, frequency and the length of hold times in the cycle. There has been little work to explore the interaction between these testing variables and the environmental effect. One such study by Coffin[58] shows that the low-cycle fatigue life of an iron-base superalloy, A286, is greater in vacuum than in air at 1100°F. The fatigue life of this material shows a strong frequency dependence in air, but little frequency dependence in vacuum. This suggests that over the frequency range studied, 0.2 to 10 cycles per min., the frequency effect in air tests is associated with oxidation. In this study, the tests were run under strain control so the effects of frequency on creep are minimized. In stress-controlled tests over a wider range of frequencies in air on nickel-base superalloys: U-700 polycrystals at 1400°F (Fig. 19)[59] and MAR-M200 single crystals at 1400° to 1700°F[60], the initial increase in fatigue

life with increased frequency is shown to result from a reduced creep component and a reduced time for oxidation. With a further increase in frequency, all cracks are initiated below the specimen surface and the resultant changes in fatigue life are associated with the degree of planar slip dispersal rather than oxidation.

The creep component in the cycle may, itself, be altered by the environment. Shahinian and Achter[61-64] have shown in a series of nickel-and iron-base alloys that the creep life in vacuum is greater than that in air where oxidation is limited; high stresses and low temperatures. But, the life in air becomes greater than in vacuum where more extensive oxidation occurs; low stresses and high temperatures. Differences in creep lives in air and vacuum may be associated with the stress level, oxidation of grain boundary phases, the blockage of dislocations by a thin adherent oxide and the cracking of thicker oxides[65,66]. In thin sections, differences in creep rates may be associated with tensile stresses in the matrix generated by oxide film formation[67].

Fatigue properties as a function of the temperature have also been conducted on superalloy single crystals[68]. Fig. 20 shows the endurance limit (stress range required to produce failure in 10^6 cycles) for low carbon MAR-M200 single crystals as a function of temperature in air and vacuum. At all stress ranges at room temperature the fatigue life in vacuum is greater than that in air, at 1400°F the lives are about the same, and at 1700°F the

life in vacuum is less than that in air.

At room temperature and 400°F, crack initiation occurs (Fig. 21) at the specimen surface. At 800°F and above, crack initiation in vacuum tests is at the surface, but crack initiation in the air tests is in the specimen interior (Fig. 22). Crack propagation is on {111} planes at temperatures between 70° and 1400°F. At 1550° and 1700°F crack propagation is initially in the Stage II mode but there is a transition to Stage I with increasing crack length. It is important to note that in the air tests at 800°F and above there were no secondary surface-connected cracks, except at 1700°F.

Since crack initiation in the air tests over the intermediate temperature region is in the specimen interior, the initiation and initial stages of propagation are in a vacuum. Thus, it may be concluded that the similar fatigue lives observed in air and vacuum result from the fact that in each case most of the specimen life is spent in vacuum.

One of the most dramatic observations of the beneficial effect of oxygen on the elevated temperature fatigue of nickel-base superalloys is the change from surface to subsurface crack initiation [69,70] as the temperature of testing is increased. Crack initiation at room temperature in most materials occurs at the surface because of the greater slip activity associated with a free surface and because of the detrimental effect of the environment on both initiation and propagation processes. But in the temperature regime of 800° to 1550°F, a

thin adherent oxide forms on the specimen and this suppresses crack initiation. Pre-oxidation of a specimen followed by testing under conditions at which crack initiation normally occurs at the surface had no effect; crack initiation was still at the surface. This indicates that a static oxide is not sufficient to produce the beneficial effect. On the other hand, when specimens were tested at high strain ranges in air and vacuum at 1400°F, surface slip was more uniformly distributed and less intense in air than in vacuum (Fig. 23). It is thought that oxygen atoms impinging on freshly formed surface slip offsets form a thin oxide on the step and reduce the degree of slip reversibility in air compared to that in vacuum. The oxide work hardens the slip band and slip is generated in adjacent regions (Fig. 24). More specific models involving dislocation-oxygen interaction have been presented by Fujita[71]. It is expected that the planar slip generated at micropores in the interior of the specimen is more heterogeneously distributed, similar to that generated at the surface of vacuum specimens, and this leads to interior crack initiation.

The observations are in agreement with those reported by Smith and Shahinian for Type 316 stainless steel[72]. They find at temperatures between 77°F and 1472°F that the surface hardness increases with cycling when tests are conducted in an environment containing more than a critical partial pressure of oxygen. Furthermore, the effect is reversible; if the pressure of oxygen is reduced then the

surface hardness falls. These results indicate the importance of the continual presence of oxygen to saturate newly formed slip steps. Actual observations of surface slip distribution were made by Smith and Shahinian in the case of Inconel X at 932°F [73]. Slip was finer and more homogeneously distributed in tests conducted in 1 torr of oxygen compared to those conducted in 6×10^{-7} torr.

Specimens tested in air at 1700°F are unlike those tested at somewhat lower temperatures in that, although the main fracture is initiated in the specimen interior, there are numerous secondary surface-generated cracks (Fig. 25a and b) [4,7,70]. At this higher temperature, a thicker oxide is formed that is easily cracked. The crack runs along the surface in the oxide layer then proceeds into the interior. At 1700°F, deformation is homogeneous and non-planar at moderate strain rates and as a result the initial stage of propagation is in the Stage II noncrystallographic mode [47]. The plastic blunting model proposed by Laird [74] is a satisfactory description of the fracture process. According to this model, the crack is blunted during the tensile half cycle and is resharpened during the unloading cycle. Oxidation of alloys produces a volume expansion. Thus, when oxide forms on crack surfaces, the crack cannot be resharpened to the same degree as in vacuum and the rate of crack growth is slowed (Fig. 26).

Aqueous Environments

A. Ferrous Alloys

In an early review paper, McAdam[75] described a number of experiments on corrosion including his own results on carbon-nickel, high-chromium, and chromium-nickel steels in various aqueous environments. He suggested that corrosion fatigue depends on both the corrosion intensity and the stress range, and that the "corrosion fatigue limit" depends on the strength of the material as well as on corrosion resistance.

From these results, McAdam developed a series of experiments to test such variables as water composition, alloying, heat treatment, and corrosion resistance. The effect of prior corrosion on subsequent fatigue behavior in air was also studied. In tests conducted on steels, specimens were corroded first in fresh water for various lengths of time and then dried, oiled and tested in air. The resulting S-N curves were similar to those of tests conducted in air only, but fatigue life and the fatigue limit were lowered increasingly with increased time of corrosion (Fig. 27). The data also indicated that the relative detrimental effect of static corrosion increased with increase in tensile strength of the steel. Similar results were obtained on specimens mechanically notched, and McAdam concluded that the damage was due to pits formed in the corrosive media.

R. R. Moore also studied the effect of prior corrosion on the fatigue life of steel[76,77]. Subjecting steel to a 40 day spray of

20 percent sodium chloride solution reduced the fatigue limit by 22 percent. It is interesting to note, however, that life obtained when both a corrosive environment and stress were applied simultaneously was considerably shorter than for any of the tests performed with prior corrosion[78].

McAdam also demonstrated that the effects of corrosion fatigue could be represented by means of a three-dimensional plot of stress range, cycles to failure, and test time (frequency)[79] (Fig. 28). From these plots, a relationship between the corrosion fatigue behavior of steels in calcium carbonate solutions and in distilled water was established. This relationship confirmed his previous conclusions that the influence of stress range and frequency on pitting behavior is practically the same. Additionally, a summary of a number of experiments indicated that there was an empirical relationship between stress and time:

$$R = CS^n \qquad (10)$$

where R is equal to the rate of damage, S is the alternating stress and C and n are constants[80].

The effects of solution concentration and temperature on the fatigue behavior of steels were studied by Gould[81,82] and by McAdam[79,83]. Gould performed experiments on mild steel specimens in distilled water and in various concentrations of KCl. His results indicated that solutions ranging from 2 molal to 1/40 molal have similar effects on corrosion fatigue, but that at concentrations below 1/40 molal the

effect approached that of distilled water (Fig. 29).

These experiments established that over a wide range of corrosivity, fatigue behavior of steels is reduced to a constant level. In mildly corrosive environments, on the other hand, fatigue behavior is markedly affected by solution concentration; fatigue life improving with decreasing solution strength. Similarly Duquette and Uhlig[84] have also shown that over an order of magnitude of applied anodic current (30-300$\mu a/cm^2$), fatigue life is essentially constant in deaerated 3% NaCl solutions and that at lower applied currents fatigue life is improved (Fig. 30).

McAdam[79,83] also studied the effect of different waters including: (a) a hard well water with an alkalinity of 100ppm (as $CaCO_3$), 100-200 ppm chloride, and 50 ppm sulfate, (b) a soft water of zero hardness containing 30 ppm sulfate and 5 ppm chloride, (c) a river water of one-sixth to one-third the salinity of sea water, and (d) a fresh water containing up to 20 ppm alkalinity and 5 ppm chloride. The hard and soft waters were about equally damaging, but the salt water was considerably more damaging that the "fresh" water.

Gould's tests[82] on mild steel in artificial sea water in a constant-temperature room at 15°C, 25°C, 35°C and 45°C showed an appreciable effect of temperature, with fatigue life being approximately halved for 10^7 cycles when the temperature was raised from 15° to 45°C (Fig. 31). This is in contrast to the normal air fatigue behavior of steel which shows no appreciable effect of temperature

in this range. At temperatures approaching the boiling point of water (82°C) Cornet and Golan[85] found that drill rod tested in 2.5 percent NaCl solutions showed definite improvement in fatigue behavior when compared to room temperature tests. The authors attributed this beneficial effect to the difference in pitting attack at high temperature, the pits being more uniformly distributed and shallower, and suggested that the ratio of cathodic to anodic areas is higher at lower temperatures.

The effect of stress frequency on corrosion fatigue has been studied by a number of investigators but is still not completely understood. For example, Gough[5], in his review of corrosion fatigue, noted that it is difficult to compare the corrosion fatigue properties of metals exposed to like environments in view of the fact that data reported are usually taken at different frequencies. In general, a given time was found to produce more damage at a higher frequency, but a given number of cycles was found to produce greater damage at low frequencies. Water and Henn[86] found that with low alloy steels in fresh water, a frequency of 1450 cycles/min. produced failure in 10^6 cycles requiring 11½ hours, but that at a frequency of 5 cycles/min. failure occurred in 0.11×10^6 cycles or 400 hours. This conclusion was also supported by the work of Endo and Miyas[87], their curves, however, converging at low stresses (long endurances) indicated that failure tended to be predominantly dependent on time (Fig. 32).

The method of applying stress to corrosion fatigue specimens and

its effect on subsequent behavior have been studied by a number of investigators [85-88]. For example, Gough and Sopwith [88,89] found ratios of fatigue life at 50 x 10^6 cycles in direct tension versus bending tests of 0.86 to 1.26 for various steels in a salt spray. Gould [90], on the other hand, found that the endurance of steel subjected to fatigue tests in sea water was several times as great in direction tension as in bending. He attributed this to a stretching of all the anodic areas in bending, whereas only some of these areas were stretched in direct tension, thus resulting in more pronounced attack in bending tests. The reverse effect has been noted in air fatigue tests with bending tests producing greater fatigue strengths than direct tension tests [91].

To date the effect of pH of aqueous solutions on corrosion fatigue behavior has not received extensive study. Simnad and Evans [92] studied the effect of 0.1 N HCl on the fatigue life of steels and found greater damage in this medium than in neutral KCl solutions. Radd, Crowder and Wolfe [93] conducted tests in alkaline media, concluding that at a pH above 12.1 a fatigue limit is regained, this limit improving at still higher pH's (Fig. 33). From these results, Radd, et.al., concluded that corrosion fatigue is a result of differential aeration cells producing pits in the metal surface and that a high pH provides an oxygen diffusion barrier of ferrous hydroxide on the surface. Higher fatigue limits at high pH are explained in terms of a "better and more perfect film barrier". These results generally agree with

those of Duquette and Uhlig who showed that fatigue life is reduced in solutions of pH less than 4, remains constant a pH's between 4 and 10, and increases markedly at pH > 10, a true fatigue limit being observed at pH's greater than 12[84].

Thum and Holzhauer's work[94], performed on boiler steels at 275°C, showed that additions of 0.7 g/l NaOH to distilled water improved the fatigue limit by approximately 20 percent, but that increasing the NaOH concentration to 200 g/l lowered the fatigue limit by approximately 10 percent. At the higher alkaline concentrations, intergranular, as well as transgranular, cracking was observed indicating that caustic cracking (stress corrosion cracking) was also occurring during normal fatigue cracking.

Although, in a few cases, annealing has been shown to be beneficial[95,96], alloying and heat treatment of steels usually have little effect on the corrosion fatigue characteristics unless the alloying is undertaken specifically to improve corrosion resistance. Thus, the use of low alloy steels and high carbon steels is not beneficial in most corrosive media, whereas in air their fatigue limits increase directly with their ultimate tensile strengths. The work of Inglis and Larke[97] on mild steel and on low alloy steels in river water and that of Burnham[98] on marine piston rods in sea water confirmed these results.

Gough's review paper[5] suggested that there was considerable evidence for the importance of dissolved oxygen to the mechanism of

corrosion fatigue. For example, Lehmann[99] noted an improvement in the fatigue life of steel specimens when the specimens were completely immersed at 96°C. He concluded that this improvement was due to the limited solubility of oxygen at this temperature. Binnie[100] noted that sodium chloride solution dripped through air was extremely damaging to fatigue specimens. On the other hand, when the specimens were surrounded with a commercial hydrogen atmosphere, he observed higher fatigue life, with still further improvement as the purity of hydrogen was increased. Similar effects were observed by Fuller[101] in aerated and deaerated steam.

Mehdizadeh, et.al[102] have reported the results of fatigue tests conducted in sodium chloride solutions containing air, hydrogen sulfide and carbon dioxide on the fatigue behavior of both normalized and quenched and tempered 1035 steel. These authors noted that, while hydrogen sulfide was not particularly damaging in the absence of air, carbon dioxide, was equally damaging in the presence or absence of air. Perhaps more importantly, their results showed that complete deaeration of sodium chloride solutions caused a reappearance of the fatigue limit observed in dry air tests, thus indicating that dissolved oxygen is essential to the corrosion fatigue mechanism in neutral pH solutions (Fig. 34). This result was also confirmed by other investigators[103] for 3% NaCl solutions and for distilled water. The presence of the chloride ion alone in deaerated solutions, however, is sufficient to lower fatigue life although it does not affect the

fatigue limit (Fig. 35).

B. Non-Ferrous Alloys

Copper-Base Alloys

As in the case of ferrous alloys, much of the early corrosion fatigue work on non-ferrous alloys was conducted by McAdam and his co-workers[104], and their results are reported in tabular form for Cu, Ni-Cu, Monel, Al, Al_2-Mn and duraluminum in a number of journal articles. Results for phosphor, aluminum and beryllium bronzes were also reported by Gough and Sopwith who showed that the corrosion fatigue resistance of bronze compares favorably with that of stainless steel; beryllium bronze showing exceptional resistance to damage[105]. McAdam and Geil[106] showed that in two-phase aluminum bronzes, corrosion fatigue associated pits are confined to α-phase regions and grow at a pronounced angle to the specimen surface, probably because of the Stage I fatigue cracking usually associated with these alloys.

Single phase aluminum bronzes also exhibit considerable corrosion fatigue resistance in salt water, fatigue lives being equivalent to or somewhat better than stainless steels[107].

Pure copper is exceptionally resistant to corrosion fatigue damage in neutral waters, fatigue life being identical in air and in aqueous environments. Only under the imposition of large anodic amounts ($\simeq$ 100 $\mu A/cm^2$) does copper show a significant reduction in fatigue life due to corrosion[108].

Aluminum-Base Alloys

Although pure aluminum is known to pit in chloride containing aqueous media, its fatigue life is relatively unaffected by these environments. Aluminum alloys, particularly those which have been alloyed to exhibit high yield and tensile strengths, on the other hand are highly susceptible to corrosion fatigue.

Pre-corrosion of duraluminum sheet for a period of 5-10 days by 20% NaCl water sprays, while showing no reduction in tensile strength, showed a marked (25%) decrease in ductility and a 35% reduction in endurance limit[76]. This reduction was attributed to a notch effect created by intergranular corrosion. Similar results were also reported after an 18 hour immersion in artificial sea water[77,109]. During conjoint exposure of Al-Mg alloys to cyclic stresses and 3% NaCl solutions, cracking was shown to be associated with transgranular precipitates rather than grain boundaries[110] with maximum resistance corresponding to an air cooled 8% Mg alloy. Fatigue tests conducted on Al 0.6Mg 1Si alloys in tap water and in 3% NaCl solutions showed dramatic reductions in fatigue strength; the endurance limit being reduced 50% in tap H_2O and 75% in the NaCl solution[111]. The influence of anionic, cationic and non-ionogenic wetting agents on the corrosion fatigue resistance of Al-7% Mg alloys has also been studied in distilled H_2O and, 3% NaCl, HCl and NaOH solutions. While anionic agents increase the corrosion fatigue resistance, cationic and non-ionogenic agents have little or no effect. These authors ascribe the

action of wetting agents to a reduction of surface energy combined with changes in the surface films formed in the metal[112].

In an extensive study of fatigue crack initiation and propagation in high strength aluminum alloys, Forsyth and Stubbington[113-121] have shown that the fatigue behavior of Al-Zn-Mg alloys (of the 7075 type) is markedly affected by the presence of NaCl solution. These authors observed that under corrosive conditions crack initiation was generally transgranular, although in the peak aged condition at low frequencies cracking was occasionally observed to occur at grain boundaries and then propagate transgranularly (stress corrosion cracks in these alloys are generally intercrystalline - associated with grain boundary precipitates). A similar observation has been made for aluminum 8% magnesium alloys[122]. When continuous grain boundary precipitates were present corrosion fatigue cracking was entirely intercrystalline while with discontinuous precipitation cracking initiated at the grain boundary but reverted to a transcrystalline mode a short distance below the specimen surface. Forsyth and Stubbington also noted that at low applied stresses the crystalline mode of cracking (Stage I) is not only extended but the fracture path shifts from a (111) plane to an apparent (100) plane. Pelloux[123] has also noted this shift of crack plane for precracked 2024 Al alloys under the influence of applied anodic currents (Fig. 36). Forsyth and Stubbington attributed the reduction of fatigue strength of these high strength aluminum alloys to preferential slip band corrosion due to

electrochemical heterogeneity arising from plastic deformation; the dislocation pile-ups in the slip bands being anodic to the metal matrix.

The combined interaction of corrosive environments and ultrasonic frequency on aluminum alloys has been studied by Hockenhull, Monks and Sala[124] who concluded that the same types of effects occur even at very high frequency (20 kHz) i.e., that in the presence of aggressive solutions fatigue lives are shortened and endurance limits eliminated, but that at least part of the damaging effects were due to mechanical wedging of a growing crack by the liquid.

A relatively recent innovation in the evaluation of corrosion fatigue crack propagation has been provided by the introduction of fracture mechanics concepts to cyclic deformation-environmental interactions. While these techniques, which consist of monitoring the growth of fatigue cracks under the influence of controlled stress concentrations, present some difficulties for theoretical interpretation, they provide useful engineering criteria for failure predictions. This approach has been particularly useful in dealing with aluminum alloys used for aerospace applications. While a comprehensive treatment of this field is beyond the scope of this review, it should be pointed out that several review articles on this subject are currently available. Specifically, these are the proceedings of three recent symposia[125-127] and two recent articles by Johnson and Paris[128] and by Wei[129] concerning the growth of fatigue

cracks under environmental conditions.

Miscellaneous Alloys

While the corrosion fatigue behavior of few alloys other than ferrous and aluminum alloys has been studied, the behavior of lead and lead alloys has been investigated in air and in 38% H_2SO_4, the H_2SO_4 solution resulting in a much lower fatigue life. The author attributed this reduction to a notch effect created by grain boundary corrosion[130]. Magnesium-aluminum alloys are also highly susceptible to corrosion fatigue, accelerated crack initiation being attributed to galvanic effects between intracrystalline precipitates and the matrix alloy[110].

C. Protective Measures

Several investigators have reported some protection against corrosion fatigue either by inducing compressive stresses at the metal surface, by adding inhibitors to the aqueous environment, or by applying external currents. For example, protection against corrosion fatigue has been obtained by shot peening[131], surface rolling[132,133], and by nitriding[97,134,96]. Portevin and Mailander reported beneficial effects and Dolan and Benniger[135] also found a 50 percent increase in fatigue life at 10^8 cycles in fresh water due to nitriding. Junger[136] found that the protective action of surface compression, although effective in short-time tests, decreased considerably in long-time tests in sea water. On the other hand, nitrided steels showed no rusting and a 500-800 percent increase in fatigue trength without showing a true fatigue limit. Nitriding and surface compression have also been shown to be beneficial

for improving fatigue behavior in air. Karpenko and Ischenko have also noted that surface rolling is beneficial in the presence of surface active agents[137].

Inhibitors have been shown to be beneficial, although a higher concentration of inhibitor was required than is normally needed to prevent uniform corrosion in the same solution. Speller, McCorkle and Mumma[138,139] studied the effect of chromates and dichromates in concentrations of 25-30,000 ppm sodium chloride. Their results indicated that more inhibitor was required at higher chloride concentrations, and that dichromate of 200-800 ppm is superior to chromate of equivalent concentration (Fig. 37). Crevice corrosion was observed at a solution-rubber washer interface in these solutions. Daeves, Kamp and Hotthaus[140], Gould[81], and Gould and Evans[141] also reported improved fatigue behavior by the addition of 0.001 M to 2 M chromates in 0.001 M to 1 M KCl solutions. Greater than 1 M chromates were shown to be especially beneficial. Fink, Turner and Paul[142] observed that saturation with zinc yellow pigment was more effective than equivalent additions of potassium chromate in preventing corrosion fatigue in chloride solutions but noted that as the inhibitor was added, results became scattered and no true fatigue limit could be obtained for long-time tests. This anomalous behavior was attributed to local breakdown of passive films and subsequent attack. Speller et.al.[143] noted that a high concentration of chromate was required to initiate a passive film, but that lower concentrations sufficed to maintain it. Sodium

carbonate[31] was shown to be effective in preventing corrosion fatigue in distilled water, and Holtzhauer[144] and Thum and Holtzhauer[94] noted that trisodium phosphate was also beneficial.

Various cathodic, anodic and inert coatings have also been investigated to prevent corrosion fatigue. Cathodic coatings are generally only effective if the coating remains unbroken, and accordingly several investigators have shown that breaks in the coating accelerate corrosion fatigue behavior, probably by accelerating corrosion at the breaks (Fig. 30a). Thus, Kenyon[145] found copper coatings to accelerate damage. On the other hand, Cazaud[146] found electrodeposited nickel and chromium to be slightly beneficial in fresh water, and Inglis and Larke[97] and Wilson[147] found nickel to be beneficial in river water and in salt spray, respectively.

Chromium plating was also found to be beneficial for corrosion fatigue resistance of high strength steels, especially if the plating was applied to shot peened or ball rolled surfaces. Case hardening and chromium coatings were still more resistant to corrosion fatigue and zinc coatings were also shown to be beneficial although not so much as the chromium coatings[148]. The state of stress of chromium coatings has also been shown to be important with residual tensile stresses being damaging to the steel under corrosion fatigue conditions,[149,150] but that improvement in behavior could be realized if the pores in the coating were sealed with linseed oil. Coating steels with corrosion resistant steels by metallizing has also been attempted with some

improvement of fatigue life even in air, but only if the surface was carefully polished to avoid crack initiators[151]. This process, as with many metallizing processes, is not effective at high applied stresses because of the inherent brittleness of the coatings. Chromizing (reaction of steel surfaces with Cr to produce an adherent coating) has also been shown to be effective in improving fatigue life under corrosive conditions[152].

Anodic metal coatings, on the other hand, have generally been shown to be beneficial even when the film was locally ruptured (Fig. 20b)[153,154]. Haigh's experiments with galvanized steel wires were the first indication that zinc could be used to markedly increase the fatigue life of steels[155]. Further experiments by Krystof[156], Harvey[157] and Schrens confirmed Haigh's results and indicated that electroplated zinc was superior to galvanizing in preventing corrosion fatigue[6,141,158,159]. Other investigators have studied the behavior of zinc and cadmium electroplates on steel specimens in various aqueous solutions, and all have arrived at the same conclusion. Huddle and Evans[160] also showed that zinc-rich paints could be beneficial for steels in salt solutions.

The effect of anodizing to protect aluminum alloys from corrosion fatigue has also been studied with somewhat mixed results, some authors showing no effect[161] and others a mixed effect with improvement of fatigue life in corrosive solutions but a reduction in air[162]. Sprayed metallic coatings have also been shown to be effective[163,164]

if stresses are not so large as to rupture the coatings.

Organic and inorganic coatings have been investigated by Gough and Sopwith [165], Speller and McCorkle [166], and others [136,167]. Each of these investigators concluded that the only purpose these coatings served was as a physical barrier to surrounding solutions and that they were not effective unless absolutely continuous.

Applying cathodic current as a means of reducing corrosion fatigue of steel wire specimens in neutral KCl solutions was first investigated by Evans and Simnad [168]. Although it was possible to completely prevent failure in these solutions, a lower fatigue limit was observed, this limit being a function of applied current (Fig. 39). In acid solutions (0.1 N HCl), on the other hand, these authors [92] noted some improvement of fatigue life with applied cathodic current, although it was not possible to completely inhibit failure. Analyses of dissolved iron at high currents (~ 2 ma) indicated no corrosive attack, but these investigators concluded that any iron dissolved at the tip of a crack was redeposited at the mouth of the crack. It was also noted that a higher current was required at higher stresses in order to prevent accumulation of dissolved iron in solution.

Glikman and Suprun [169] studied high medium (0.37 percent) steels in 3 percent NaCl and noted that the protection afforded by applied cathodic currents was directly proportional to current density (1 amp/cm^2, max.), with anodic currents decreasing life to the same extent. Spähn also noted, however, that he was unable to completely

protect against failure in acid solutions and suggested that it remained to be shown whether or not cathodic protection against corrosion fatigue in acids was possible. Cathodic polarization of mild steels was also investigated by Minami and Takada[170] and Spähn[171]. In each case, a fatigue limit identical to that observed in air was observed at sufficiently active potentials in neutral solutions. Minami and Takada noted that even at potentials where a significant amount of hydrogen was absorbed, strength was not significantly affected.

Duquette and Uhlig were able to show complete protection of mild steels by cathodic polarization in both neutral and acid solutions[84,163] (Figs. 40 and 41). Significantly the critical potential for complete protection from corrosion fatigue is identical to the calculated open circuit potential of iron in equilibrium with ferrous ion in solutions below the fatigue limit (Fig. 43). In low pH solutions (pH 2), copious amounts of hydrogen are liberated with no apparent affect on the fatigue limit. At stresses abcve the fatigue limit in these solutions, however, cathodic polarization results in a marked increase in fatigue life - an as yet unexplained result. Pelloux has also shown that cathodic currents are effective in reducing crack propagation rates in aluminum alloys even when cracks are of significant length[123].

The possibility of anodic protection against corrosion fatigue was also investigated by Spähn[171,172], who studied the fatigue

behavior of a 0.48 percent C steel in an acetate buffered solution of pH 4.6 under potentiostatic conditions. Although fatigue life of the steel remained constant throughout most of the passive region of the polarization curve (+200 to +900 mv versus S.C.E.), failure always occurred. It should be noted that the current observed throughout the passive region was relatively high, (3-4 ma/cm^2). Spähn concluded that this high passive current was the result of a non-protective passive film due to the high proportion of pearlite in his specimens. The fatigue life observed at this current agreed qualitatively with that observed in the active region of the polarization curve e.g. failure occurred in the passive region in 5×10^5 cycles at a stress level equal to 90 percent of the fatigue limit and in 4×10^5 cycles at an active anodic current of 3 ma/cm^2 at the same stress level.

The reappearance of a fatigue limit in solutions of pH 12 and greater can probably also be attributed to the presence of a protective passive layer which reduces corrosion to a rate below a certain critical value [84,103].

D, The Mechanism of Aqueous Corrosion Fatigue

Theories of corrosion fatigue have generally relied on one or more of the following mechanisms: (1) stress concentration at the base of hemispherical pits created by the corrosive medium, (2) electrochemical attack at plastically deformed areas of metal with non-deformed metal acting as cathode, (3) electrochemical attack at ruptures in an otherwise protective surface film, and (4) lowering of surface energy of the

metal due to environmental adsorption and increased propagation of microcracks.

Early investigators of corrosion fatigue [173,174] favored the stress-concentration pit theory. Their conclusions were based on the physical examination of failed specimens. Such examinations revealed a number of very large cracks originating at large hemispherical pits at the metal surface. Recently, Romanov [175] favored this mechanism as the first stage of failure.

Pit formation in metals and alloys in aggressive environments undoubtedly does lead to a reduction in fatigue life. However, it is important to note that the corrosion fatigue phenomenon also occurs in environments where pitting does not occur. For example, low carbon steels are highly susceptible to corrosion fatigue in acid solutions, where pits are not observed [184,168]. Additionally, reduced fatigue lives can be induced in steel specimens by the application of small anodic currents in deaerated solutions where pits do not form. Conversely, fatigue tests performed in 3 percent NaCl + NaOH solution of pH 12 where only a few randomly distributed pits are observed show fatigue limits identical with those observed in air [34]. Results of this kind are perhaps not unexpected since corrosion induced pits tend to be hemispherical in nature and the stress intensity factor associated with surface connected hemispherical defects is not large [176].

Further evidence that corrosion induced pitting cannot be responsible for early crack initiation in corrosion fatigue was shown by Duquette and Uhlig[103] In a series of experiments aimed specifically at the initiation process, low carbon steels fatigued in neutral 3 percent NaCl solutions for small percentages of total fatigue life were sectioned and examined metallographically. Although some hemispherical pits were observed in the specimen surface, no cracking could be attributed to their presence. Rather, accelerated corrosion of initiated Stage I cracks was noted, with a deep "pit-like" configuration being oriented at approximately 45° to the specimen surface (Fig. 42). No fatigue cracks were observed emanating from these pits, and an examination of specimens cycled for longer periods showed that the extent of growth of initiated fatigue cracks was always equivalent to "pit" depth, with no "normal" fatigue cracks associated with pits. It may be concluded then, that in many cases, the pits observed at failure by previous observers are not the cause of corrosion fatigue cracking but rather the result.

Whitwham and Evans[177] studied the effect of preliminary air fatigue on subsequent corrosion fatigue behavior in order to determine the effect of preferential dissolution of distorted metal on fatigue life. Results indicated that preliminary dry fatigue had little or no effect on corrosion fatigue life of annealed and cold-drawn wires. Transgranular cracks originating in slip bands at the steel surface were the principal causes of failure, although a small percentage of

intergranular cracks was also observed. From these observations, the authors concluded that failure due to corrosion fatigue is caused by distorted metal acting as anode with unidistorted metal acting as cathode; very fine cracks then advance by a combination of electrochemical-mechanical action. They further suggested that this mechanism acts only when the metal is being cyclically stressed and when the atoms at the tip of the crack are very "hot"; the "hot" atoms being electrochemically active to the surrounding "cooler" atoms. When the atoms are cool (static), they cease to be susceptible to attack. A variation of this model (cyclic stress altering structure and causing sensitivity to attack) was proposed by Lihl[178] and by Glikman and Suprun[179], wherein cyclic stresses cause breakdown in the homogeneity of the metal structure. Lihl suggested that an undefined precipitation within the grains destroys the "mosaic" structure, while Glikman and Suprun suggested that electrochemical heterogeneity arises during the course of cyclic stressing creating conditions for increased attack.

Surface film rupture as the principal cause of the corrosion fatigue phenomenon of steels was proposed as early as 1933 by Laute[180]. He proposed that a film of varying thickness forms, which is ruptured by mechanical stress causing increased corrosive attack at the rupture. Low frequencies allow repair of the film and very long life is noted. Evans and Simnad[92,168] also suggested that film rupture might be important in neutral solutions but that structural changes in the

metal predominate in acid solutions. Ryabchenkov[181] noted that the electrode potential of a steel drops markedly in fatigue tests with a higher rate of change being noted at higher stresses. This potential drop continues throughout a particular alternating stress experiment, but reaches a steady-state in static tests. This investigator attributed the continuous lowering of electrode potential to opening of microcracks and destruction of a protective film. Additionally, it was noted that in a grooved steel specimen under alternating stress, the bottom of the groove was anodic to the sides of the notch and to the surface of the specimen.

Investigating the corrosion fatigue behavior of steel under cathodic polarization in neutral and alkaline solutions, Ryavski and Vedenkin[182,183] concluded that the action of protective currents is due to a local change of electrolyte pH at the specimen sufficient to generate a passive film, thus providing protection. On separating the specimen (cathode) from a platinum anode with a connecting agar-agar bridge, it was noted that the pH of the anolyte decreased and the pH of the catholyte increased to 11, this increase being sufficient to protect the specimen against further corrosion. From these results, it was concluded that the protective action of cathodic currents was due not to the suppression of a stressed-unstressed metal galvanic couple, but that the observed change in the potential of the stressed areas is a consequence rather than a cause of cracks. These authors felt that their results disproved the usual electrochemical theory of corrosion

fatigue (i.e., the electrochemical theory in this instance refers to the stressed-unstressed metal galvanic couple theory).

Spähn[184] attributed the shift of the potential in the active direction to the appearance of slip bands on the surface in the early stages of deformation, with localized corrosion occurring as the subsequent step, a resultant notch causing stress concentration and final failure. This apparent change in the electrochemical behavior was also noted by Simnad and Evans[160] and was attributed to (1) a diminution of polarization of both cathodic and anodic areas of the metal, the anodic shift being more dominant, (2) a reduction in resistance of the electrolyte path joining anode and cathode, or (3) a possible bodily shift of the anode potential in the active direction (Fig. 43).

The effect of adsorbed species from a surrounding liquid environment on the mechanical properties of solids and its relevance to fatigue behavior was discussed by Benedicks[185] in 1948. Arguing that the mechanical properties of steels (tensile strength fatigue strength, etc.) could be reduced by wetting the surface with water or alcohol and increased when wetted with other organic agents, this investigator concluded that corrosion fatigue and other environment sensitive mechanical characteristics (e.g., caustic embrittlement, season cracking or soldering brittleness) can be explained by a wetting effect. The liquid wetting the surface caused a dilatation of the solid body due to a reduction of surface energy, and subsequent deformation was thereby made easier, the effect increasing with

increasing surface tension of the liquid.

This theory, based on reduction of surface energy affecting subsequent fatigue behavior, has received much attention from Russian experimenters, notably G. Karpenko [186-190] and P. Rebinder and co-workers [191]. Karpenko first suggested that the corrosion fatigue mechanism consisted of the sum of two separate steps [186]. The first step is the appearance of fatigue cracks due to environmental adsorption, and the second step consists of a corrosion reaction within the nucleated cracks. This mechanism was based on experiments performed on mild steel specimens in distilled water with and without 1 percent addition of saponine, a surface active agent. Cracks appeared in specimens in the saponine solutions but were markedly absent in untreated distilled water [187]. In another set of tests, Karpenko noted in comparing two steel specimens, one in air and the other in distilled water at a stress level slightly below the fatigue limit that cracks were noted only in the specimen tested in water. All growing cracks were normal to the specimen surface and were filled with corrosion product. These results were interpreted in support of the Rebinder effect whereby adsorption accounted for the multiplication of pre-existing ultramicrocracks on deformation with subsequent growth occurring by electrochemical dissolution. Experimental evidence for this mechanism is also cited in later publications by this investigator [188,189] which explain the beneficial effect of surface compressive stresses as a suppression of the adsorption factor.

In a later report on the mechanism of corrosion fatigue, Karpenko attempted to correlate the effect of cathodic and anodic currents on fatigue behavior. The reduction in fatigue strength of a 0.3 percent C steel in an electrolytic bath was attributed to hydrogen adsorption at cathodic areas, and it was concluded that failure under cyclic stress in corrosive media could take place by one of three mechanisms: (1) at high amplitudes, hydrogen embrittlement of cathodic areas dominates, (2) at moderate amplitudes the combined adsorption-electrochemical theory, due to corrosion at anodic areas, controls, and (3) at low amplitudes, crack appearance and growth is due mainly to an electrochemical corrosion mechanism (Fig. 44). Karpenko claimed that in case (3) the corrosion is favored by cyclic stresses which lower the electrode potential in highly stressed areas and destroy oxide films which would otherwise be protective. Thus, this mechanism includes the theories of distorted metal activity and film rupture, as well as the adsorption-electrochemical theory, the stress range determining the controlling mechanism.

It is likely that no one mechanism completely governs the entire corrosion fatigue process; however, the corrosion fatigue crack initiation step appears to be much more specific.

For example, neither the pitting models, the preferential dissolution models or the film rupture models of crack initiation can apply for all metal-environment combinations. Thus their specificity would imply that, although they may be relevant in some limited

circumstances, a more general mechanism must operate. Of the mechanisms cited, the Rebinder or reduction of surface energy mechanism by adsorption would appear to be the most attractive to explain the premature crack initiation process. However, even this model has some severe limitations. For example, it has been shown that steels in neutral aqueous solutions do not suffer corrosion fatigue in deaerated solutions, even when strongly adsorbing ions such as Cl^- are present. It has also been shown that definite, although small, corrosion rates must be maintained to induce crack initiation[103]. These results would appear to be inconsistent with a surface adsorbate theory unless one concludes that the role of the adsorbate is to assist in removing the outermost layer of surface atoms. This mechanism has been suggested for metals being deformed in strongly adsorbing soap solutions with metal-soap complexes being detected in solutions[192].

The extremely small anodic current required to initiate fatigue cracking below the fatigue limit of steels ($\approx 2\mu A/cm^2$) is equivalent to an overall corrosion rate of 1×10^{-4} layers of atoms per stress cycle, obviously indicating that overall corrosion cannot be responsible for corrosion fatigue crack initiation[34]. It is likely, however, that selective corrosion of specific sites on the specimen surface serves to remove small amounts of anodic material. It is accordingly proposed that accelerated fatigue crack initiation in corrosive environments is a result of this selective corrosion process occurring at

newly created metal surface at the metal-environment interface (by the slip step emergence or by an intrusion-extrusion mechanism). While it is clear that the selective corrosion occurring at the freshly exposed metal is not a thermodynamic process, it is likely that metal atoms contained in slip bands would have a lower activation energy for reaction with the environment; thus activation depolarization of anodic sites would accelerate localized corrosion at emerging metal.

In the case of steels, where the normal fatigue process causes crack propagation only above a specific stress, it has been postulated that dislocations are locked and further slip accordingly inhibited by a Cottrell locking process below the fatigue limit. Accordingly, the corrosive attack would effectively "unlock" otherwise blocked slip thus leading to crack initiation and ultimate failure. For example, it has been shown that the joint application of cyclic stresses and corrosive environment leads to extrusion-intrusion broadening in steels (Fig. 45). For other metals, which do not exhibit a definite fatigue limit, it has been shown that the dislocation structure at the metal surface can be quite different from that inside the metal [193-196]. If this region is viewed as an effectively work hardened region, due to dislocation interaction, localized corrosion of emerging slip steps or extrusion would effectively soften specific surface regions leading to accelerated crack initiation. Thus, rather than a surface energy reduction leading to increased slip and subsequent crack nucleation, the proposed mechanism consists of metal removal from specific highly deformed

regions in the metal surface (Fig. 46).

It is significant to note that a number of investigators have shown that over wide ranges of corrosion rates fatigue life (and presumably crack nucleation time) is independent of corrosion rate [34,103]. For example, fatigue lives below the fatigue limit of steels have been observed to be constant over a range of applied anodic currents equivalent to overall corrosion rates of 0.05 to 0.5 atom layer per second and similarly constant in either air saturated or oxygen saturated salt solutions where corrosion rates increase by a factor of 5 respectively. According to the proposed mechanism for crack initiation, these corrosion rates would be sufficiently high so that they are greater than the local rate required to dissolve dislocation blocking sites as they occur.

Conclusions

On reviewing existing data on the phenomenon of both gaseous and aqueous corrosion fatigue, it becomes apparent that little is actually known of the quantitative mechanisms which govern either process. In the gaseous case, surface energy reductions by adsorbing gaseous species resulting in accelerated crack growth are at best speculative although such a model appears to be a reasonable qualitative explanation for observed results. More basic information in the form of specific gas-metal atomic reactions must be available before a truly quantitative understanding can be achieved.

For aqueous environments, the scientific situation seems to be

even less well defined than for gaseous environments. Few experimental programs have been developed to study the basic aspects of either corrosion fatigue crack initiation or propagation. Rather, speculative models have been developed based on phenomenological observations of cyclic stress/environment-failure relationships. Until the micro-mechanical/electrochemical nature of metal surfaces under cyclic stresses in corrosive environments is better understood, corrosion fatigue will remain somewhat of an enigma.

Acknowledgments

The support of the U. S. Navy Office of Naval Research under Contract #N00014-67A-0117-0012, NR036-093 is gratefully acknowledged.

List of References

1. B. P. Haigh, J. Inst. Metals 10, 55 (1917).
2. M. Achter, ASTM STP 415, 181 (1967).
3. H. J. Gough, J. Inst. Metals 49, 17 (1932).
4. P. T. Gilbert, Met. Rev. 1, 379 (1956).
5. H. J. Gough, J. Inst. Metals 49, 93 (1932).
6. H. J. Gough and D. G. Sopwith, J. Inst. Metals 72, 415 (1946).
7. H. J. Gough and D. G. Sopwith, J. Inst. Metals 52, 55 (1935).
8. N. J. Wadsworth and J. Hutchings, Phil. Mag. 3, 1154 (1958).
9. N. J. Wadsworth, Phil. Mag. 6, 387 (1961).
10. N. Thompson, N. J. Wadsworth and N. Louat, Phil. Mag. 1, 113 (1956).
11. R. L. Stegman and M. Achter, Trans. TMS-AIME 239, 742 (1967).
12. D. J. Duquette and M. Gell, Met. Trans. 2, 1325 (1971).
13. H. H. Smith and P. Shahinian, Trans. ASM 62, 549 (1969).
14. C. Laird and A. R. Krause, Trans. TMS-AIME 242, 3339 (1968).
15. K. U. Snowden, Phil. Mag. 3, 1411 (1958).
16. K. U. Snowden and J. N. Greenwood, Trans TMS-AIME 212, 91 (1958).
17. K. U. Snowden and J. N. Greenwood, Trans TMS-AIME 212, 627 (1958).
18. K. U. Snowden, Phil. Mag. 6, 321 (1960).
19. K. U. Snowden, Nature (London) 189, 53 (1961).
20. K. U. Snowden, Acta Met. 12, 295 (1964).
21. K. U. Snowden, Phil. Mag. 10, 435 (1964).

22. J. M. Jacisin, Trans. TMS-AIME 239, 821 (1967).

23. W. Engelmaier, Trans. TMS-AIME 242, 1713 (1968).

24. M. Shen, S. E. Podlaseck and I. R. Kramer, Acta. Met. 14, 341 (1966).

25. M. J. Hordon, Acta. Met. 14, 1173 (1966).

26. D. A. Meyn, Trans. ASM 61, 53 (1968).

27. T. Broom and A. Nicholson, J. Inst. Met. 89, 183 (1960).

28. F. J. Bradshaw and C. Wheeler, Mat. Res. 2, 112 (1966).

29. C. Laird and G. C. Smith, Phil. Mag. 8, 1945 (1963).

30. F. E. Fujita, Acta. Met. 6, 543 (1958).

31. R. M. N. Pelloux, Trans. ASM 62, 281 (1969).

32. J. C. Grosskreutz and C. Q. Bowles, Environment Sensitive Mechanical Behavior, Gordon and Breach (1963), p. 67.

33. J. C. Grosskreutz, Fracture 1969 Proc. Int. Conf. on Fracture, Brighton, Chapman and Hall (1969), p. 731.

34. J. C. Grosskreutz, Surface Sci. 8, 173 (1967).

35. W. A. Wood, S. McK. Cousland and K. R. Sargant, Acta. Met. 11, 643 (1963).

36. G. J. Danek, Jr., H. H. Smith and M. R. Achter, Proc. ASTM 61, 775 (1961).

37. K. U. Snowden, J. Appl. Phys. 34, 3150 (1963).

38. H. H. Smith, P. Shahinian and M. Achter, Trans. TMS-AIME 245, 947 (1969).

39. A. Kelly, W. R. Tyson and A. H. Cottrell, Phil. Mag. 15, 567 (1967).

40. A. R. C. Westwood, C. M. Preece and N. H. Kamdar, Trans. ASM 60, 723 (1967).

41. K. R. L. Thompson and J. V. Craig, Met. Trans. 1, 1047 (1970).

42. C. A. Stubbington and P. J, E. Forsyth, Metallurgia 74, 15 (1966).

43. M. Gell and J. Vandersande, MERL, P&W Aircraft, Middletown, Conn. unpublished research.

44. D. I. Golland and P. L. James, Met. Sci. J. 4, 113 (1970).

45. P. Beardmore and P. Thornton, Ford Sci. Lab., Dearborn, Mich. private communication.

46. J. K. Tien and R. P. Gamble, Met. Trans. 2, 1933 (1971).

47. M. Gell and G. R. Leverant, Fracture 1969 Proc. 2nd Int. Conf. on Fracture, Chapman and Hall Ltd., London 1969, p. 565.

48. C. H. Wells and C. P. Sullivan, Trans. ASM 61, 149 (1968).

49. M. Gell, G. R. Leverant and C. H. Wells, Achievement of High Fatigue Resistance in Metals and Alloys, ASTM STP 467, 113 (1970).

50. G. F. Paskiet, D. H. Boone and C. P. Sullivan, MERL P&W Aircraft, Middletown, Conn., unpublished research (1971).

51. J. R. Johnston and R. L. Ashbrook, NASA TN D-5376 Aug. 1969.

52. M. A. H. Howes, NASA CR 73738, May 1970.

53. C. G. MacMahon and L. F. Coffin, Jr., Met. Trans. 1, 3443 (1970).

54. B. Hodgson, Met. Sci. J. 2, 235 (1968).

55. M. Gell and D. J. Duquette, Proc. Int. Conf. on Corrosion Fatigue, Storrs, Conn. (1971) to be published.

56. A. J. Nachtigall, S. J. Klima, J. C. Freche and C. A. Hoffman, NASA TN D-2898, June 1965.

57. M. R. Achter, Proc. Environ. Sci. 1963, p. 385.

58. L. F. Coffin, Jr., Proc. Int. Conf. on Corrosion Fatigue, Storrs, Conn. (1971) to be published.

59. F. E. Organ and M. Gell, Met. Trans. 2, 943 (1971).

60. M. Gell and G. R. Leverant, MERL, P&W Aircraft, Middletown, Conn., unpublished research.

61. P. Shahinian, Trans. ASM 49, 862 (1957).

62. P. Shahinian and M. R. Achter, Nav. Res. Lab. Report No. 5036, October 1957.

63. P. Shahinian and M. R. Achter, Nav. Res. Lab. Report No. 5037, October 1957.

64. P. Shahinian and M. R. Achter, Nav. Res. Lab. Report No. 5133, May 1958.

65. T. H. Alden and W. A. Backofen, Acta Met. 9, 352 (1961).

66. J. C. Grosskreutz, Surface Sci. 8, 173 (1967).

67. J. M. Francis and K. E. Hodgson, Mats. Sci. and Eng. 6, 313 (1970).

68. D. J. Duquette and M. Gell, Met. Trans. 3, to be published.

69. M. Gell and G. R. Leverant, Trans. TMS-AIME 242, 1869 (1968).

70. G. R. Leverant and M. Gell, Trans. TMS-AIME 243, 1167 (1969).

71. F. E. Fujita, Fracture of Solids, Interscience Publ. 657 (1963).

72. H. H. Smith and P. Shahinian, Met. Trans. 1, 2007 (1970).

73. H. H. Smith and P. Shahinian, Trans. Quart. ASM 62, 549 (1969).

74. C. Laird, Fatique Crack Propagation, ASTM STP 415 (1967), p. 131.

75. D. J. McAdam, Jr., Trans. Am. Soc. Steel Treat. 11, 355-79 (1927).

76. R. R. Moore, Proc. Amer. Soc. Test. Mat. 26 (II) 255 (1926).

77. R. R. Moore, Ibid, 27 (II) 129 (1927).

78. D. J. McAdam, Jr., Proc. Am. Soc. Testing Mat. 26, 224 (1926).

79. D. J. McAdam, Jr., Proc. Amer. Soc. Test. Mat. 31 (II) 259 (1931).

80. D. J. McAdam, Jr., Trans. Amer. Inst. Min. Met. Eng. 99, 282 (1932).

81. A. J. Gould, Engineering 136, 453 (1933).

82. A. J. Gould, Engineering 141, 495 (1936).

83. D. J. McAdam, Jr., Proc. Amer. Soc. Test. Mat. 28(II) 117 (1928).

84. D. J. Duquette and H. H. Uhlig, Trans ASM 62, 839 (1969).

85. I. Cornet and S. Golan, Corrosion 15, 262t (1959).

86. M. Vater and M. Henn, Korrosion u. Metallschütz 20, 179 (1944).

87. K. Endo and Y. Miyas, Bull. Japan Soc. Mech. Eng. 1, 374 (1958).

88. H. J. Gough and D. G. Sopwith, J. Iron and Steel Inst. 127, 301 (193[illegible]

89. H. J. Gough and D. G. Sopwith, J. Iron and Steel Inst. 135, 293 (1937).

90. A. J. Gould, J. Iron Steel Inst. 161, 11 (1949).

91. P. G. Forrest, Fatigue of Metals, Pergamon Press, New York (1962), p. 218.

92. M. T. Simnad and U. R. Evans, J. Iron Steel Inst. 156, 531 (1947).

93. F. J. Radd, L. H. Crowder and L. H. Wolfe, Corrosion 16, 415t (1960).

94. A. Thum and C.Holtzhaure, Warmë 56, 640 (1933).

95. D. J. McAdam, Jr., Trans. Amer. Soc. Mech. Eng. 51(I) 45 (1929).

96. R. Mailänder, Krupp. Monatsh. 13, 56 (1932).

97. N. Inglis and G. F. Larke, Trans. Faraday Soc. 27, 803 (1931); 28, 715 (1932).

98. T. H. Burnham, Trans. Inst. Marine Eng. 46, 1 (1934).

99. G. D. Lehmann, Engineering 122, 807 (1926).

100. A. M. Binnie, Engineering 128 199 (1929).

101. T. S. Fuller, Trans. Am. Inst. Min. Met. Eng. 90, 280 (1930).

102. P. Mehdizadeh, R. L. McGlasson and J. E. Landers, Corrosion 22, 325 (1966).

103. D. J. Duquette and H. H. Uhlig, Trans ASM 61, 449 (1968).

104. D. J. McAdam, Jr., Proc. ASTM 27, 102 (1927).

105. D. J. McAdam, Jr., and G. W. Geil, J. Res. N.B.S. 26, 135 (1941).

106. H. J. Gough and D. G. Sopwith, J. Inst. Met 60, 143 (1937).

107. J. McKeown, D. N. Mends, E. S. Bale and A. D. Michael, J. Inst. Metals 83, 69 (1954).

108. H. H. Uhlig, Proc. Int. Conf. on Corr. Fat., Storrs, Conn. (1971) to be published.

109. R. Cazaud, Rev. Met. 31, 439 (1934).

110. F. Bollenrath and K. Bungardt, Z. Metallkunde 30, 357 (1938).

111. N. P. Inglis and E. C. Larke, J. Inst. Met. 83, 117 (1954).

112. E. Gebhardt and H. Beyer, Z. Metallkunde 48, 5 (1957).

113. P. J. E. Forsyth, J. Inst. Met 80, 181 (1951).

114. P. J. E. Forsyth, Nature 171, 172 (1953).

115. P. J. E. Forsyth and C. A. Stubbington, Nature 175, 765 (1955).

116. P. J. E. Forsyth, J. Inst. Met. 83, 395 (1955).

117. P. J. E. Forsyth, Proc. Roy. Soc. A242, 198 (1957).

118. P. J. E. Forsyth and C. A. Stubbington, J. Inst. Met. 85, 339 (1957).

119. P. J. E. Forsyth, Cranfield Symposium on Crack Propagation 1961.

120. C. A. Stubbington and P. J. E. Forsyth, J. Inst. Met. 90, 347 (1961).

121. C. A. Stubbington, Metallurgia 68, 109 (1963).

122. C. Panseri, Allumino 23, 473 (1954).

123. R. M. N. Pelloux, Fracture 1969, Proc. Int. Conf. on Fracture, Chapman and Hall Ltd., London 1969

124. B. S. Hockenhull, N. A. Monks, H. Sala, Proc. Int. Conf. on Corrosion Fatigue, Storrs, Conn. (1971) to be published.

125. "Fatigue Crack Propagation" ASTM STP 415, 1967.

126. "Effects of Environment and Complex Load History on Fatigue Life", ASTM STP 462, 1970.

127. "Achievement of High Fatigue Resistance in Metals and Alloys", ASTM STP 467, 1970.

128. H. H. Johnson and P. C. Paris, Eng. Fracture Mech. 1, 3, (1968).

129. R. P. Wei, Eng. Fracture Mech. 1, 633 (1970).

130. D. J. Mack, Proc. ASTM 45, 629 (1945)

131. A. J. Gould and U. R. Evans, J. Iron and Steel Inst. 156, 531 (1947).

132. A. Thum and H. Ochs, Korrosion u. Metallshütz, 13, 380 (1937).

133. O. Föppel, O. Behrens and T. Dusold, Z Metallkunde 25, 279 (1933).

134. A. Portevin, Metaux et Corrosion 13, 43 (1938).

135. T. J. Dolan and H. H. Benniger, Proc. Am. Soc. Test. Met., 40, 658 (1940).

136. A. Jünger, Mitt. Forsch. Anstalt. Gutehoffnungshütte Oberhausen A.-G. 5, 1 (1937).

137. G. V. Karpenko and I. I. Ischenko, Nauch. Zapiski Inst. Machinoved. I Avtomatiki, Akad. Nauk. Ukr. S.S.R. 2,84 (1953).

138. F. N. Speller, I. B. McCorkle and P. F. Mumma, Proc. Amer. Soc. Test. Mat. 28 (II) 159 (1928).

139. F. N. Speller, I. B. McCorkle and P. F. Mumma, Proc. Amer. Soc. Test. Mat. 29 (II) 238 (1929).

140. K. Daeves, E. Kamp and K. Holthaus, Z.V.D.I., 78, 1065 (1934).

141. A. J. Gould and U. R. Evans, Iron Steel Inst. Spec. Rep., (24) 325 (1939).

142. C. G. Fink, W. D. Turner and G. T. Paul, Trans. Electrochem. Soc. 83, 377 (1943).

143. F. N. Speller, et al., Proc. Amer. Petroleum Inst. 17 (IV) 68 (1936).

144. C. Holtzhauer, Mitt. Materialprüf Anst. Techn. Hochscule Darmstadt 3, (1953).

145. J. N. Kenyon, Proc. Amer. Soc. Test. Mat. 40, 705 (1940).

146. R. Cazaud, Chim. et Ind. 41, 381 (1939).

147. R. E. Wilson, Metal Ind. 72, 211, 251 (1948).

148. A. V. Ryabchenkov and V. F. Abramova, Vestnik Machinostroeniya 35, 54 (1955).

149. L. A. Glikman, L. A. Suprun, L. Ya. Bogorad and E. L. Gakman, Trudy Tsentral. Nauch. Issledovatel. Inst. Morsk. Flota No. 5, 36, (1965).

150. A. P. Grahovetskii, Metalloved. I Term. Obrahotka Metal. No. 1, 21 (1963).

151. I. A. Elin, L. A. Suprun and E. F. Kostrov, Trudy Tsentral. Nauch. Issledovatel. Inst. Morskogo Flota, No. 22, 5 (1959).

152. F. Bollenrath and J. Broichhausen, Werkstoffe U. Korrosion 15, 808 (1964).

153. B. P. Haigh, Trans. Inst. Chem. Eng. 7, 29 (1929).

154. B. P. Haigh and T. S. Robertson, Engineering 138, 240 (1934).

155. J. Krystof, Metallwirtschaft 14, 305 (1935).

156. W. E. Harvey, Metals and Alloys 1, 458 (1930).

157. O. Behrens, Mitt. Wöhler-Inst. 19 (1933).

158. N. Stuart and U. R. Evans, J. Iron Steel Inst. 147, 131 (1943).

159. A. Thum and H. Ochs, Korrosion u. Metallshütz 13, 380 (1937).

160. R. A. U. Hoddle and U. R. Evans, J. Iron and Steel Inst. 149, 109 (1944).

161. D. W. Rudorff, Metallurgia 28, 157 (1943).

162. P. Inglis and E. C. Larke, J. Inst. Met. 83, 117 (1954).

163. E. A. G. Lilliard, J. A. Whittaker and H. King, First Int. Cong. Met. Corr. London, 1961, p. 482.

164. H. G. Cole and R. J. M. Payne, Metallurgia 66, 11 (1962).

165. H. J. Gough and D. G. Sopwith, J. Iron and Steel Inst. 135, 315 (1937).

166. F. N. Speller and I. B. McCorkle, Oil Gas J. 32, 73 (1932).

167. R. C. McMaster, Proc. Am. Soc. Test. Mat. 48, 628 (1948).

168. M. T. Simnad and U. R. Evans. Proc. Roy. Soc. A188, 372 (1947).

169. L. A. Glikman and L. A. Suprun, Metalloved I Obrabotka Metalov, No. 6, 10 (1955).

170. Y. Minami and H. Takada, Boshoku Gijutsu 7, 336 (1958).

171. H. Spähn, Metalloberfläche 16, 369 (1962).

172. H. Spähn, Metalloberfläche 16, 335 (1962); 16, 197 (1962). 16, 233 (1962); 16, 267 (1962).

173. D. J. McAdam, Jr. and G. W. Geil, Proc. Am. Soc. Test Mat. 41, 696 (1941).

174. B. B. Wastcott, Mech. Eng. 60, 813, 829 (1938).

175. V. V. Romanov, Metallurgiya Metallovedenie Fiziko Khimicheskie Metody Issledovaniya 13, 171 (1963).

176. H. Neuber, "Theory of Notch Stresses", J. W. Edwards, Ann Arbor, Michigan 1946.

177. D. Whitwham and U. R. Evans, J. Iron and Steel Inst. 165 (1), 72 (1950).

178. F. Lihl, Berg-U. Huttenmann Monatsh. Montan. Hochschule Leossen 95 (2) 25 (1950).

179. L. A. Glikman and L. A. Suprun, Trudy Tsentral Nauch. Issledovatel. Inst. Morsk. Flota No. 5, 25 (1956).

180. K. Laute, Oberflächentech. 10, 281 (1933).

181. A. V. Ryabchenkov, Zhur. Fiz. Khim. 26, 542 (1952).

182. S. G. Vedenkin and V. S. Sinyavskii, Zhur. Fiz. Khim. 36, 2209 (1962).

183. S. G. Vedenkin and V. S. Sinyavskii, Trudy Vses. Mezhvuz. Nauchn. Konf. Po Vopr. Bor'by Korrosiei 20 (1962).

184. H. Spähn, Metalloberfläche, 16, 299 (1962).

185. C. Benedicks, Pittsburgh Intern. Conf. on Surface Reactions, 196 (1948).

186. G. V. Karpenko, Doklady Akad. Nauk S.S.S.R. 79, 287 (1951).

187. G. V. Karpenko, Doklady Akad. Nauk S.S.S.R. 77, 827 (1951).

188. G. V. Karpenko, Korroziya Metal. I Metody Bor'by S. Neyu. Sbornik 52, (1955).

189. G. V. Karpenko, Nekotorye, Voprosy Ustalost. Prochnosti Stali S Uchetom Vliyaniya Aktivnoy Sredy Sbornik (1955).

190. G. V. Karpenko, Deyaki Pitannya Fiz. Khim. Mekhun. Metal. Akad. Nauk Ukr. R.S.R. Inst. Machinoznavstva Ta Avtomatiki, 47 (1958).

191. V. Likhtman, E. Shehukin and P. Rebinder, Physiochemical Mechanics of Metals, Acak. of Sciences, U.S.S.R., Israel Program for Scientific Translations, Jerusalem (1964).

192. I. Kramer and L. Demer, Prog. in Mat. Sci. 9 (3) 195 (1961).

193. E. E. Laufer and W. N. Roberts, Phil. Mag. 10, 883 (1964).

194. E. Levine and S. Weissmann, Trans. ASM 61, 128 (1968).

195. P. Lukáš M. Klesnil and J. Krejči, Phys. Stat. Sol. 27, 545 (1968).

196. P. Lukáš and M. Klesnil, Phys. Stat. Sol. 37, 833 (1970).

List of Figures

Fig. 13 Effect of Vacuum on the fatigue life of nickel-base superalloy single crystals (after Duquette and Gell[12]).

Fig. 14 Effect of vacuum on the fracture surface appearance of a single crystal nickel-base superalloy single crystals (after Duquette and Gell[12]).

Fig. 15 (a) Slip band cracking in a nickel-base superalloy (U-700) at room temperature; (b) grain boundary cracking in a nickel-base superalloy (U-700) at 1700°F (after Wells and Sullivan[48]).

Fig. 16 Model for fatigue crack nucleation in stainless steel at elevated temperatures (after Hodgson[54]).

Fig. 17 Oxide in intercrystalline crack in a nickel-base superalloy at elevated temperature (after Gell and Duquette[55]).

Fig. 18 Effect of vacuum on the fatigue life of polycrystalline nickel at elevated temperatures (after Nachtigall et al.[56]).

Fig. 19 Effect of frequency on the fatigue life of nickel-base superalloys (after Organ and Gell[59]).

Fig. 20 Endurance limit ($N_f = 10^6$ cycles) of nickel-base superalloy single crystals as a function of temperature (after Duquette and Gell[68]).

Fig. 21 Fatigue life of nickel-base superalloy single crystals (a) 1400°F and (b) 1700°F (after Duquette and Gell[68]).

Fig. 22 Fatigue fracture surfaces of nickel-base superalloy single crystals in air and in vacuum at 1400°F showing initiation sites (after Duquette and Gell[68]).

Fig. 23 Slip offsets on the surfaces of cylindrical nickel-base superalloy single crystals tensile tested in (a) air and in (b) vacuum (after Duquette and Gell[68]).

Fig. 24 Model to explain the effect of oxide layer on emerging slip steps in air on the slip behavior of nickel-base superalloy single crystals (after Duquette and Gell[68]).

Fig. 25 Fatigue fracture surfaces of single crystal nickel-base superalloys in (a) air and in (b) vacuum at 1700°F showing initiation sites (after Duquette and Gell[68]).

Fig. 26 Model showing effect of oxide blunting of Stage II fatigue crack in nickel-base superalloys at 1700°F (after Duquette and Gell[68]).

Fig. 27. Typical corrosion fatigue S-N curves for steels - air, fresh water and saline water (after McAdam[78]).

Fig. 28. Three dimensional plot showing corrosion fatigue behavior of 3.7% Nickel Steel in carbonate water (after McAdam[79]).

Fig. 29 Effect of solution concentration on corrosion fatigue behavior of low carbon steel in KCl solution (curve 2) curve 1 refers to fatigue behavior of steel in distilled water + Na_2CO_3 (after Gould[81]).

Fig. 30 Effect of applied anodic current on the fatigue behavior of low carbon steel in deaerated 3% NaCl solution (after Duquette and Uhlig[34]).

Fig. 31 Effect of solution temperature on the fatigue behavior of mild steel in artificial s a water (after Gould[82]).

Fig. 32 Effect of frequency (time of exposure) on the fatigue behavior of mild steel in air, in tap water and in saline solution (after Endo and Miyas[87]).

Fig. 33 Effect of solution pH on the fatigue behavior of mild steel in 3.5% NaCl solutions (after Radd et al.[93]).

Fig. 34 Effect of dissolved O_2 on the fatigue behavior of 1035 steel in 5% NaCl solutions (after Mehdizadeh et al.[102]).

Fig. 35 Effect of dissolved O_2 and chloride ion on the fatigue behavior of low carbon steel in distilled water and 3% NaCl solutions (after Duquette and Uhlig[103]).

Fig. 36 Fracture surface of 2024 aluminum alloy in sea water. The orientation of the fracture plane is changing with anodic-cathodic current reversals (after Pelloux[123]).

Fig. 37 Effect of Na_2SO_4 and $Na_2Cr_2O_7$ additions on the fatigue behavior of mild steel in NaCl solutions (after Speller et al.[138]).

Fig. 38 Schematic diagram of effect of coating breaks on corrosion behavior of emerging slip bands by cyclic deformation in corrosive environments, (a) cathodic coatings, (b) anodic coatings.

Fig. 39 Effect of applied cathodic current on fatigue behavior of mild steel in KCl solutions (after Simnad and Evans[168]).

Fig. 40 Effect of applied cathodic potentials on the fatigue behavior of low carbon steels in neutral 3% NaCl solutions (after Duquette and Uhlig[103]).

Fig. 41 Effect of applied cathodic potentials on the fatigue behavior of low carbon steels in 0.5 N Na_2SO_4 + H_2SO_4 solutions, pH 3 (after Duquette and Uhlig[84]).

Fig. 42 Surface of low carbon steel cyclically deformed in 3% NaCl to 4% of total life showing crystallographic pitting (after Duquette and Uhlig[103]).

Fig. 43 Models for preferential dissolution of deformed regions in cyclically deformed metals, (a) depolarization of cathodic and anodic areas, anodic depolarization dominant, (b) reduction in resistance of electrolyte between local anodes and cathodes, (c) shift of open-circuit potential of local anodic sites at crack tip.

Fig. 44 Schematic diagram of Karpenko mode of corrosion fatigue as a function of applied stress (after Karpenko[190]).

Fig. 45 Surface of low carbon steel cyclically stressed to $\approx$ 4% of total life in (a) air and (b) aerated 3% NaCl showing development of extrusions and intrusions (arrow in (a). Dark lines in air specimen are Stage I fatigue cracks (after Duquette and Uhlig[103]).

Fig. 46 Schematic diagram of model to explain accelerated slip and subsequent early crack nucleation in corrosion fatigue.

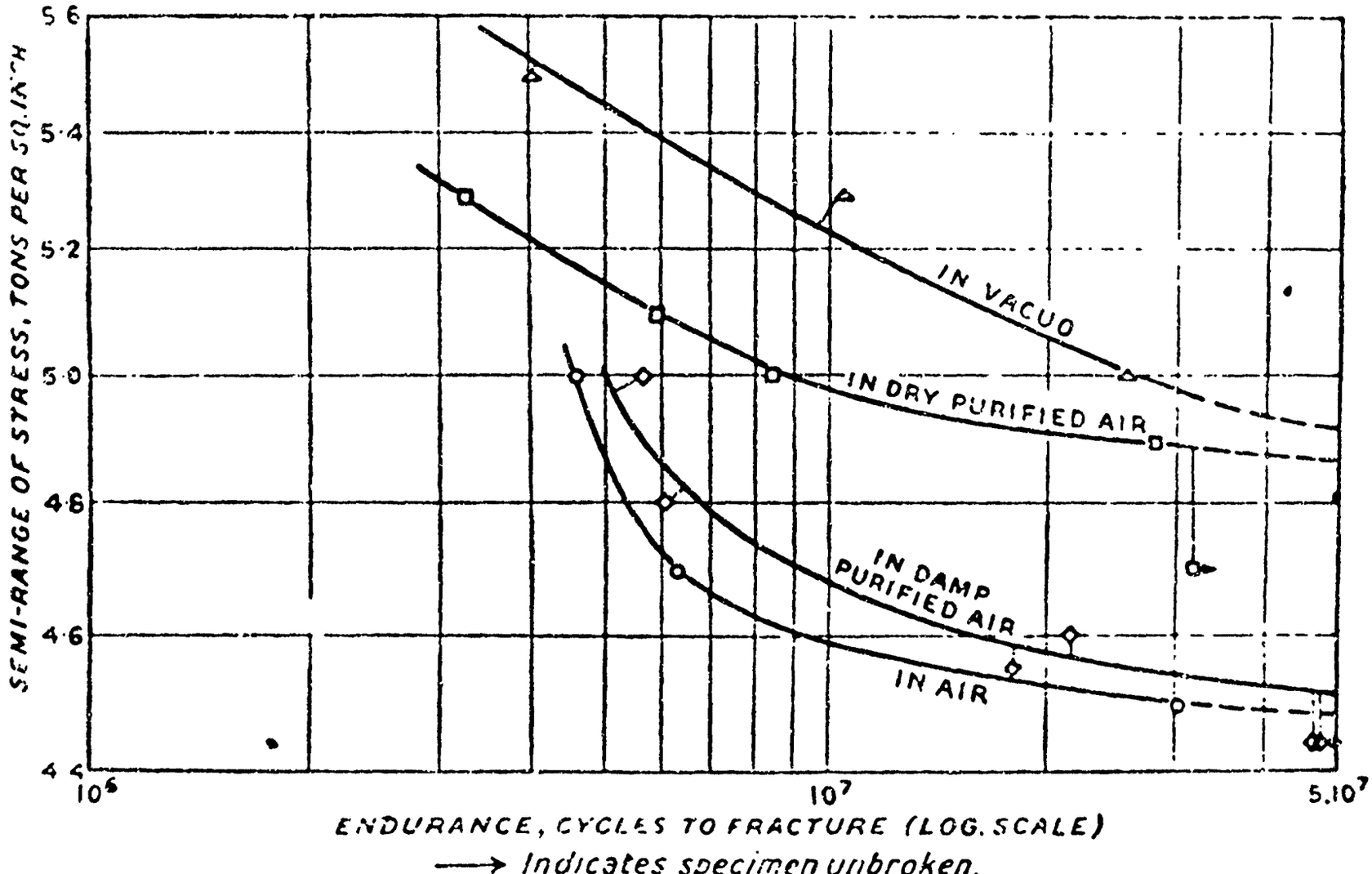

Fig. 1 Effect of gaseous environment on the fatigue life of annealed copper (after Gough and Sopwith[7]).

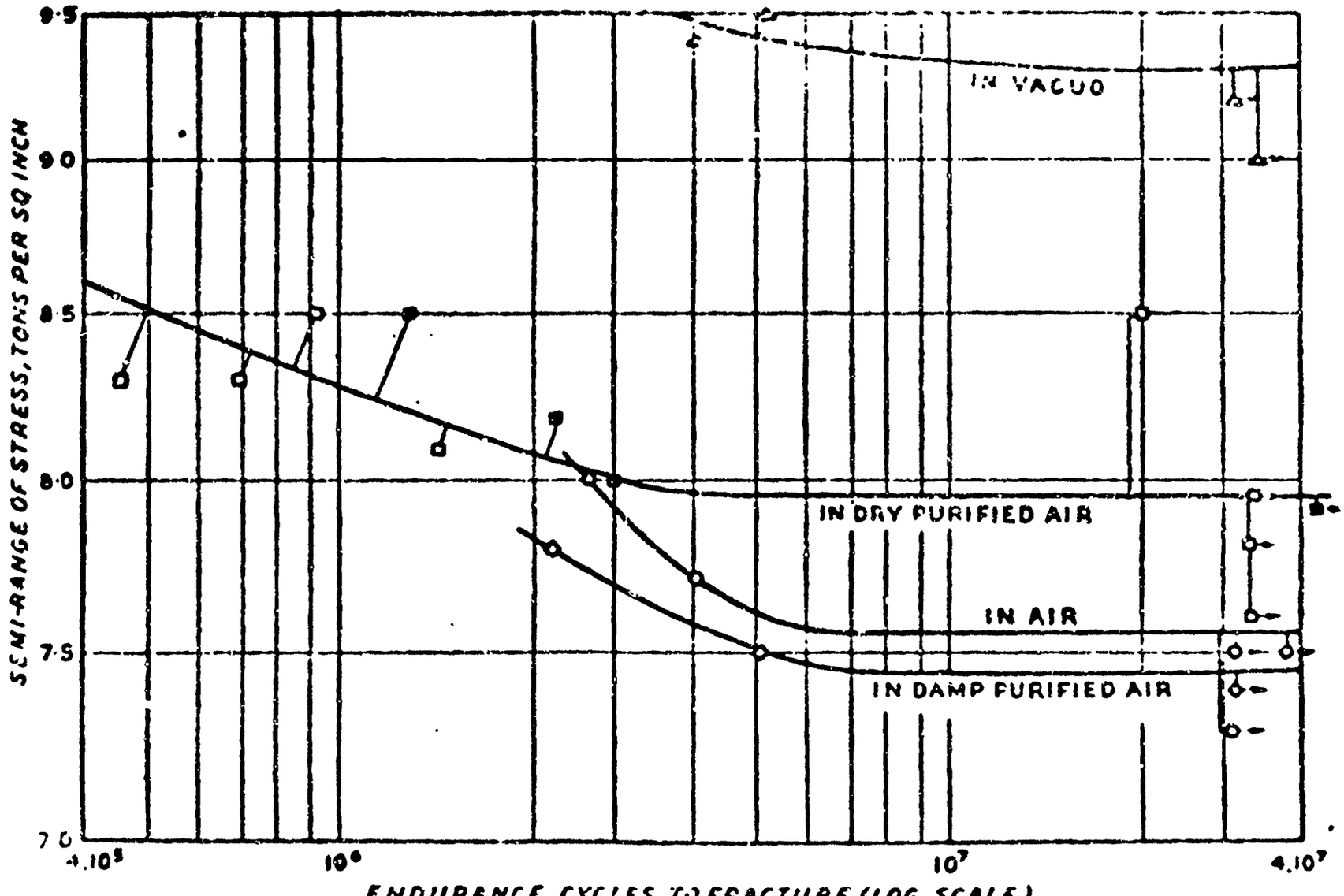

Fig. 2 Effect of gaseous environment on the fatigue life of 70:30 brass (after Gough and Sopwith[7]).

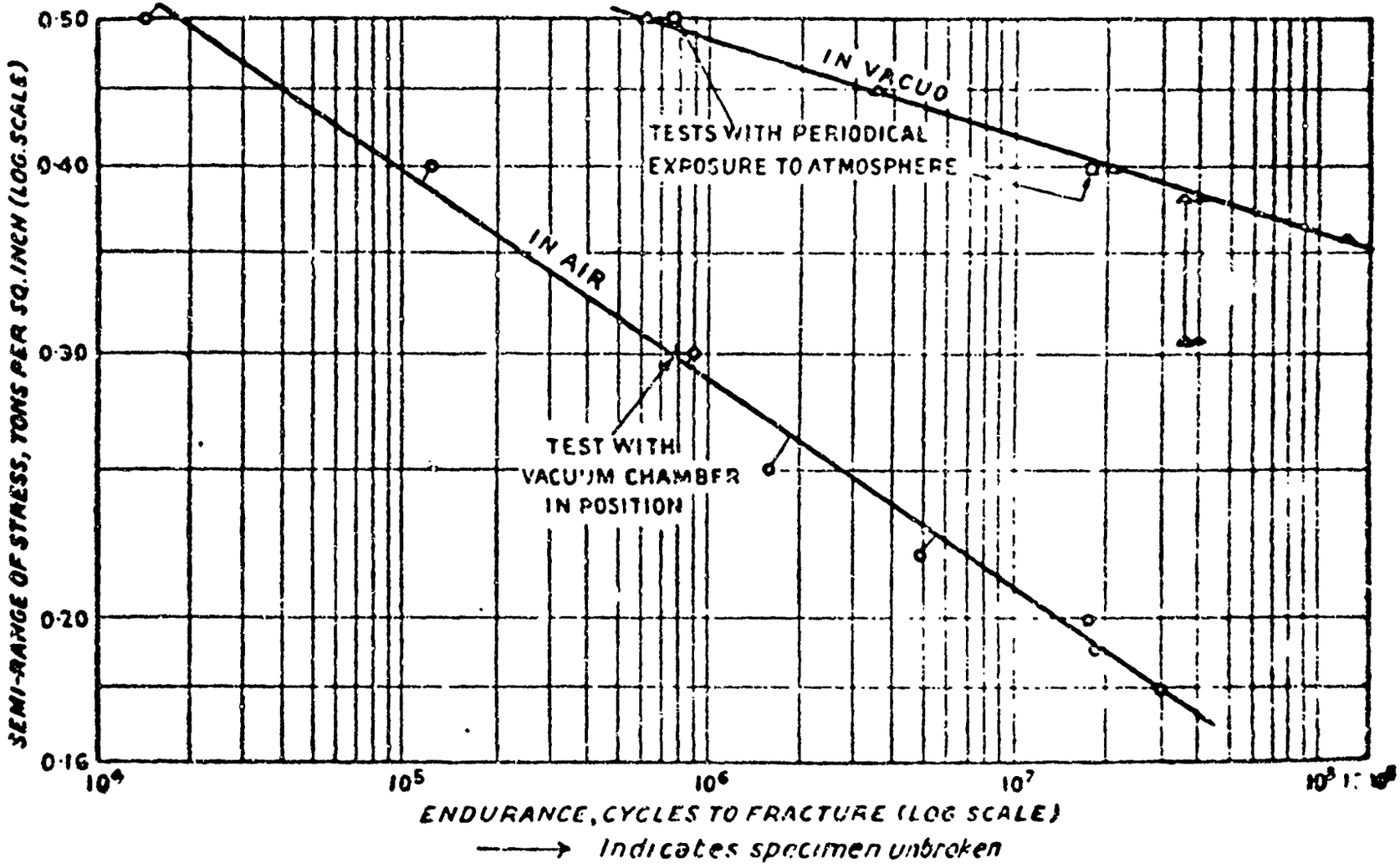

Fig. 3 Effect of gaseous environment on the fatigue life of lead (after Gough and Sopwith[7]).

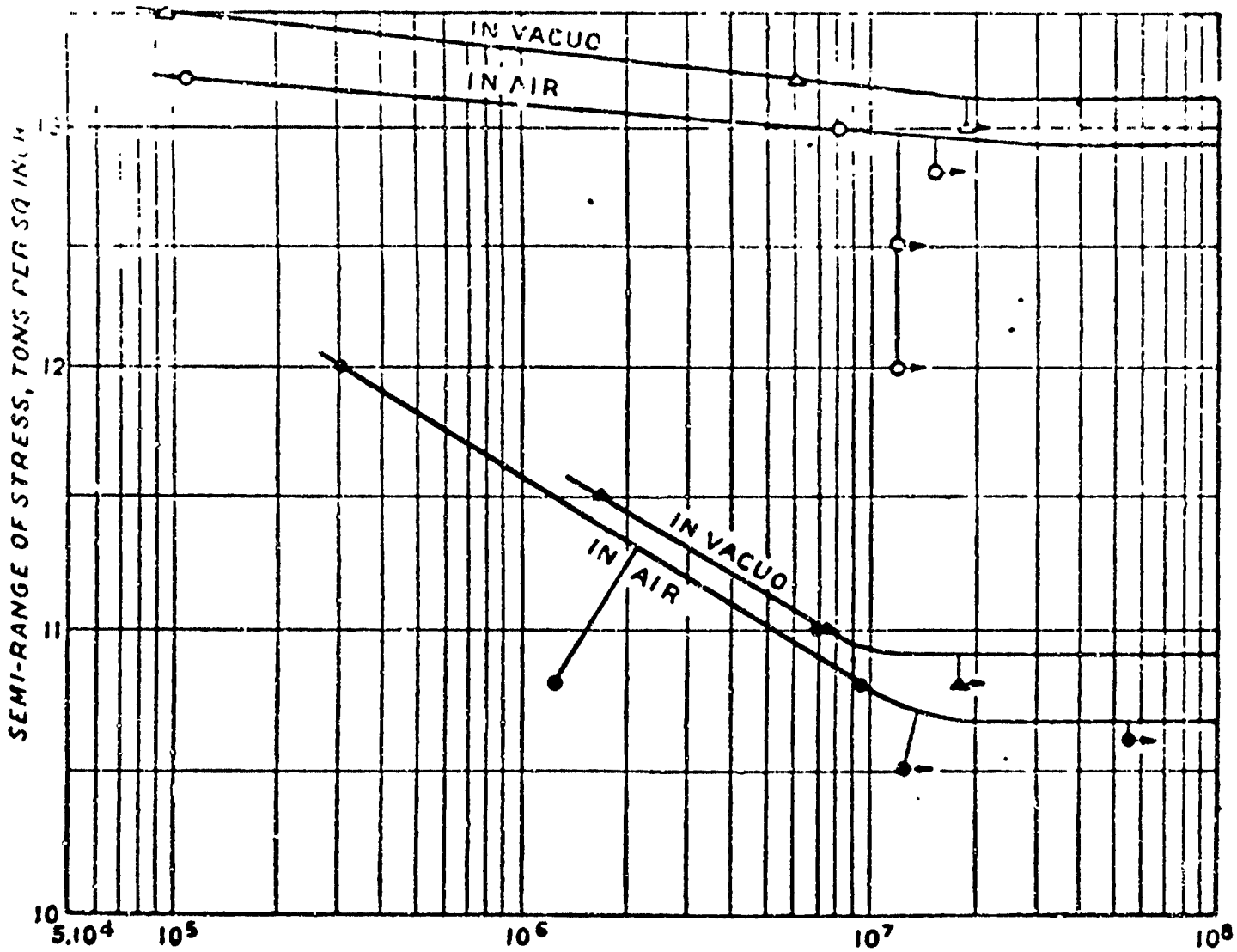

Fig. 4 Effect of gaseous environment on the fatigue life of iron (after Gough and Sopwith[7]).

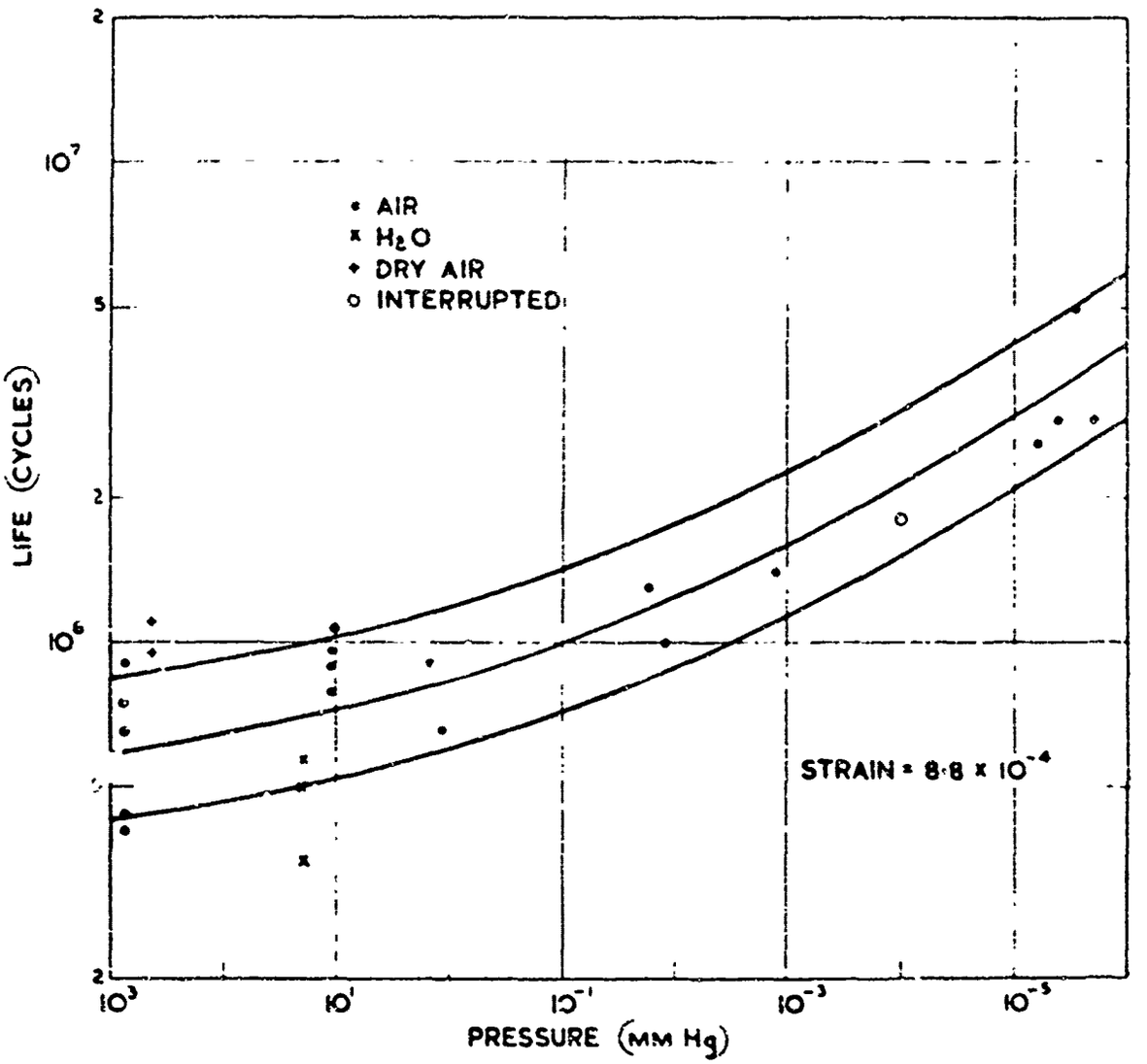

Fig. 5 Effect of gaseous environment on the fatigue life of aluminum as a function of pressure (after Wadsworth and Hutchings[8]).

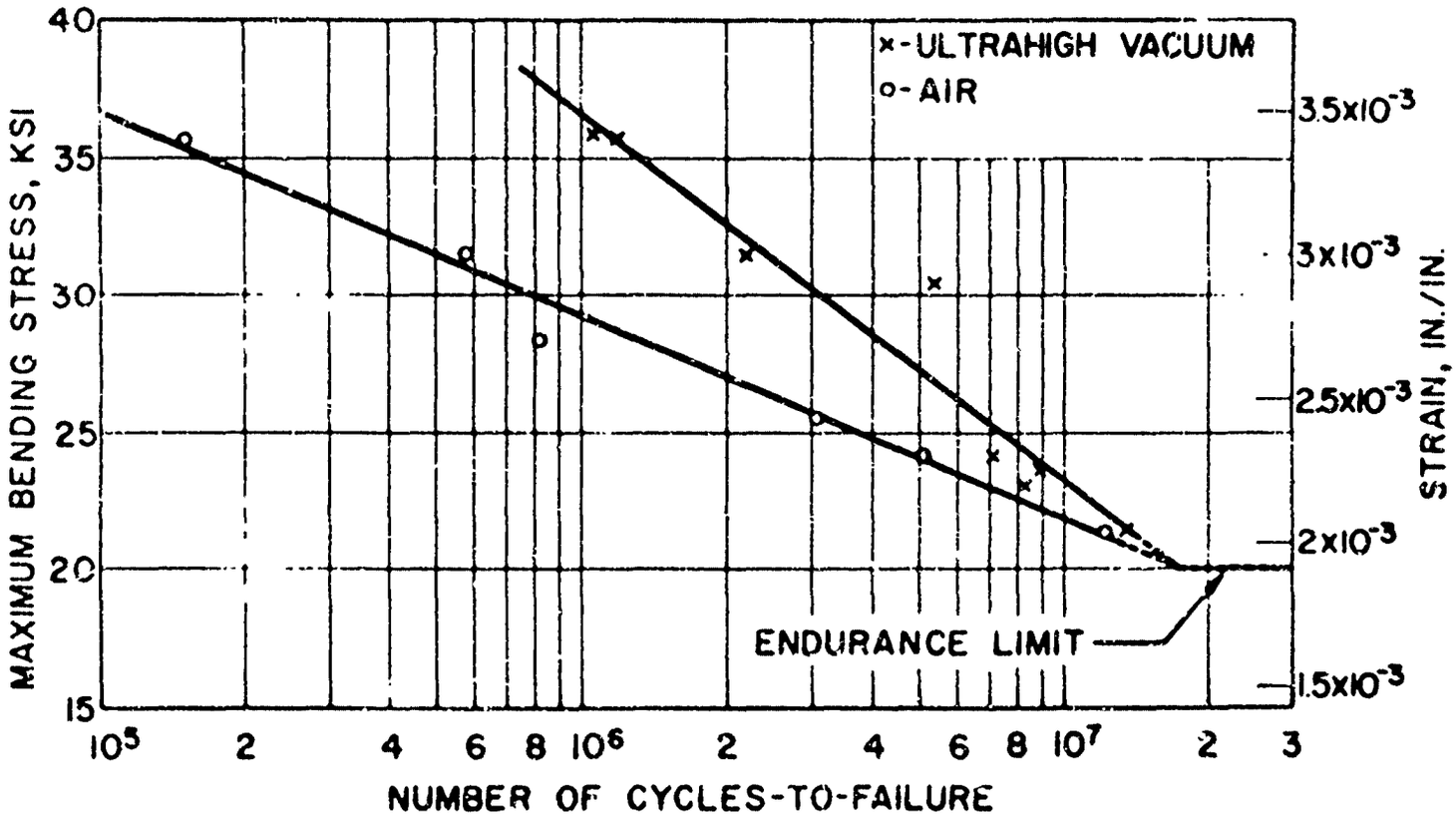

Fig. 6 Effect of vacuum on the fatigue life of aluminum alloy (after Engelmaier[23]).

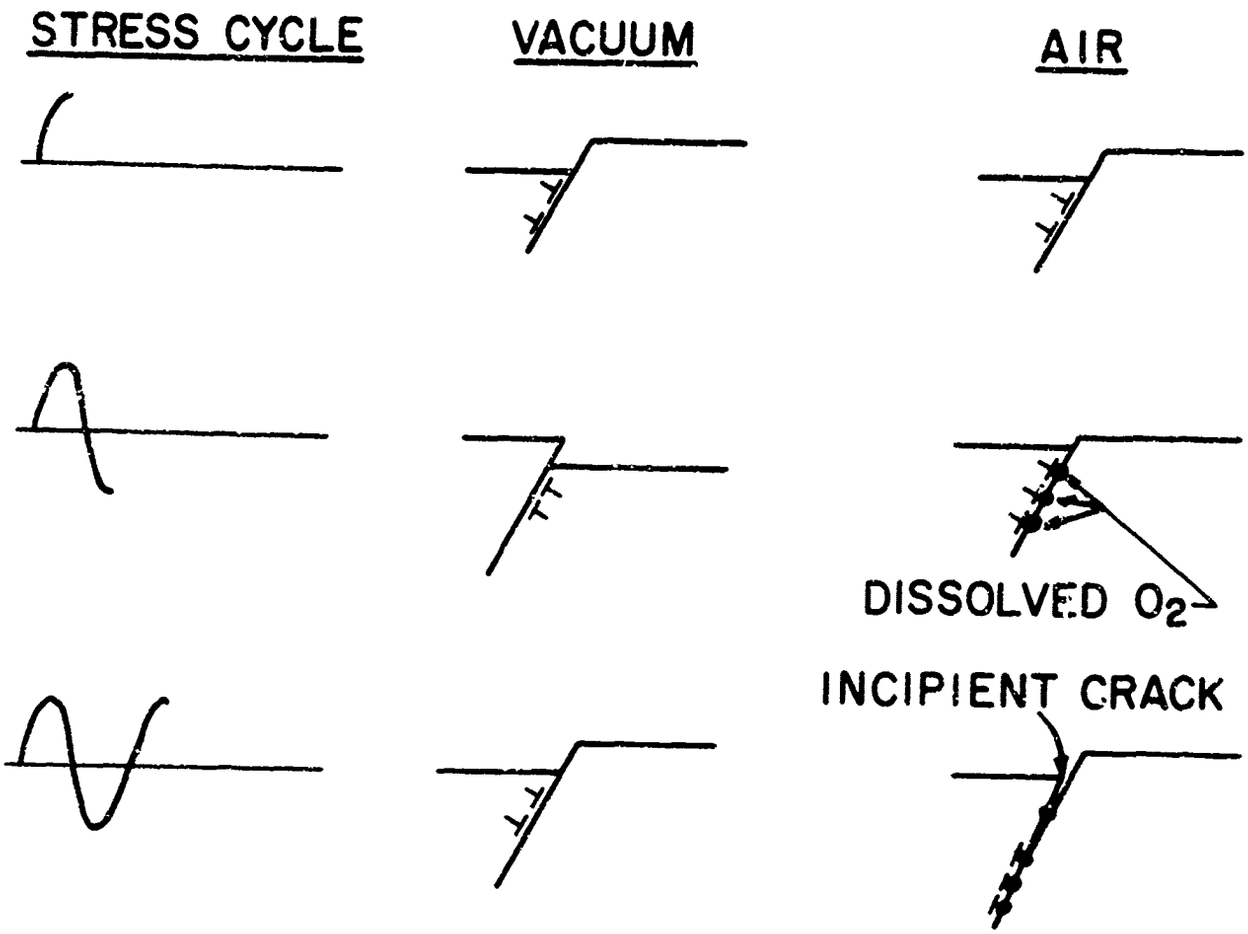

Fig. 7 Model of oxygen - slip band interaction to explain environment sensitive fatigue crack nucleation (after Thompson et al.[10]).

Fig. 8 Fracture surface of 2024-T3 aluminum alloy fatigue tested in air (lower) and in vacuum (upper). Etch pits indicate crack growth on a (100) plane in a < 110 > direction (after Pelloux[32]).

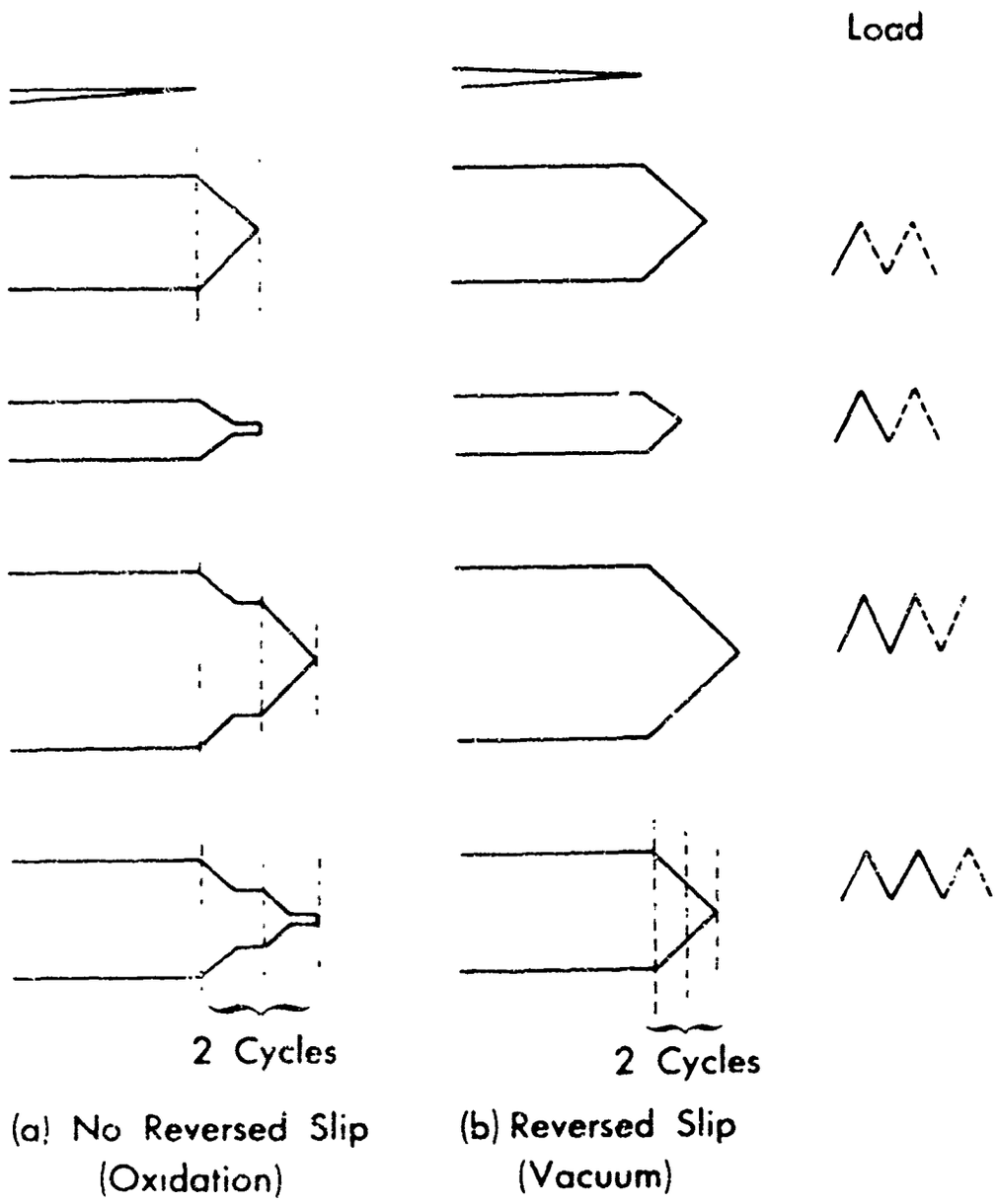

Fig. 9 Model to explain effect of environment on fatigue crack growth (after Pelloux[32]).

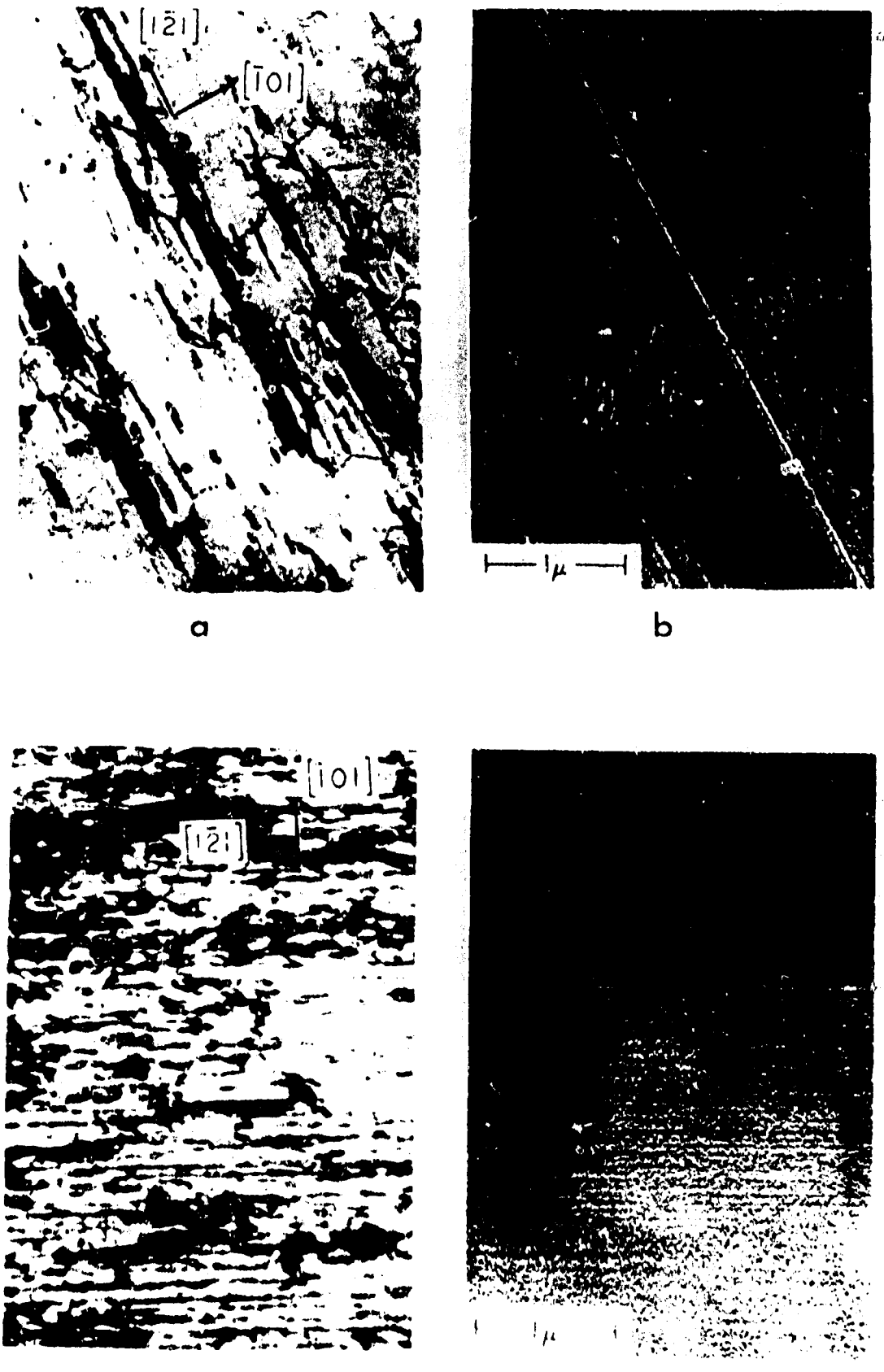

Fig. 10 Electron micrographs of surfaces of cyclically deformed aluminum crystals (a, b) in air (c, d) in vacuum, showing dislocation arrangements near the surface and resultant slip offsets (after Cross, Laird[34]).

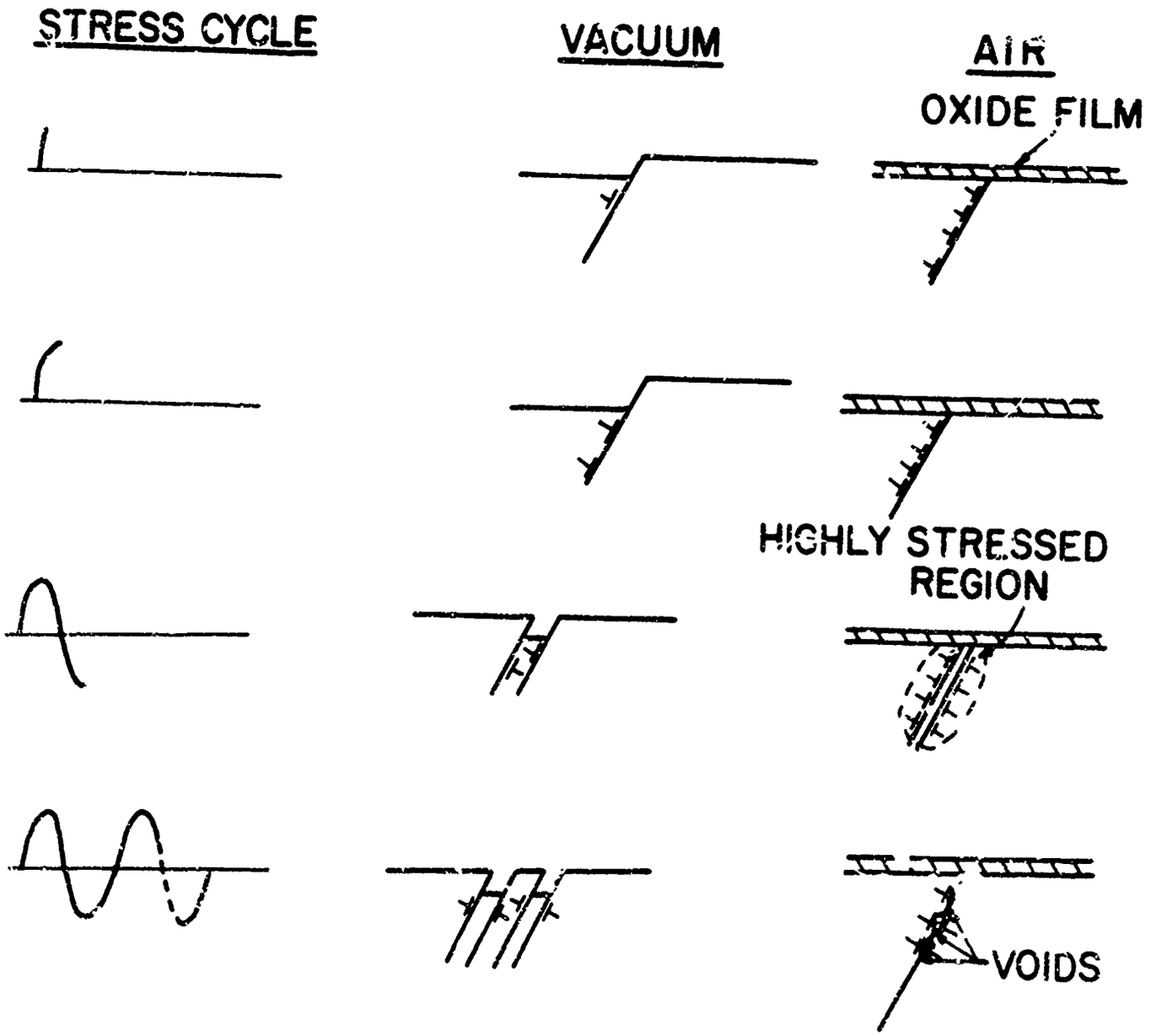

Fig. 11 Model of void nucleation under oxide films to accelerate crack initiation in gaseous environments (after Shen et al.[24]).

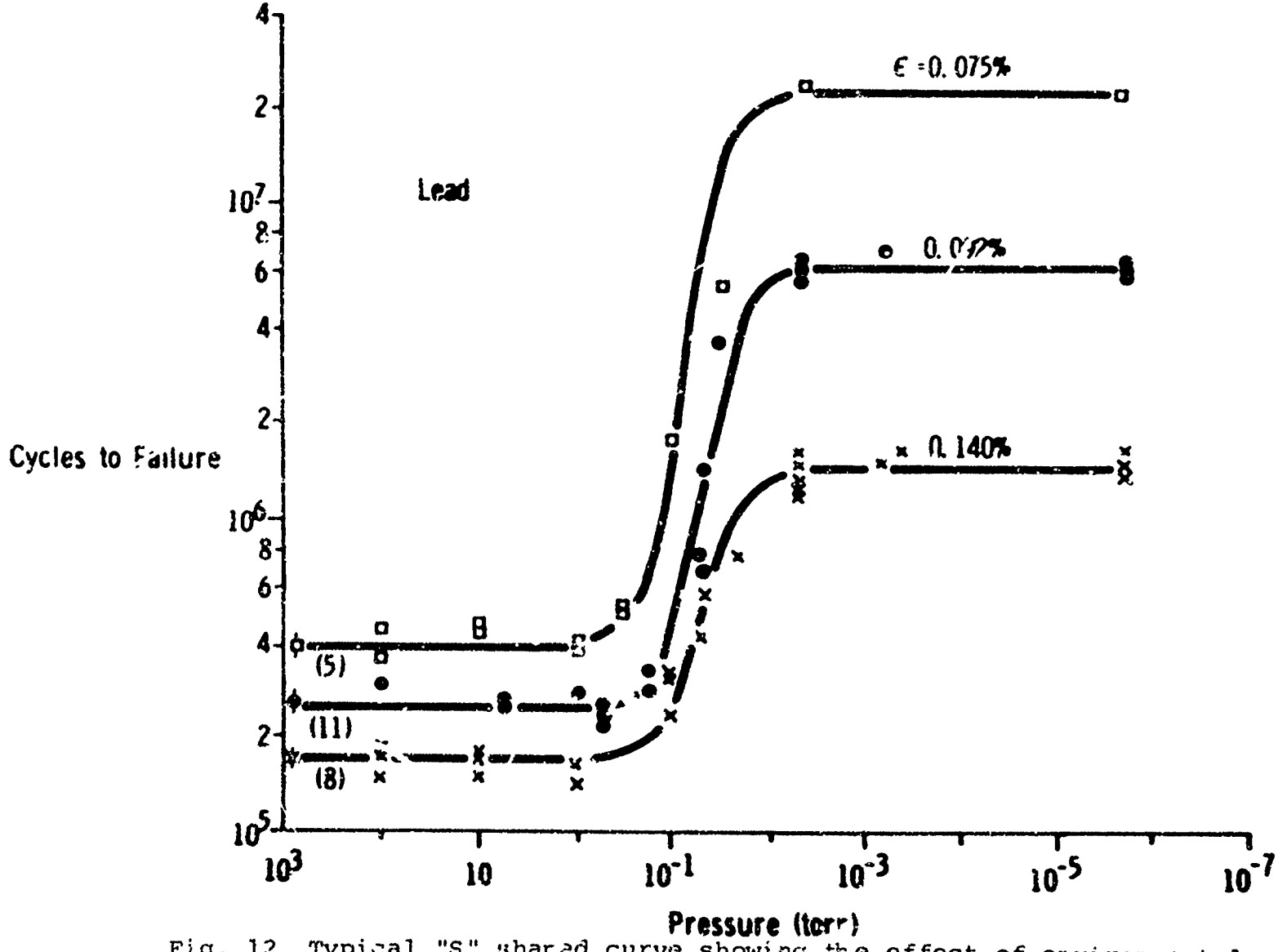

Fig. 12 Typical "S" shaped curve showing the effect of environmental pressure on fatigue life and indicating concept of "critical pressure" (after Snowden[20]).

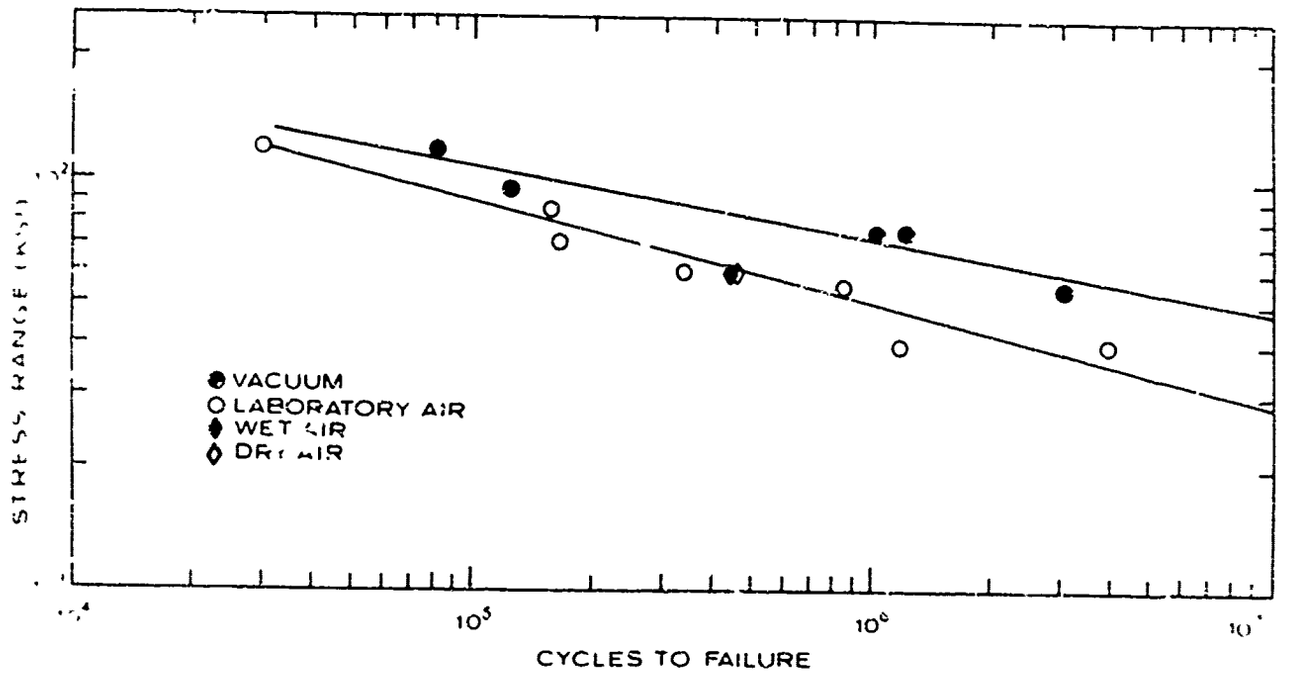

Fig. 13 Effect of vacuum on the fatigue life of nickel-base superalloy single crystals (after Duquette and Gell[12]).

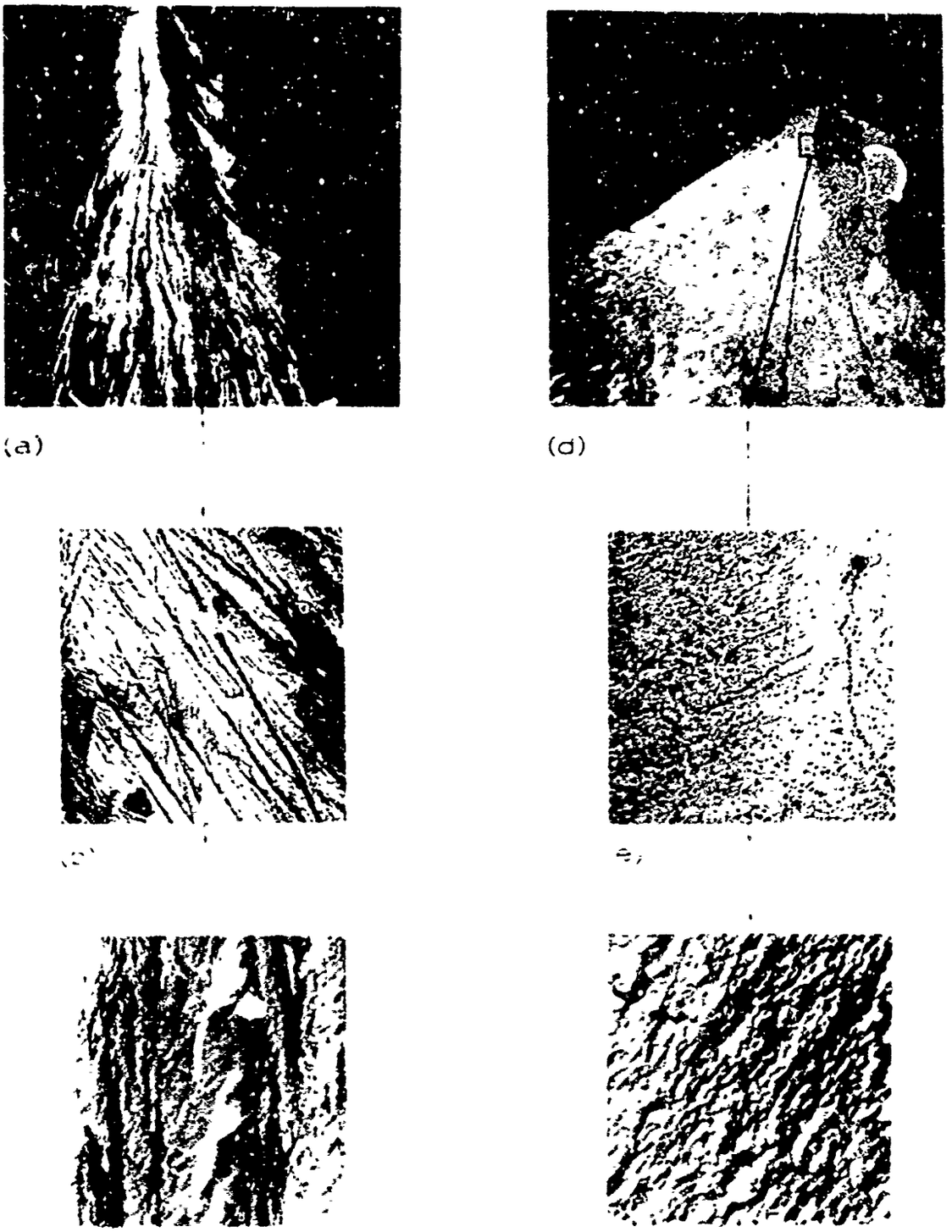

Fig. 14 Effect of vacuum on the fracture surface appearance of a single crystal nickel-base superalloy single crystals (after Duquette and Gell[12]).

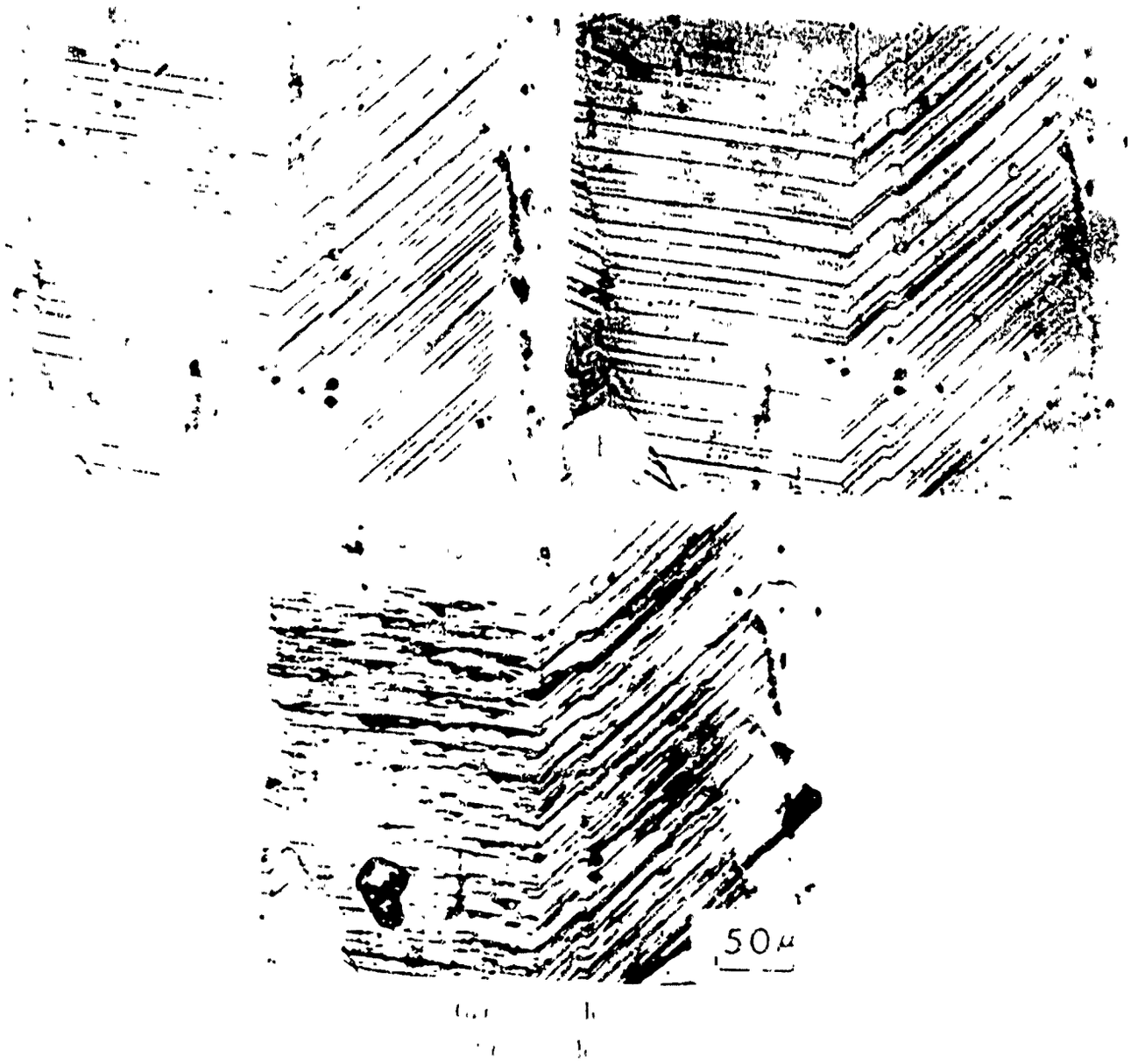

Fig. 15(a) Slip band cracking in a nickel-base superalloy (U-700) at room temperature. (after Wells and Sullivan[48]).

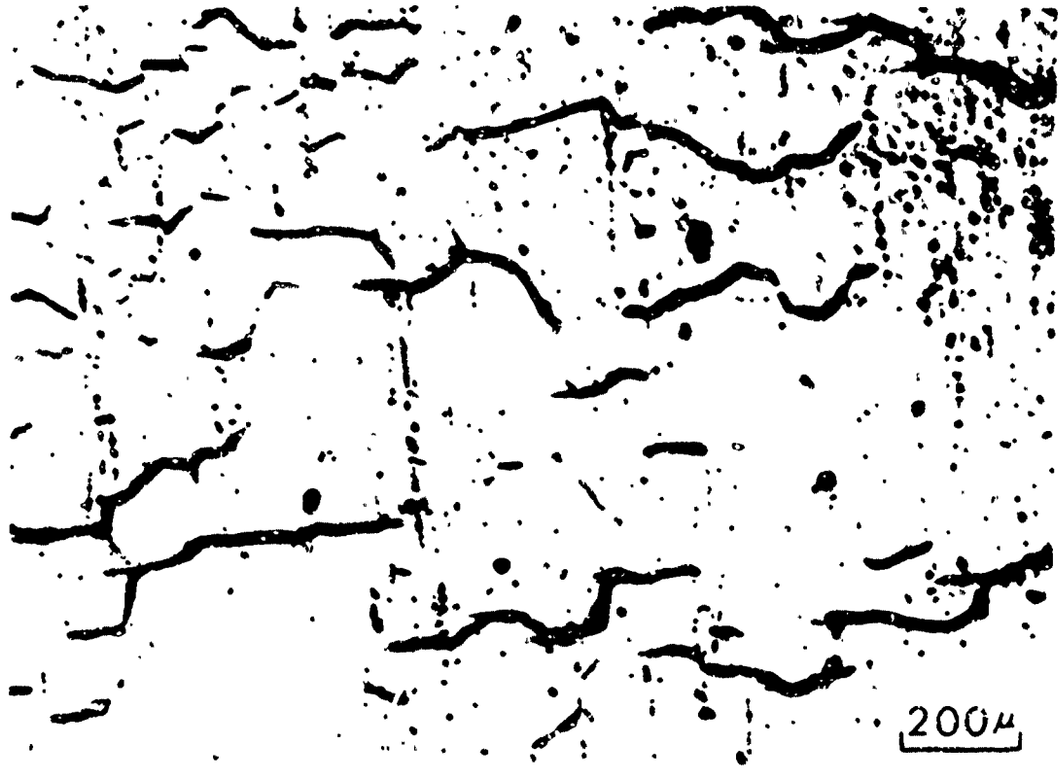

Fig. 15(b) Grain boundary cracking in a nickel-base superalloy (U-700) at 1700°F (after Wells and Sullivan[48]).

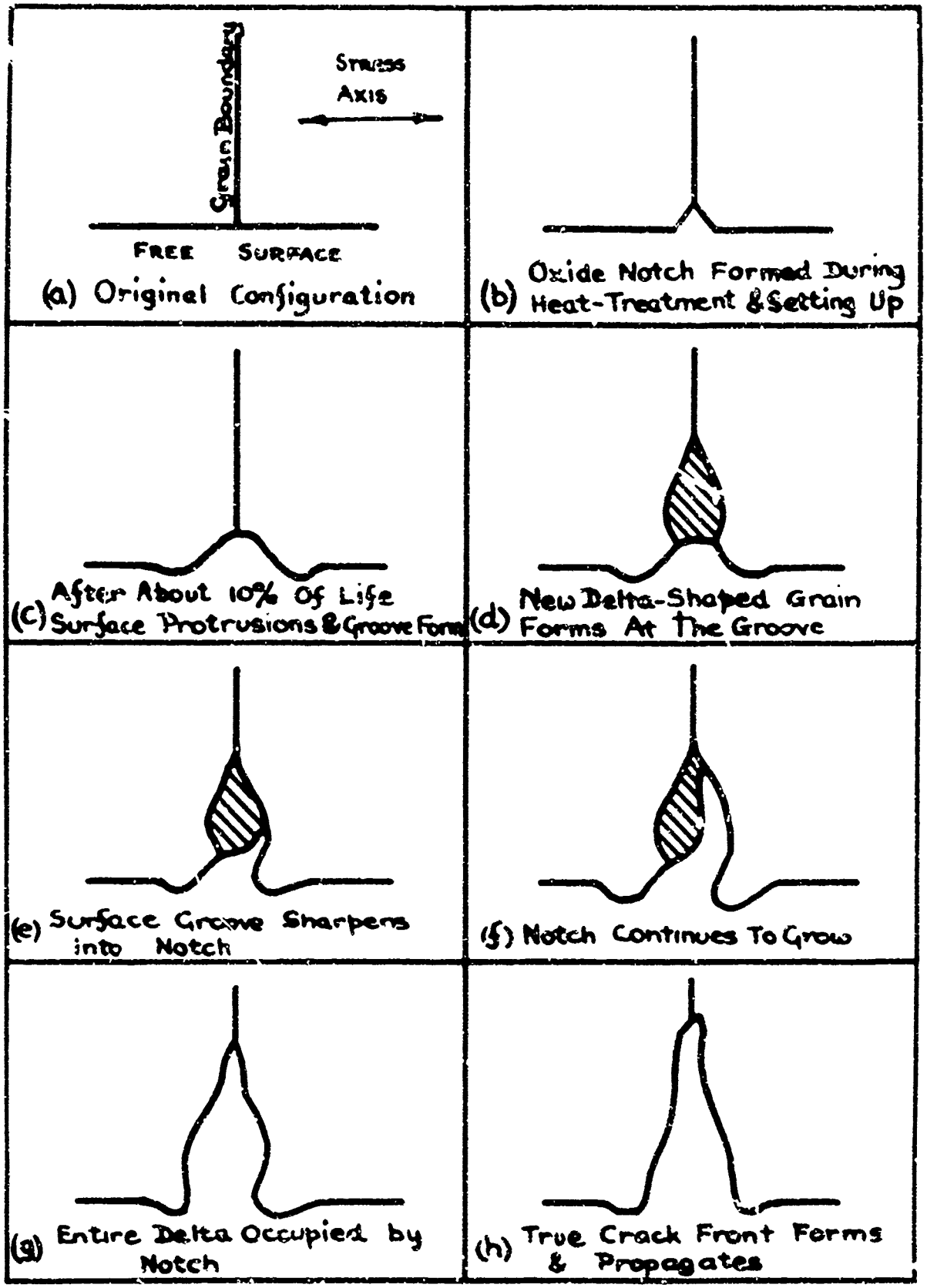

Fig. 16 Model for fatigue crack nucleation in stainless steel at elevated temperatures (after Hodgson[54]).

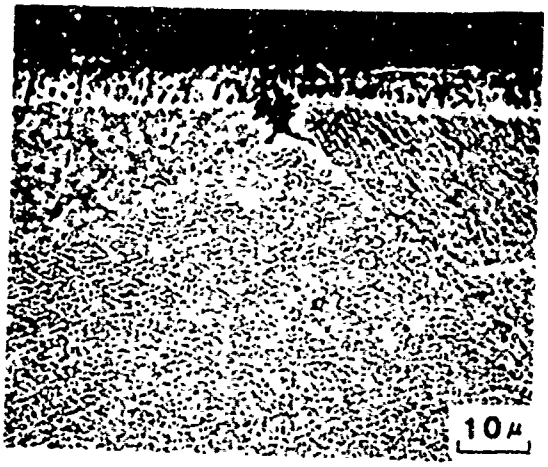

Fig. 17 Oxide in intercrystalline crack in a nickel-base superalloy at elevated temperature (after Gell and Duquette[55]).

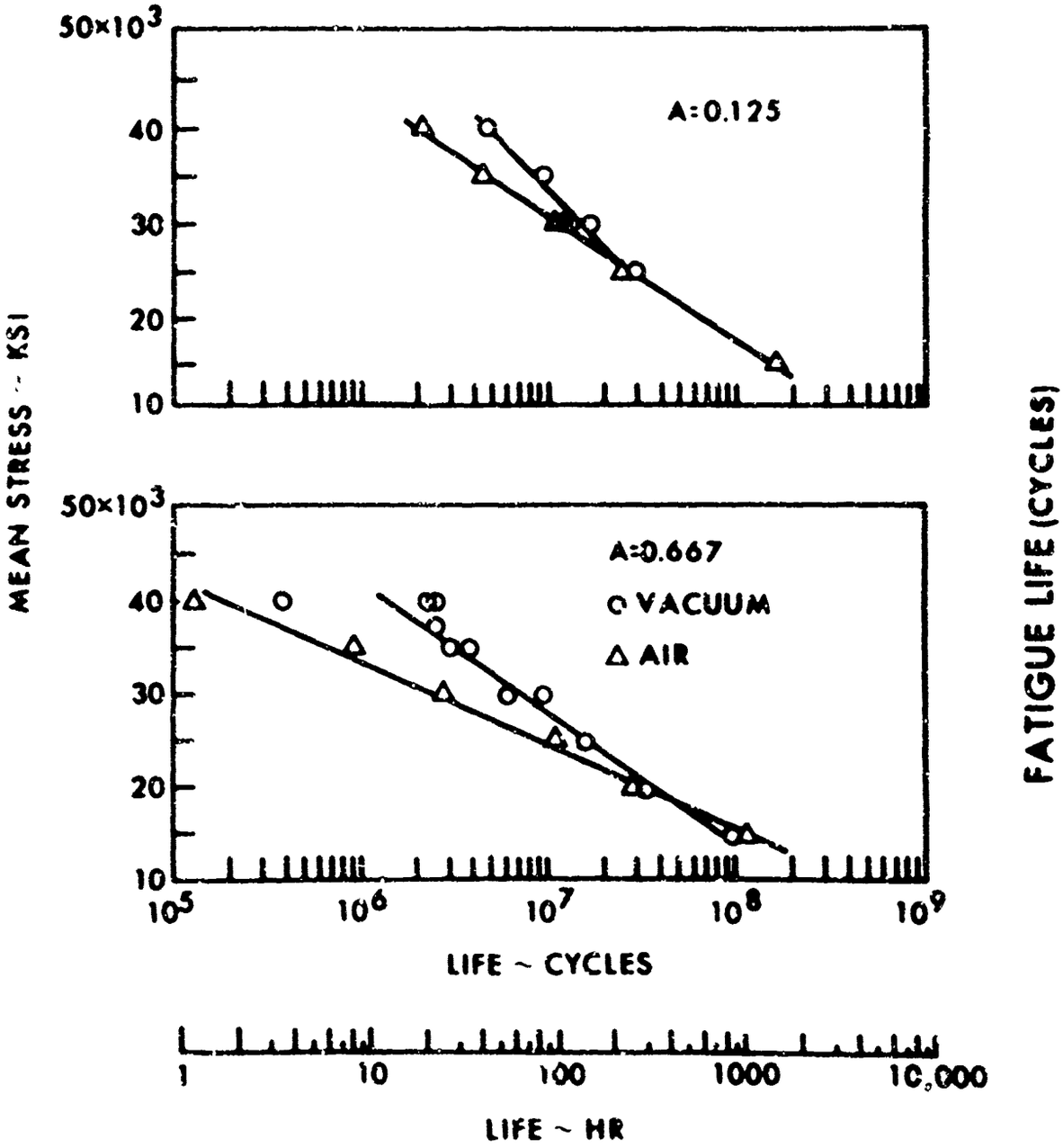

Fig. 18 Effect of vacuum on the fatigue life of polycrystalline nickel at elevated temperatures (after Nachtigall et al.[56]).

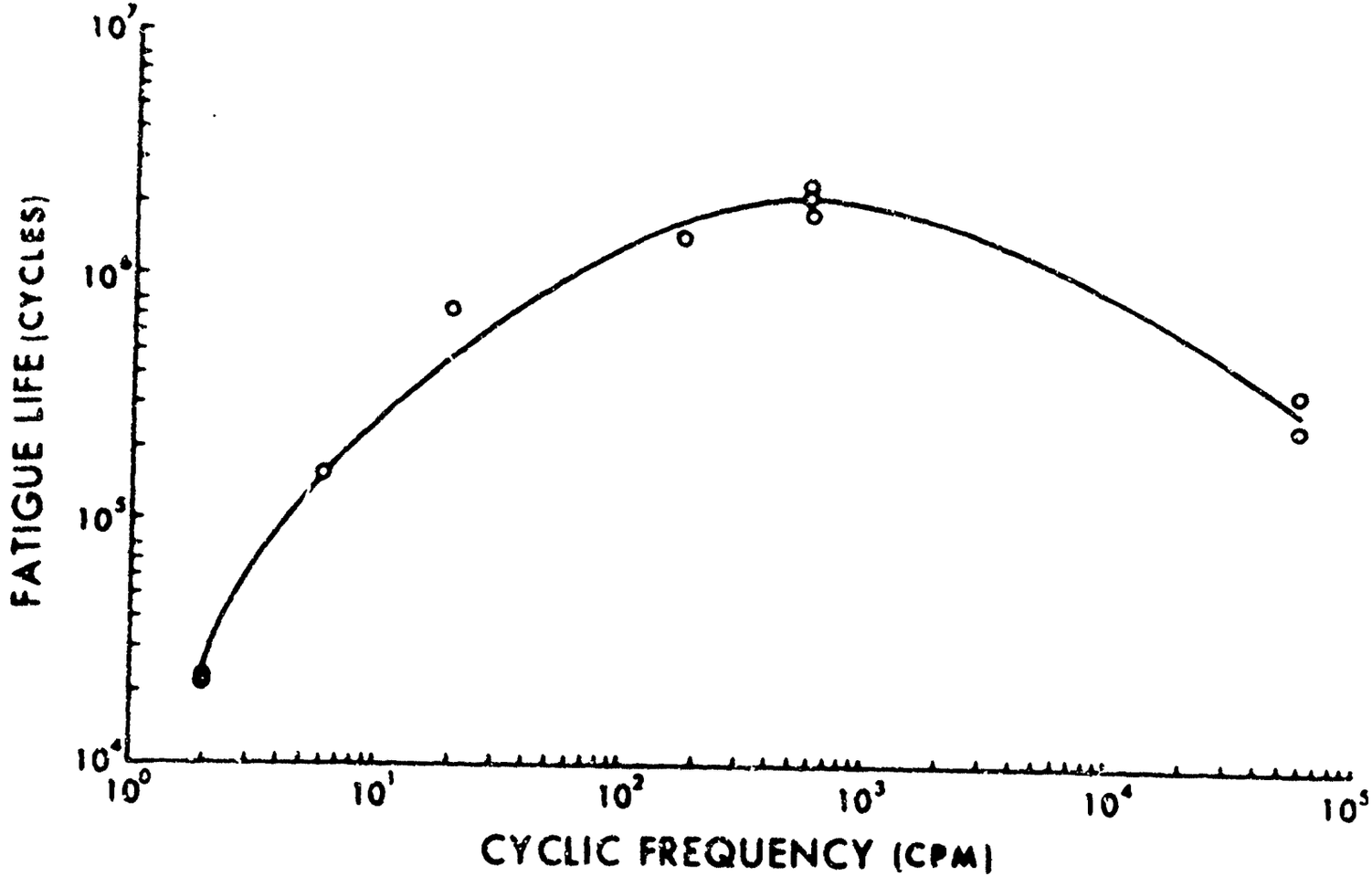

Fig. 19 Effect of frequency on the fatigue life of nickel-base superalloys (after Organ and Gell[59]).

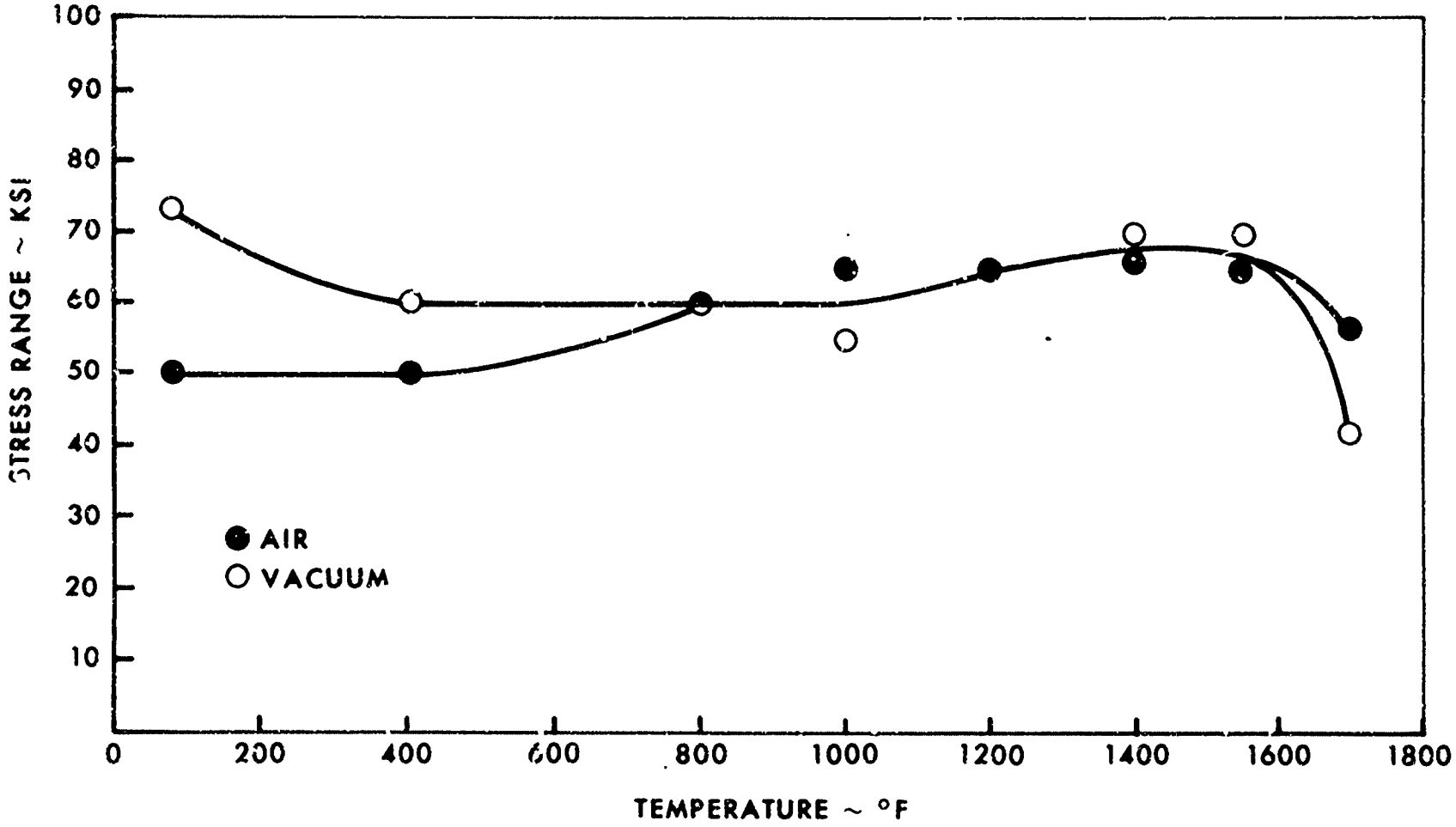

Fig. 20 Endurance limit ($N_f = 10^6$ cycles) of nickel-base superalloy single crystals as a function of temperature (after Duquette and Gell[68]).

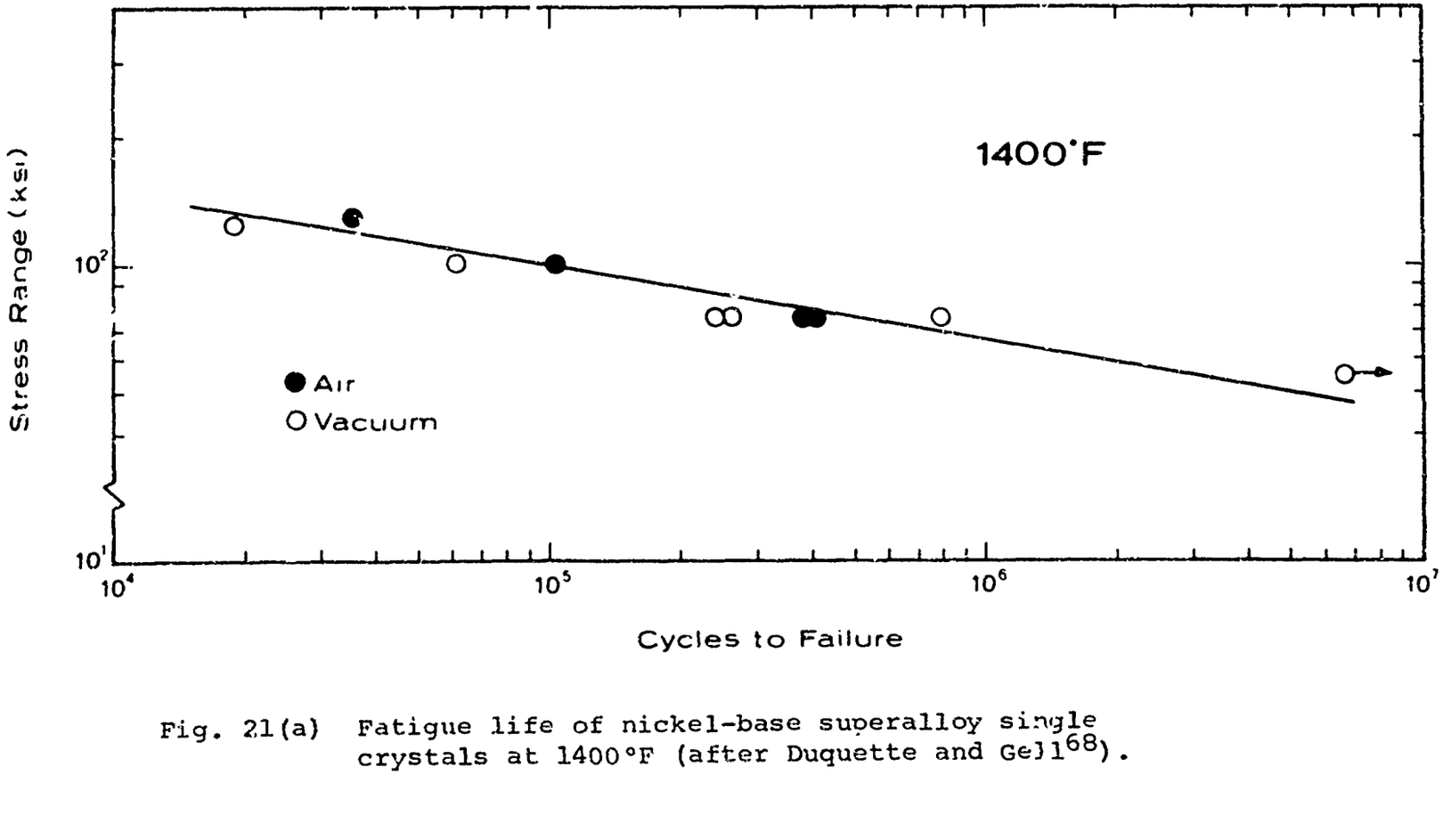

Fig. 21(a) Fatigue life of nickel-base superalloy single crystals at 1400°F (after Duquette and Gell[68]).

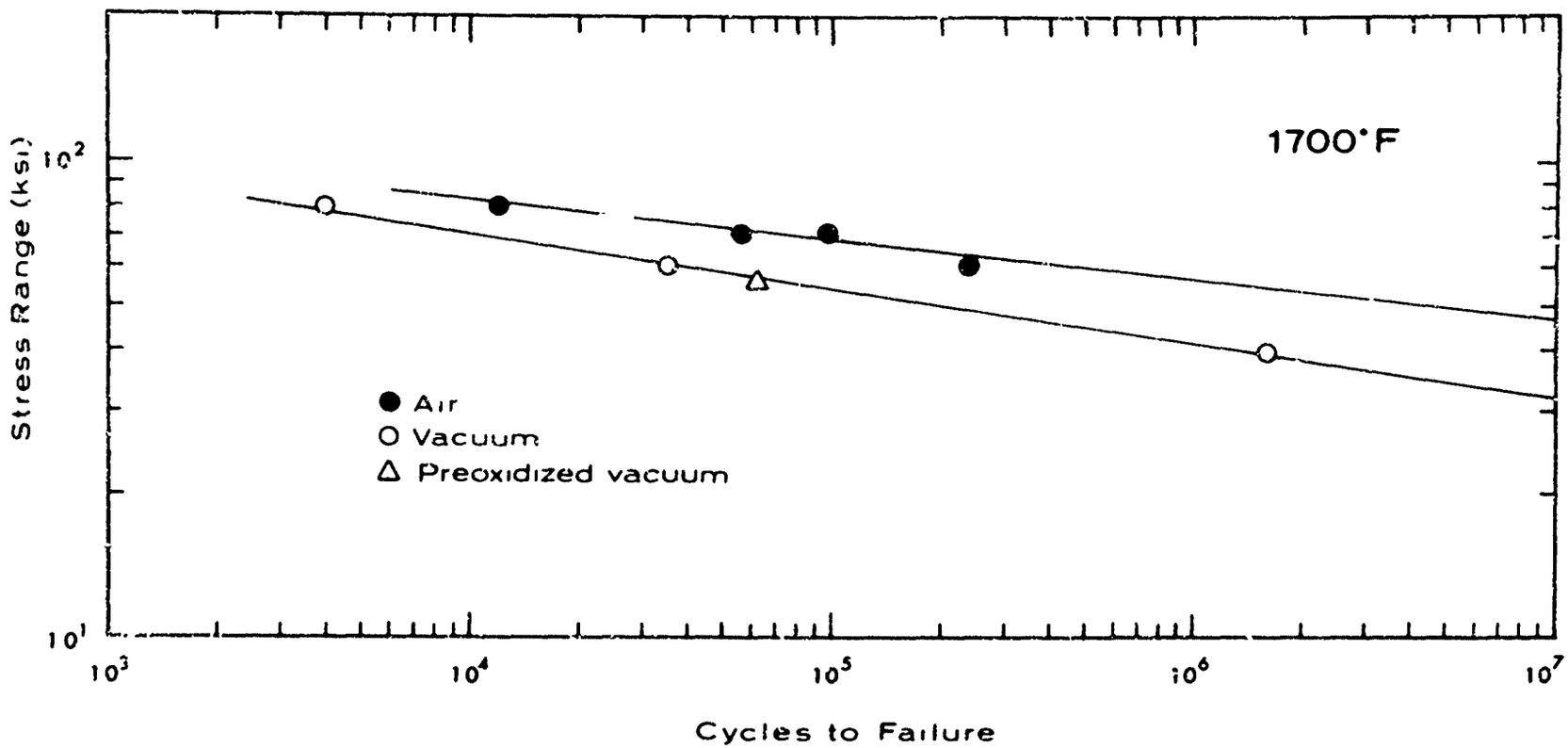

Fig. 21(b) Fatigue life of nickel-base superalloy single crystals at 1700°F (after Duquette and Gell[68]).

a

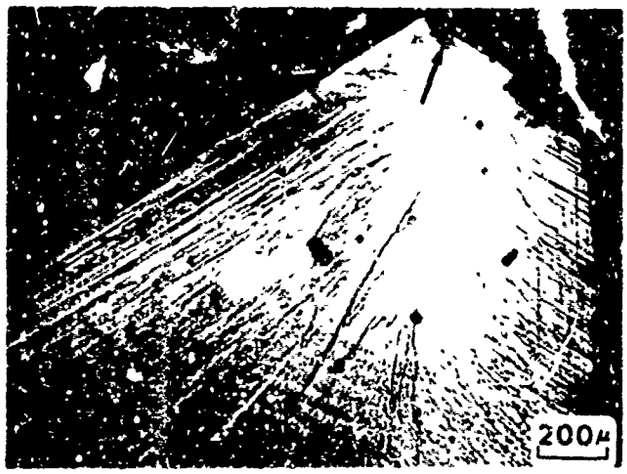

b

Fig. 22 Fatigue fracture surfaces of nickel-base superalloy single crystals in air and in vacuum at 1400°F showing initiation sites (after Duquette and Gell[68]).

Fig. 23 Slip offsets on the surfaces of cylindrical nickel-base superalloy single crystals tensile tested in (a) air and in (b) vacuum (after Duquette and Gell[68]).

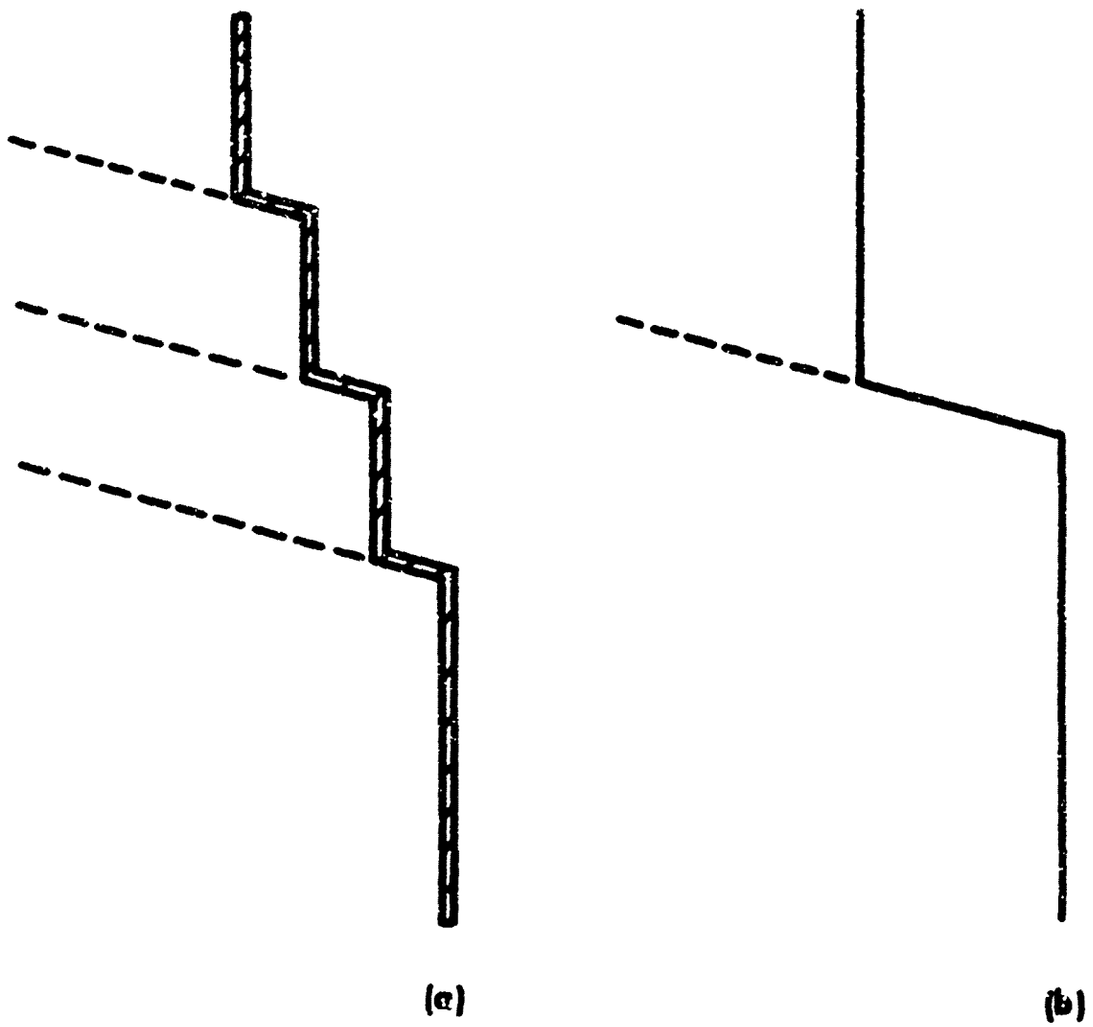

Fig. 24 Model to explain the effect of oxide layer on emerging slip steps in air on the slip behavior ofnickel-base superalloy single crystals (after Duquette and Gell[68]).

Fig. 25 Fatigue fracture surfaces of single crystal nickel-base superalloys in (a) air and in (b) vacuum at 1700°F showing initiation sites (after Duquette and Gell[68]).

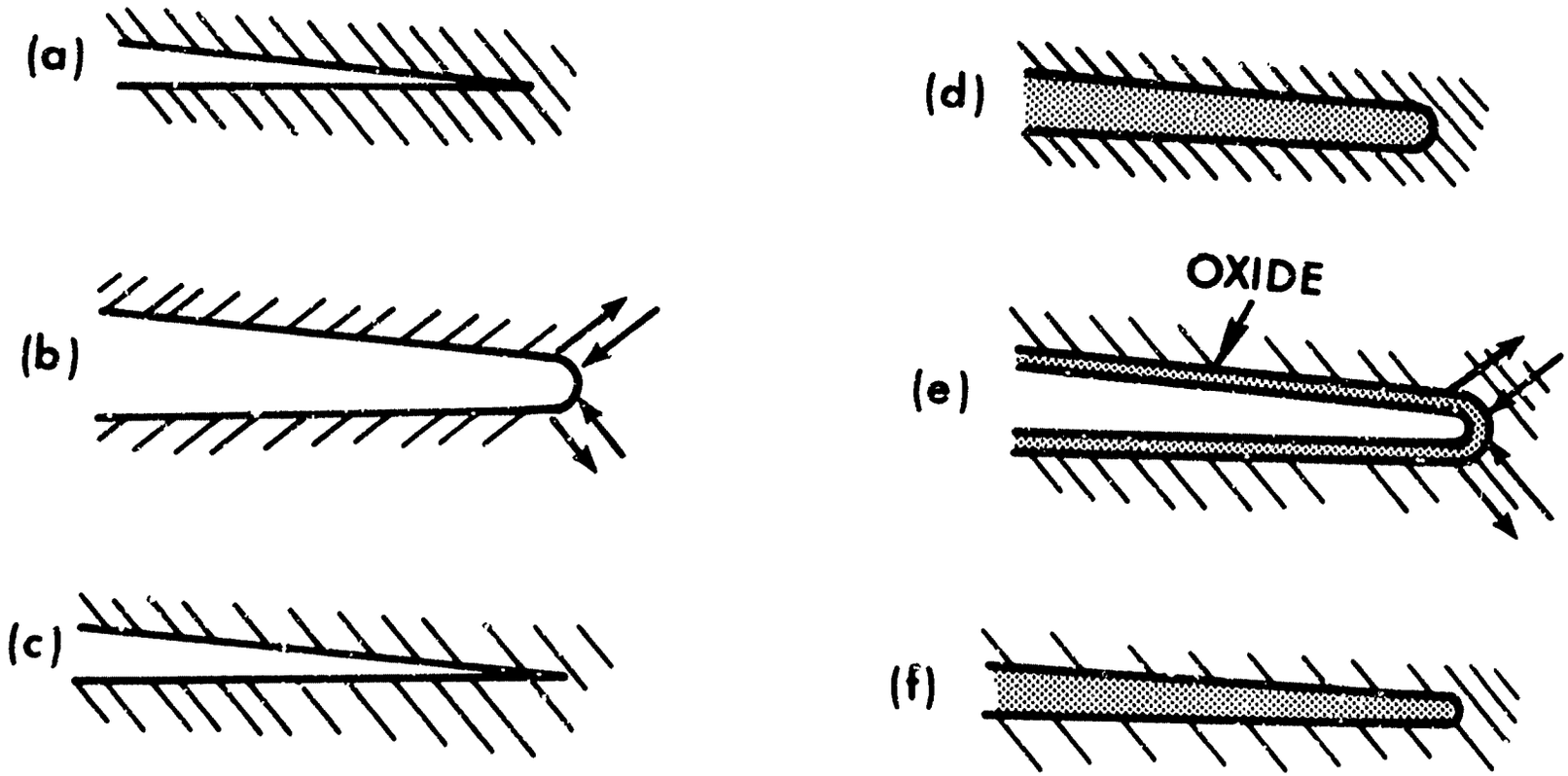

Fig. 26 Model showing effect of oxide blunting of Stage II fatigue crack in nickel-base superalloys at 1700°F (after Duquette and Gell[68]).

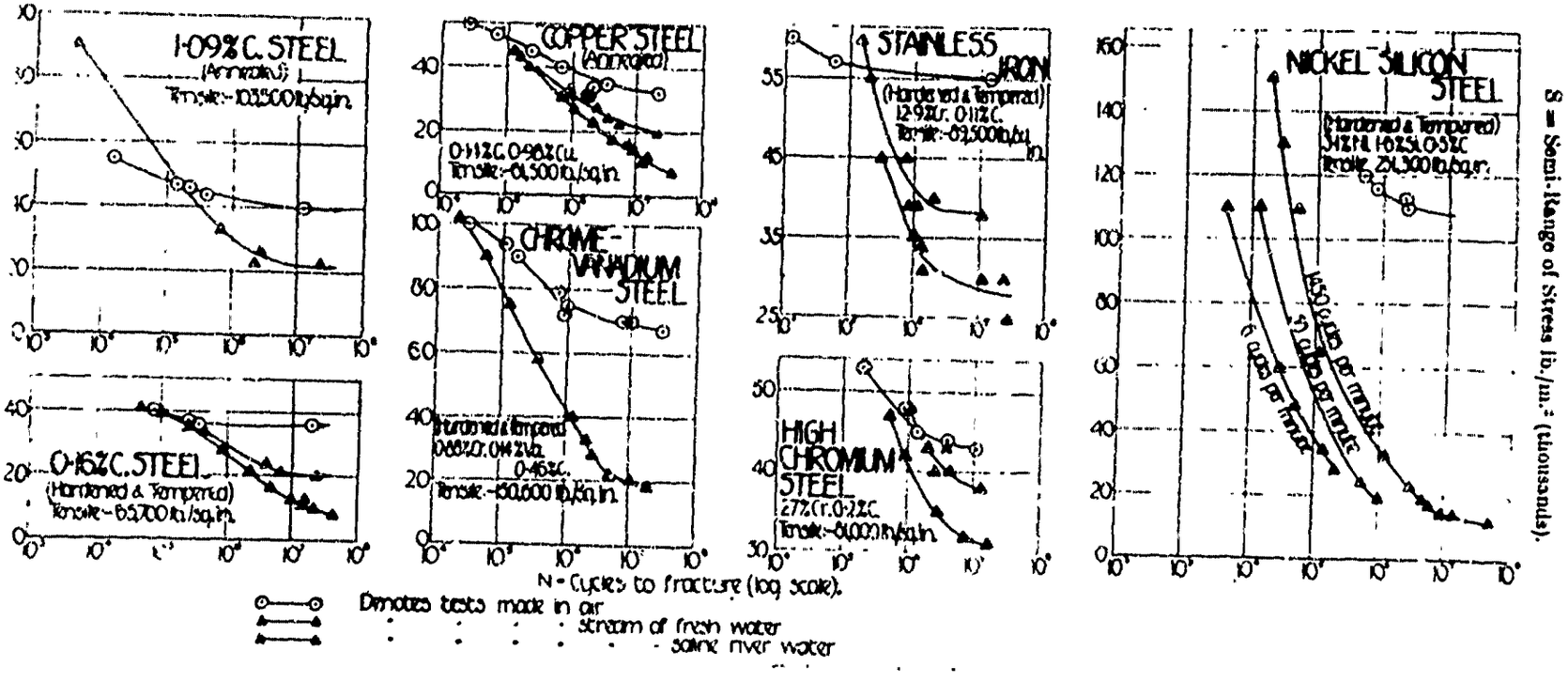

Fig. 27 Typical corrosion fatigue S-N curves for steels - air, fresh water and saline water (after McAdam[78]).

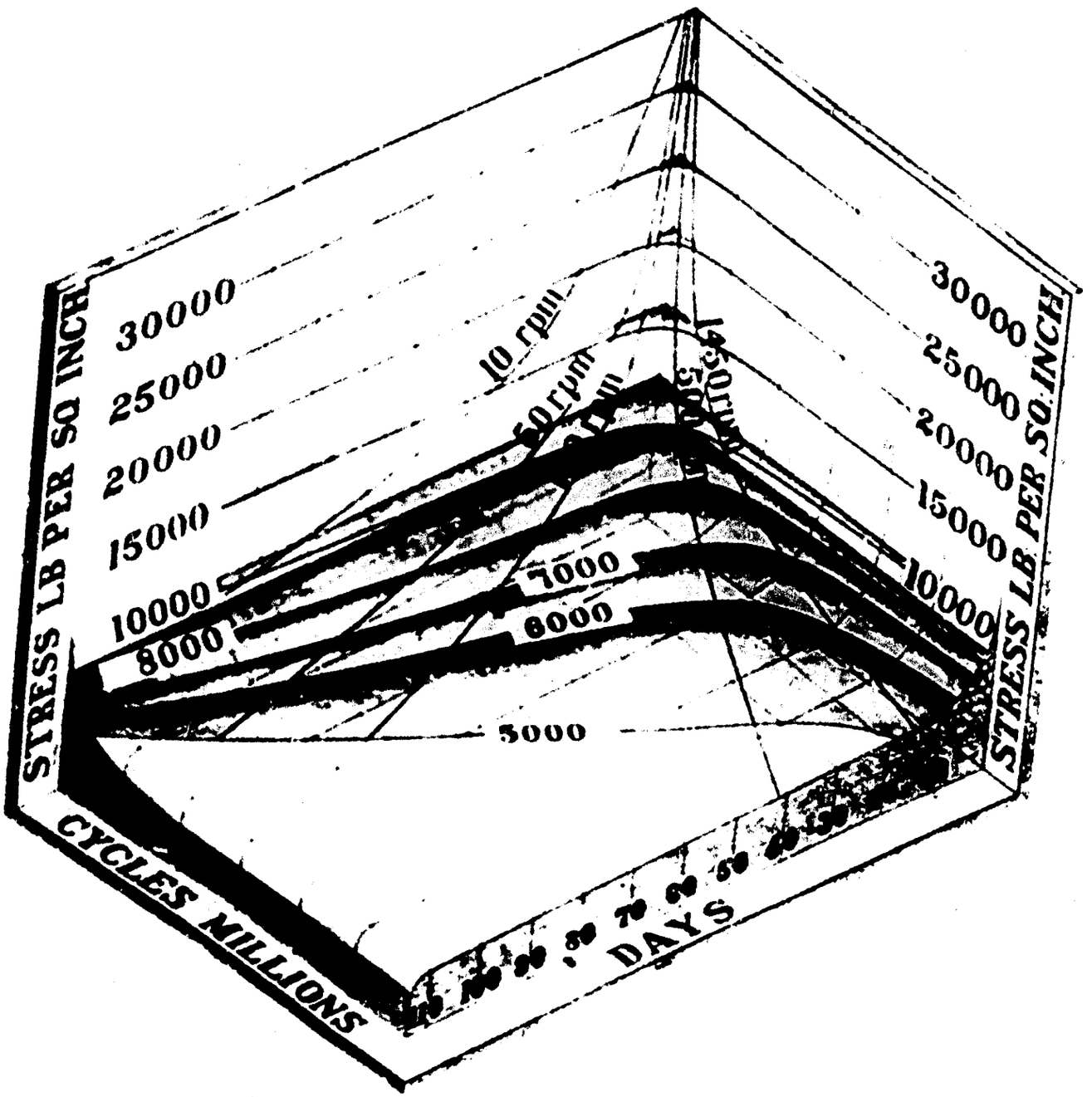

Fig. 24 Three dimensional plot showing corrosion fatigue behavior of 3.7% Nickel steel in carbonate water (after McAdam[79]).

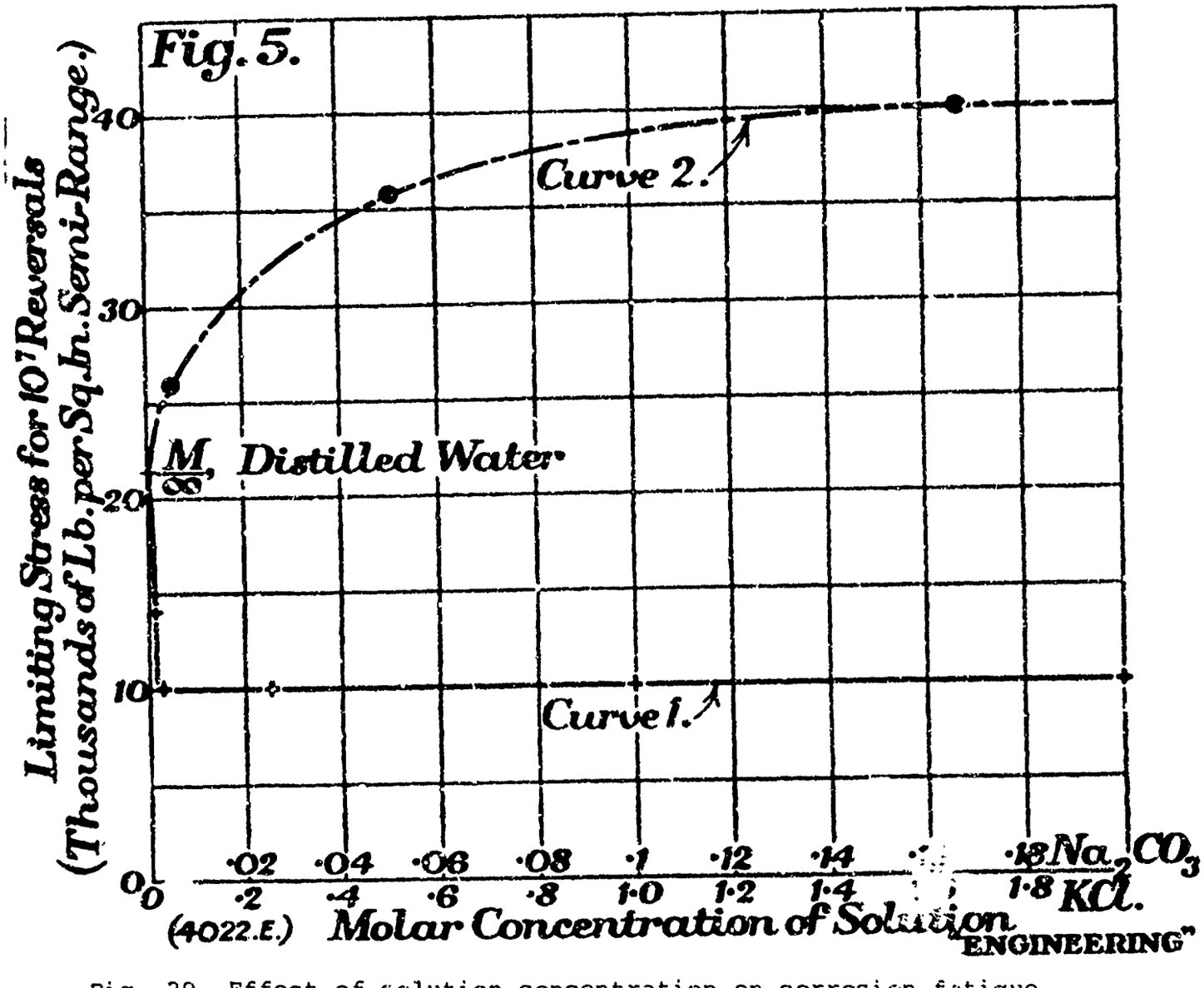

Fig. 29 Effect of solution concentration on corrosion fatigue behavior of low carbon steel in KCl solution (curve 2) curve 1 refers to fatigue behavior of steel in distilled water + Na_2CO_3 (after Gould[81]).

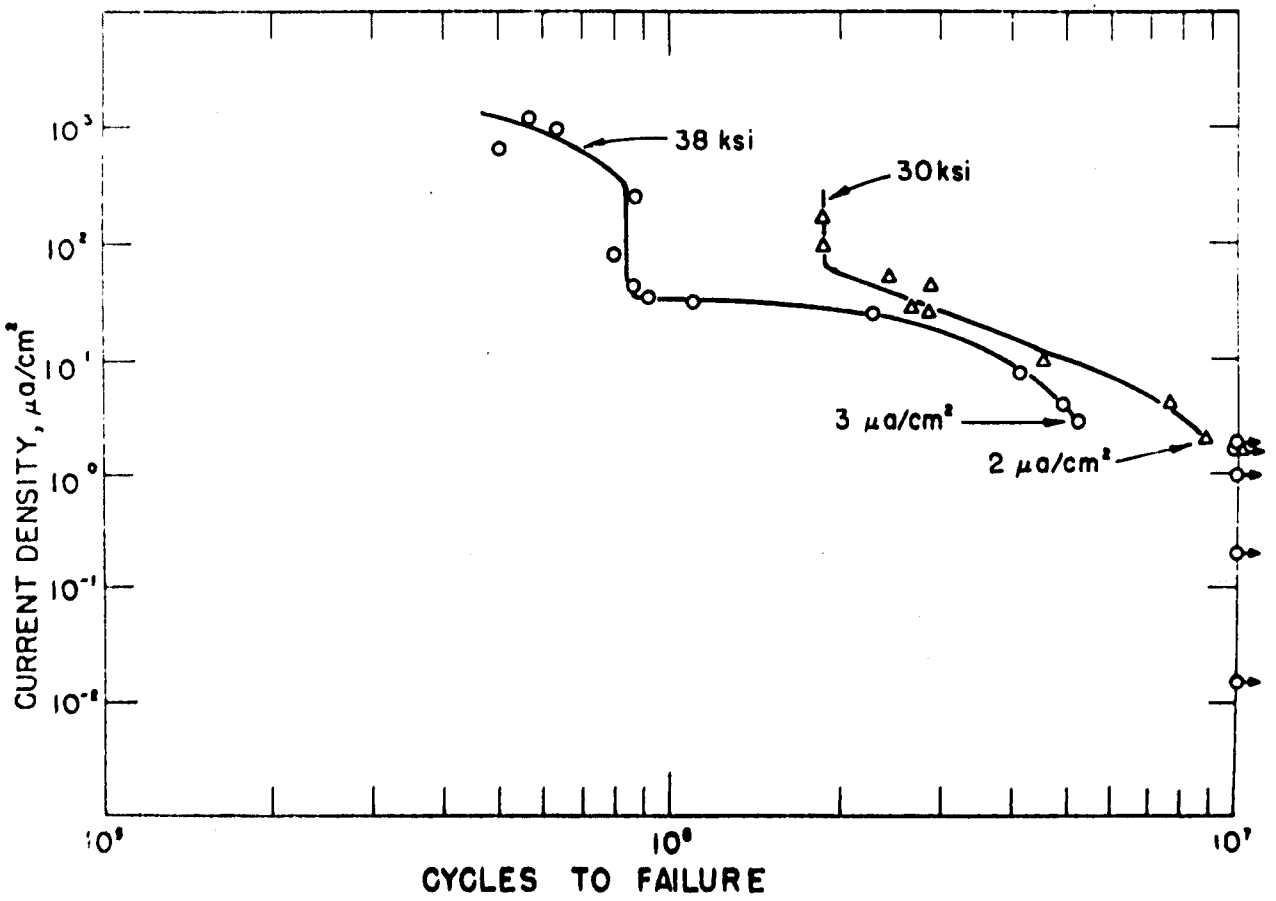

Fig. 30 Effect of applied anodic current on the fatigue behavior of low carbon steel in deaerated 3% NaCl solution (after Duquette and Uhlig[84]).

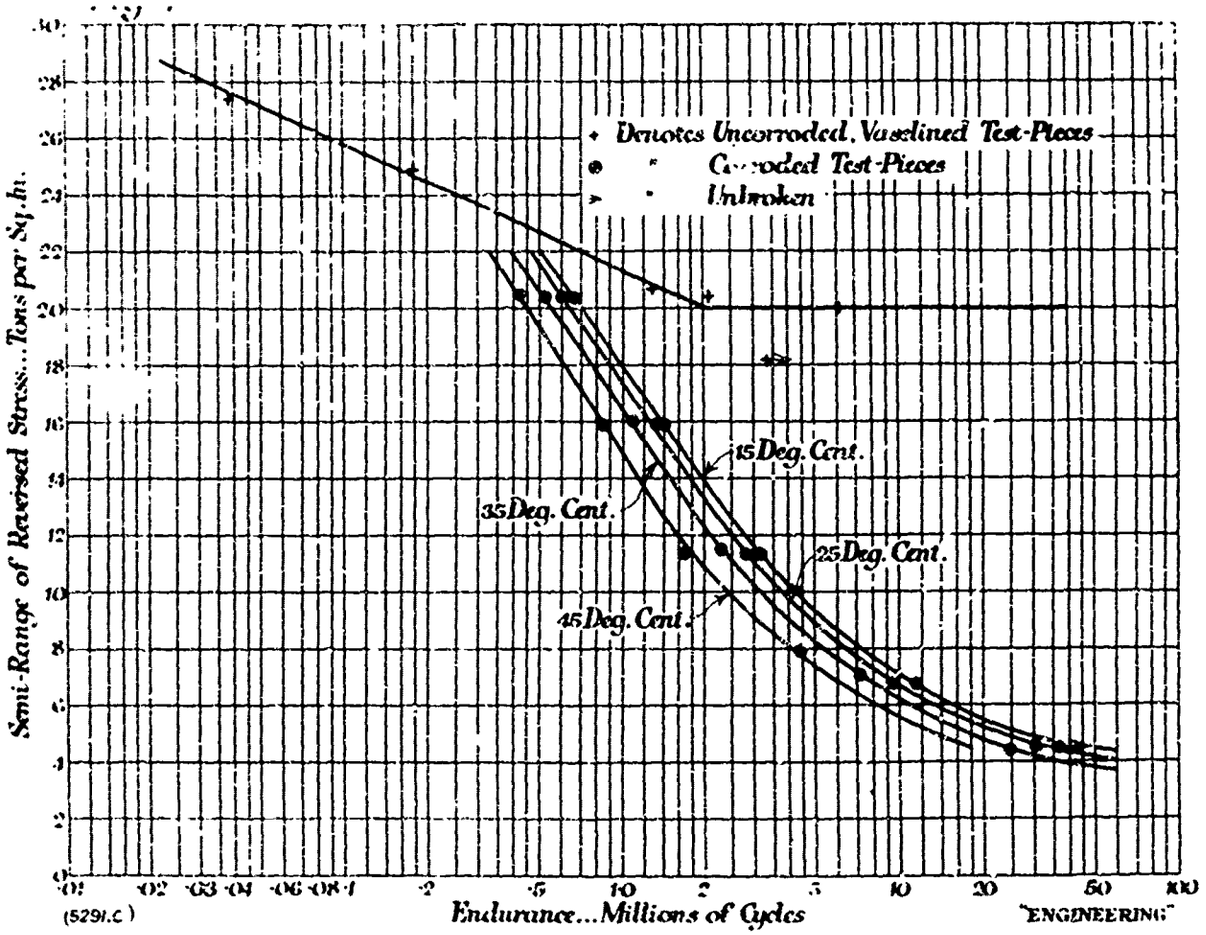

Fig. 31 Effect of solution temperature on the fatigue behavior of mild steel in artificial sea water (after Gould[82]).

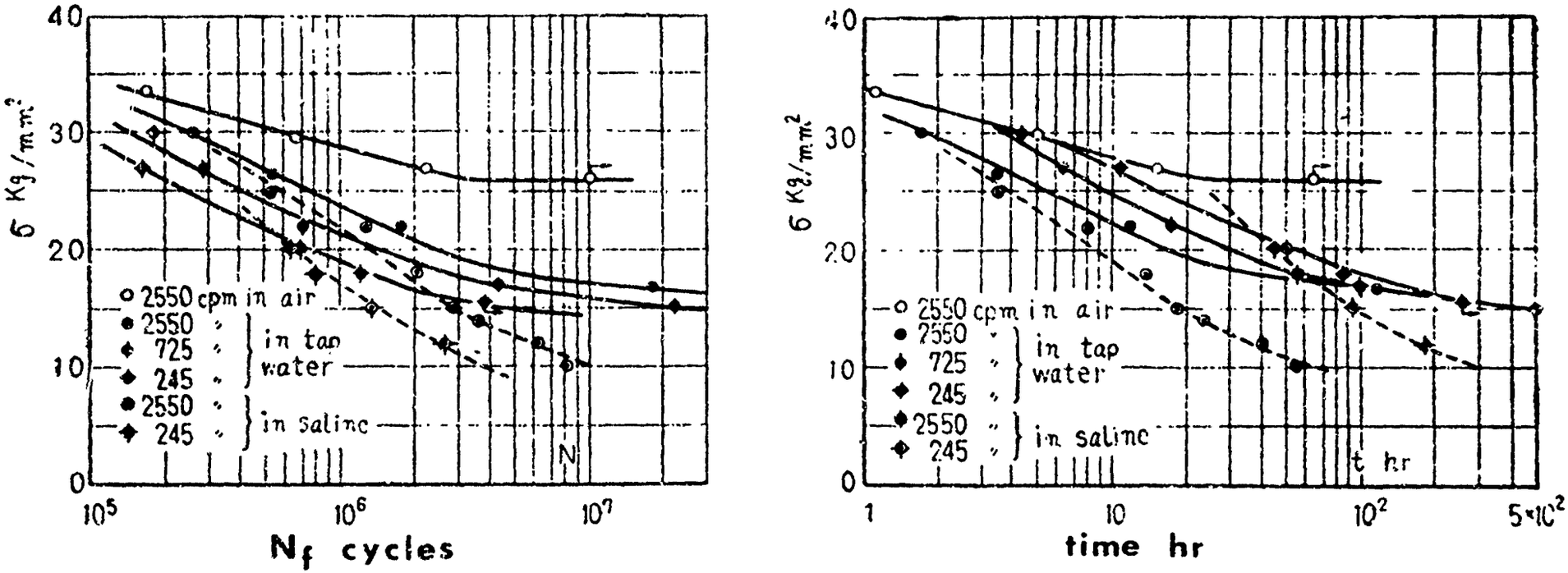

Fig. 32 Effect of frequency (time of exposure) on the fatigue behavior of mild steel in air, in tap water and in saline solution (after Endo and Miyas[87]).

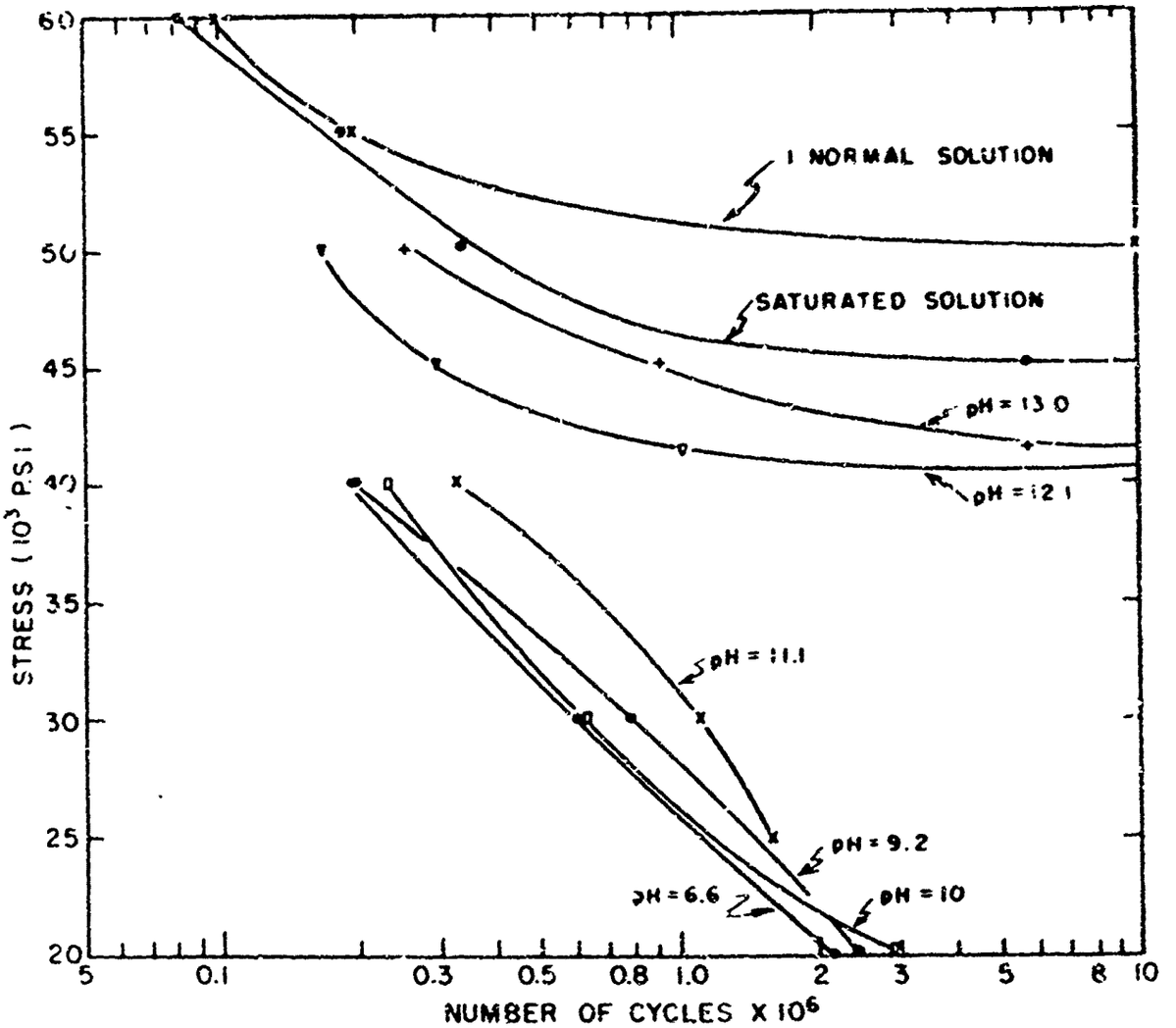

Fig. 33 Effect of solution pH on the fatigue behavior of mild steel in 3.5% NaCl solutions (after Radd et al.[93]).

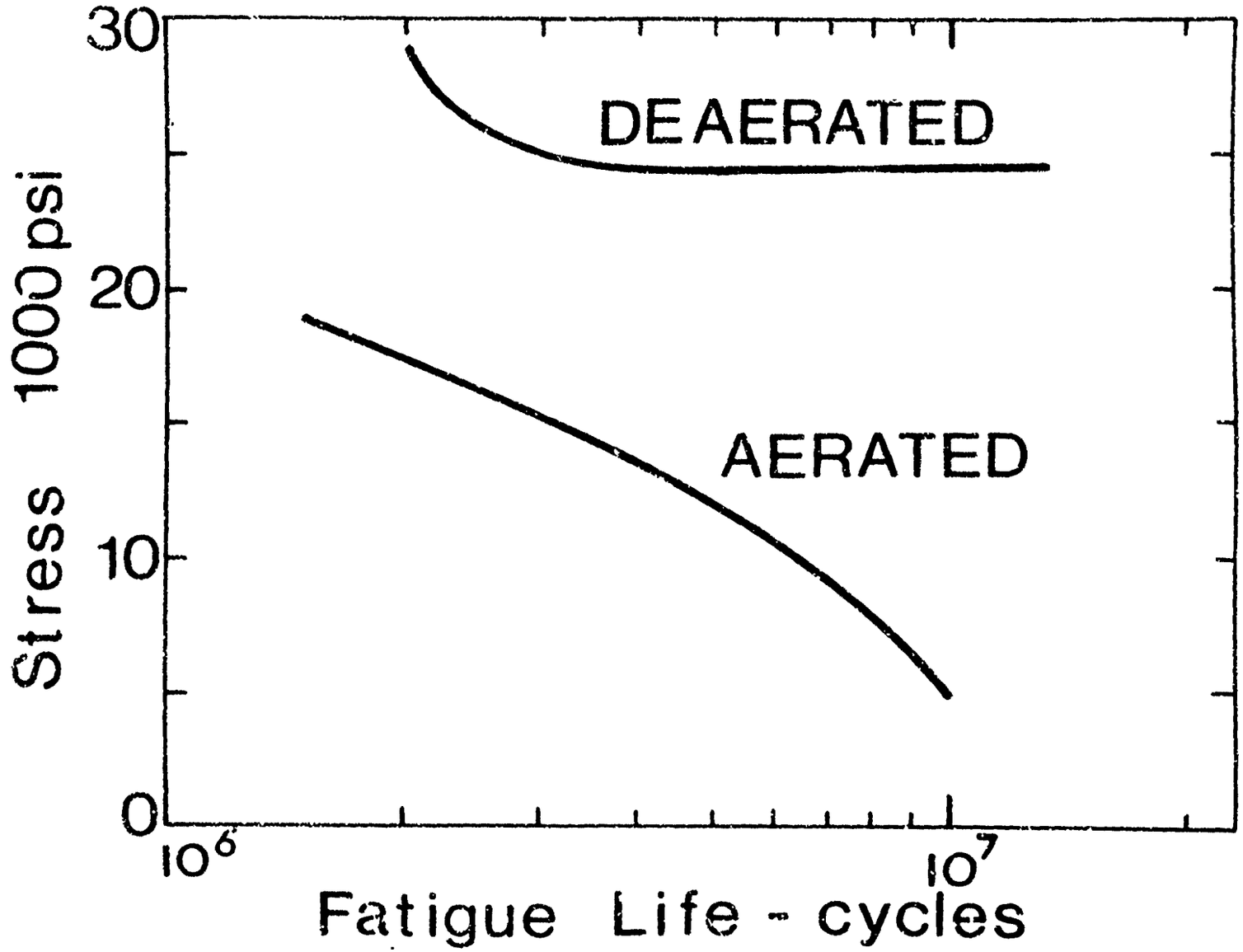

Fig. 34 Effect of dissolved O_2 on the fatigue behavior of 1035 steel in 5% NaCl solutions (after Mehdizadeh et al.[102]).

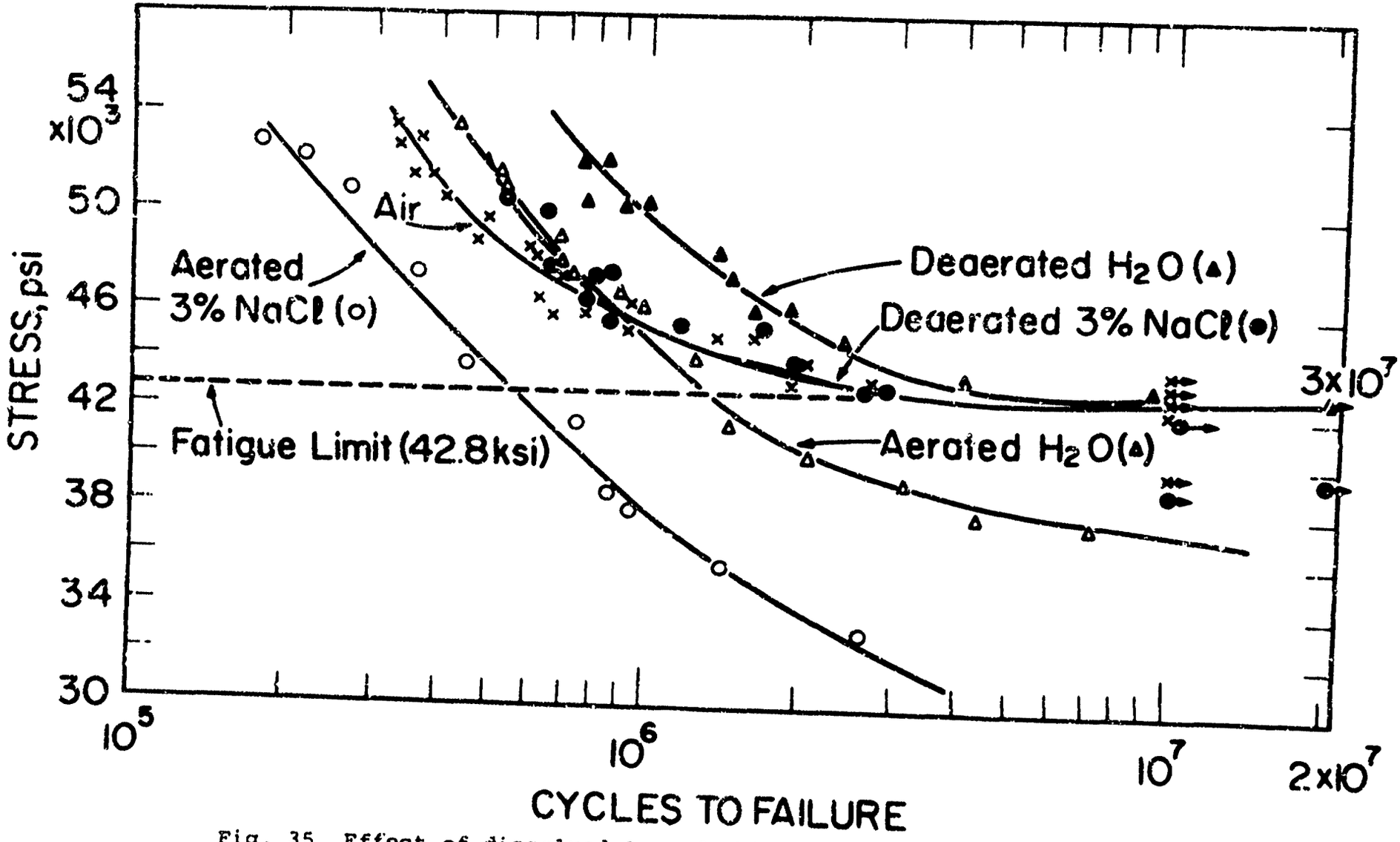

Fig. 35 Effect of dissolved O_2 and chloride ion on the fatigue behavior of low carbon steel in distilled water and 3% NaCl solutions (after Duquette and Uhlig[103]).

Fig. 3. Fracture surface of 2024 aluminum alloy in sea water. The orientation of the fracture plane is changing with anodic-cathodic current reversals (after Pelloux[123]).

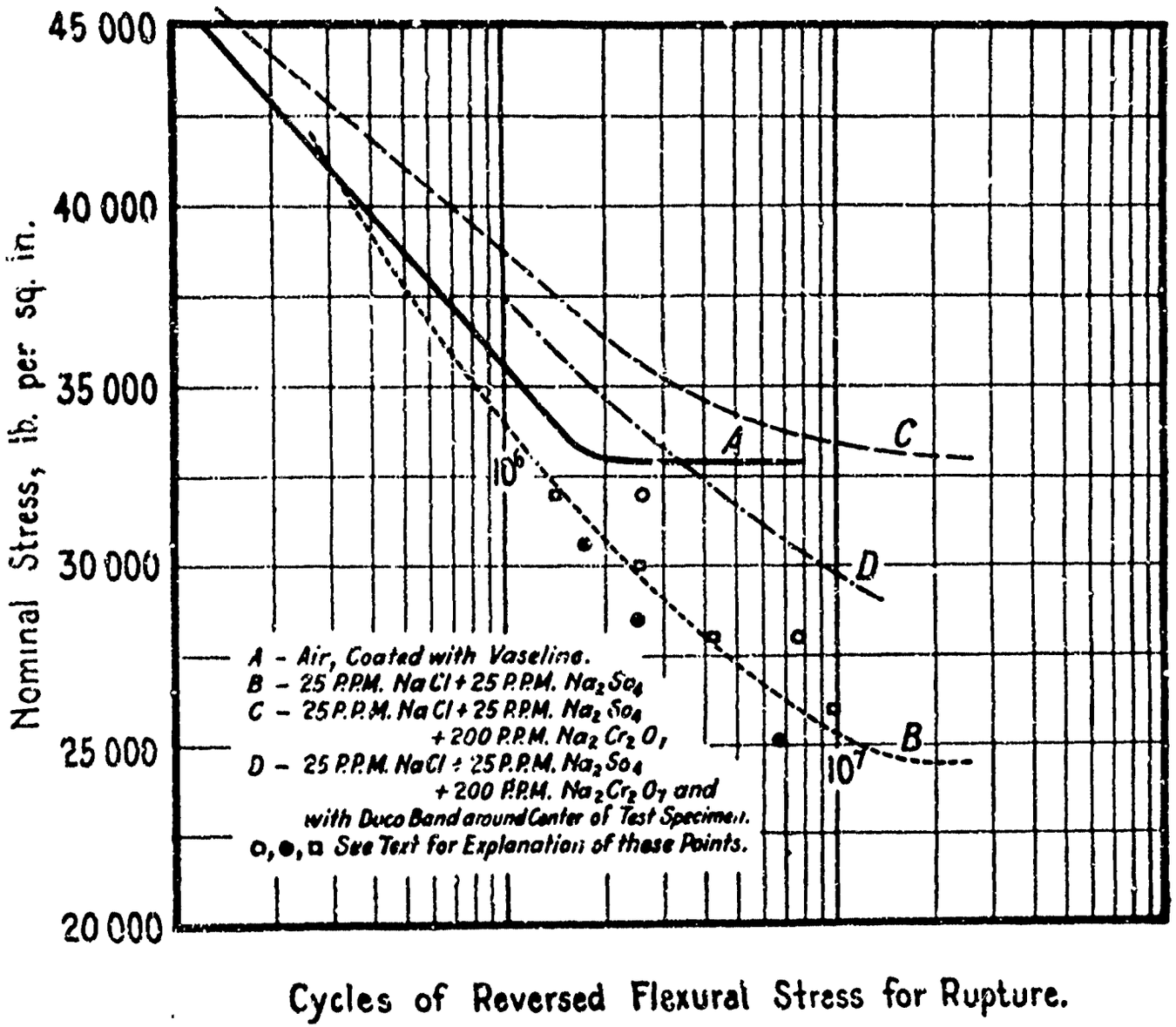

Fig. 37 Effect of Na_2SO_4 and $Na_2Cr_2O_7$ additions on the fatigue behavior of mild steel in NaCl solutions (after Speller et al.[138]).

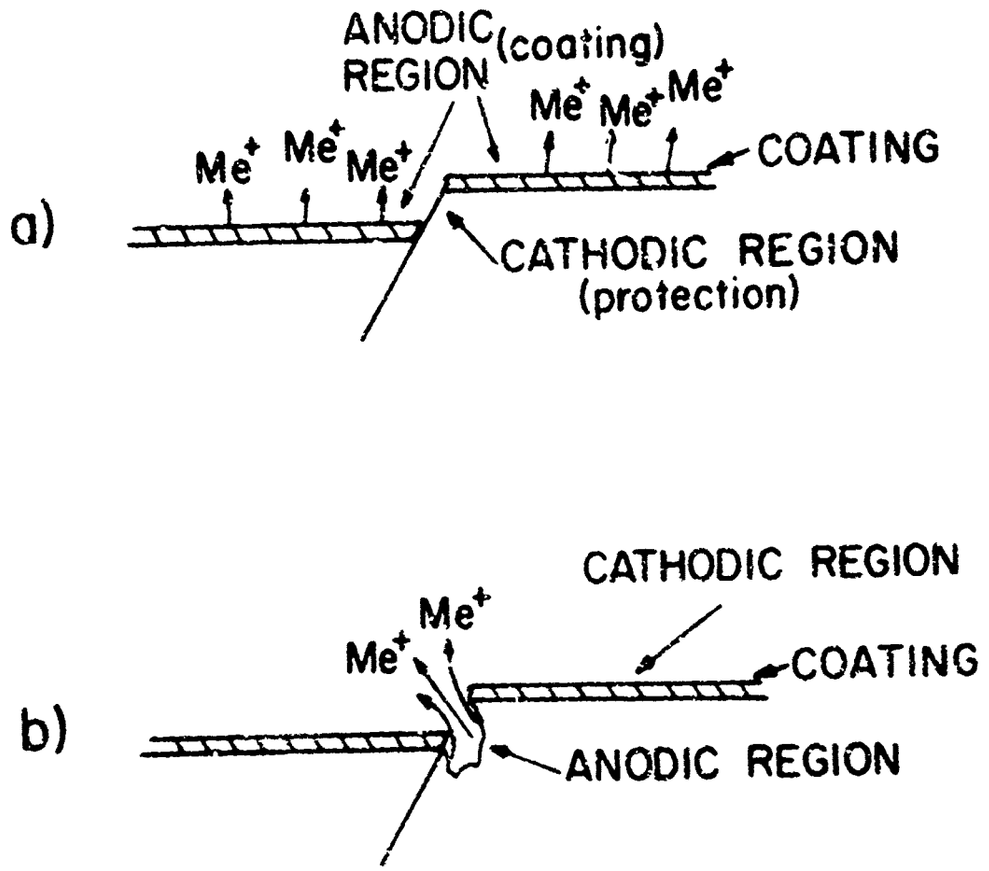

Fig. 38 Schematic diagram of effect of coating breaks on corrosion behavior of emerging slip bands by cyclic deformation in corrosive environments, (a) cathodic coatings, (b) anodic coatings.

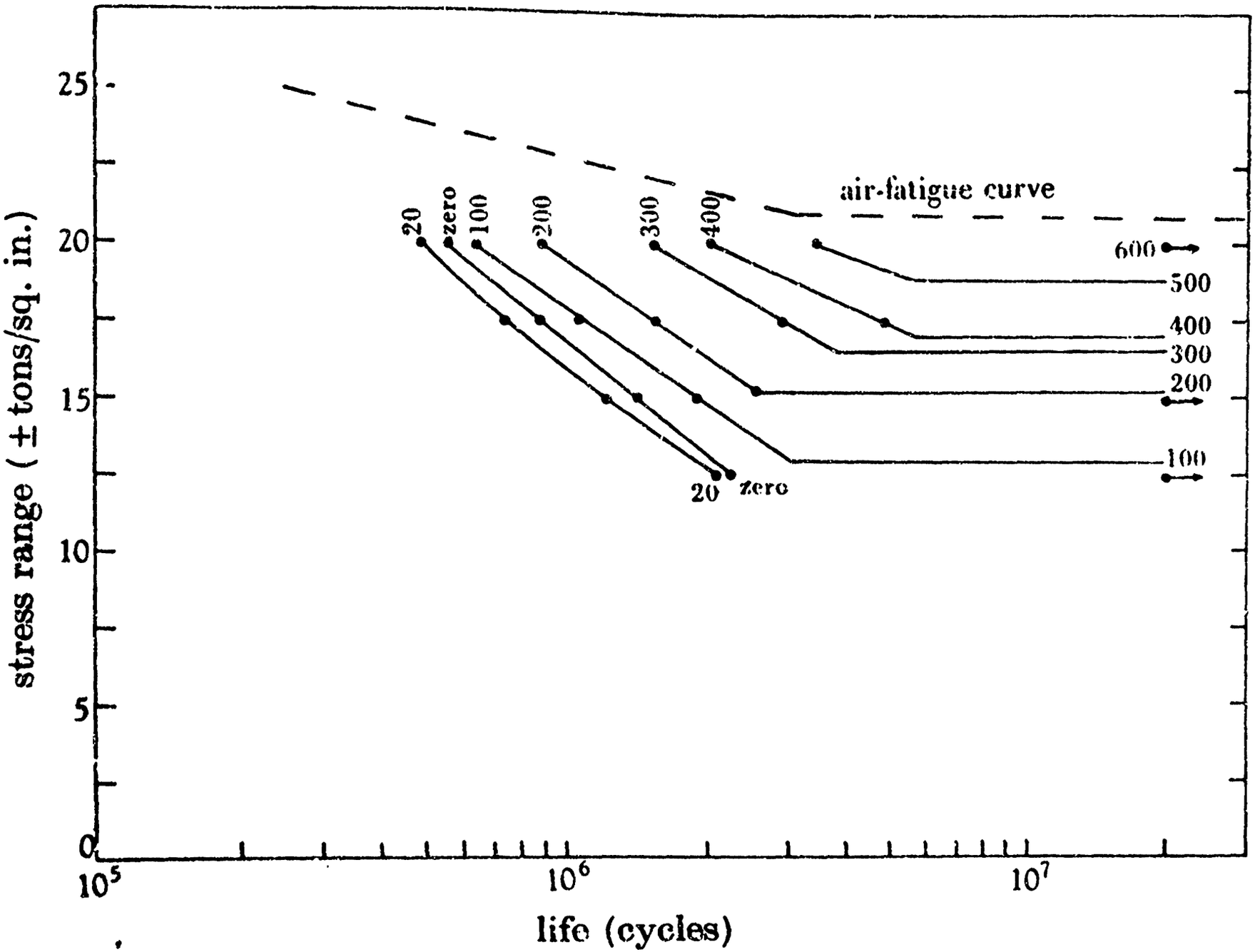

Fig. 39 Effect of applied cathodic current on fatigue behavior of mild steel in KCl solutions (after Simnad and Evans[168]).

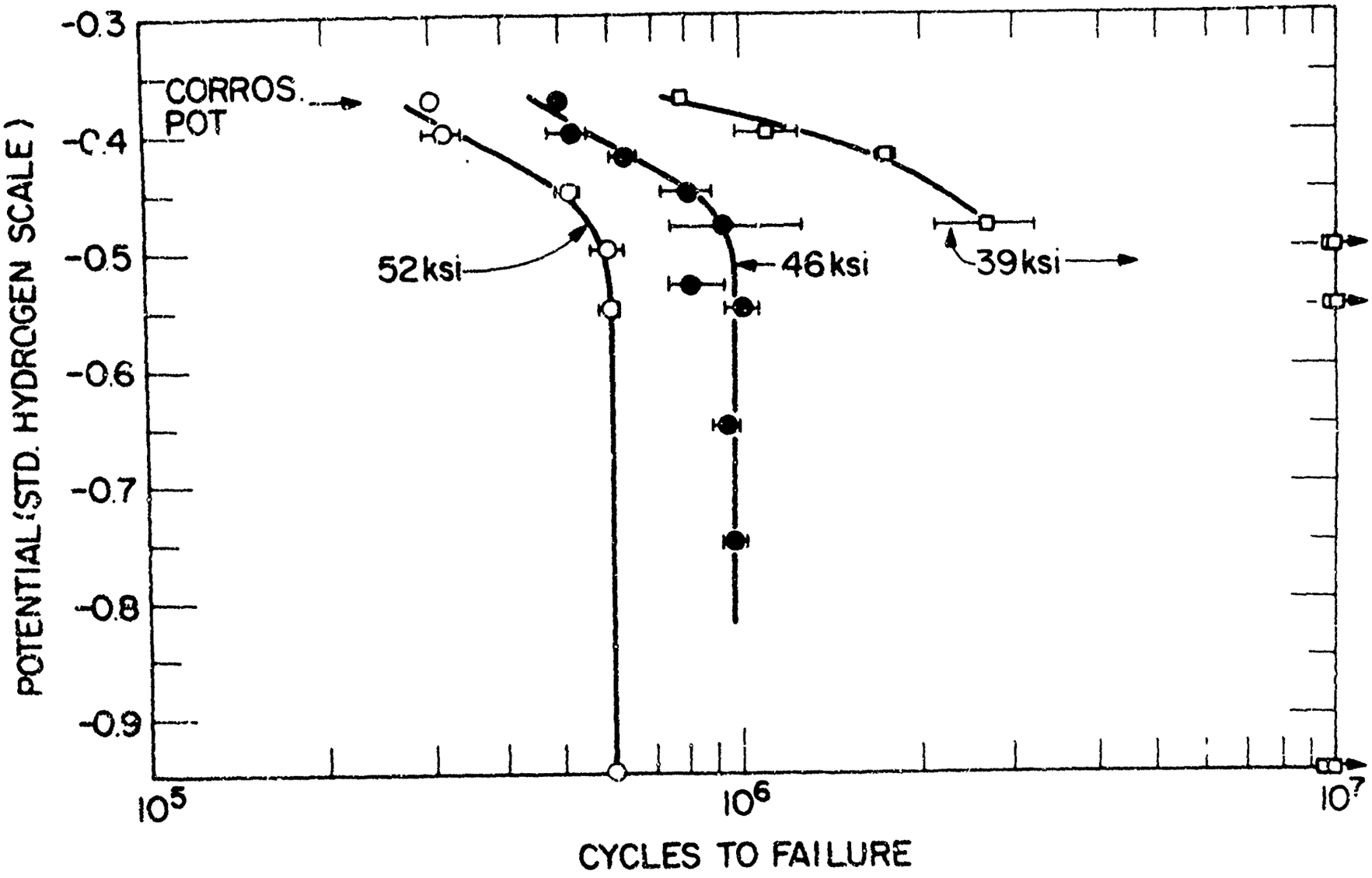

Fig. 40 Effect of applied cathodic potentials on the fatigue behavior of low carbon steels in neutral 3% NaCl solutions (after Duquette and Uhlig[103]).

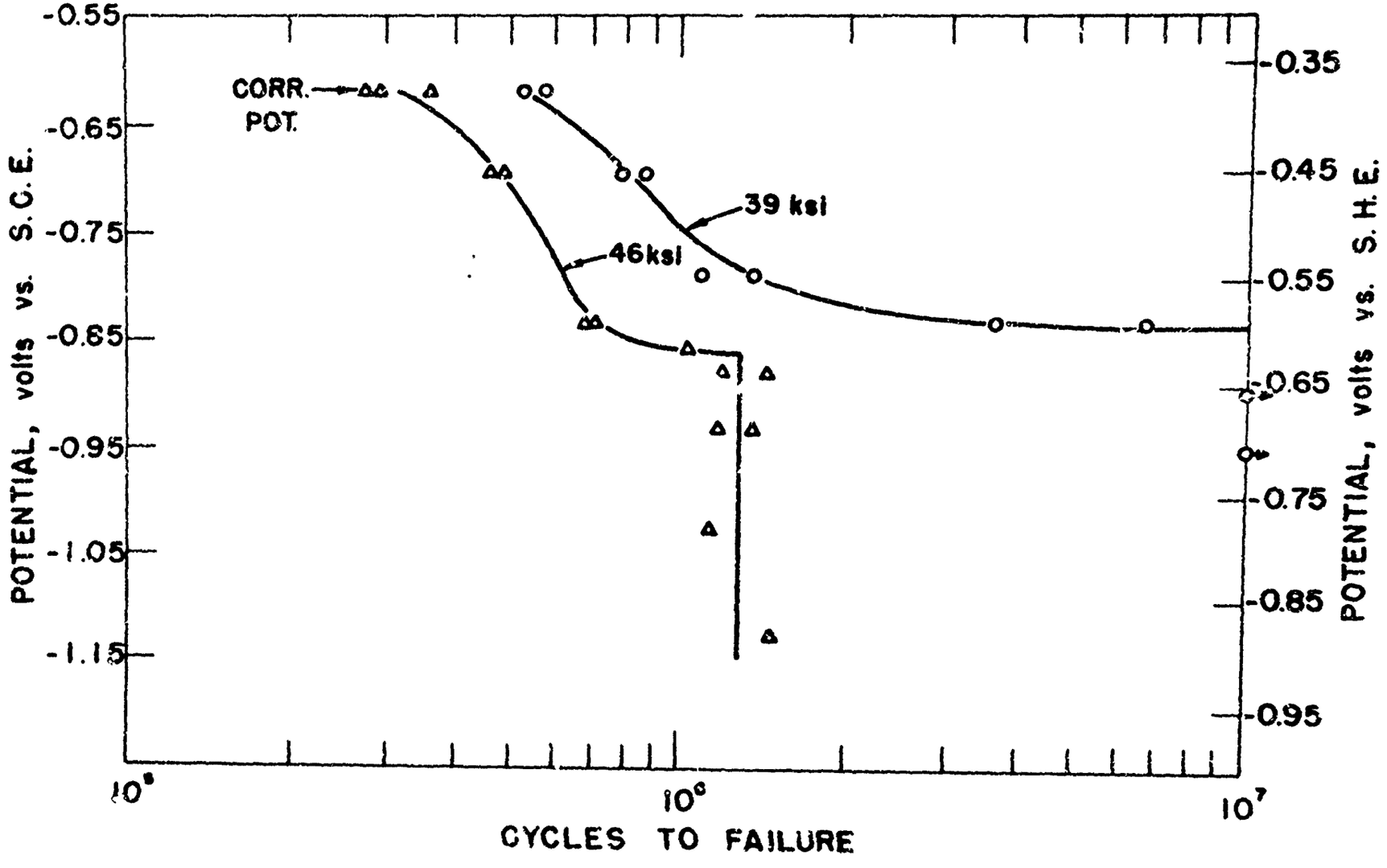

Fig. 41 Effect of applied cathodic potentials on the fatigue behavior of low carbon steels in 0.5 N Na_2SO_4 + H_2SO_4 solutions, pH 3 (after Duquette and Uhlig[84]).

Fig. 42 Surface of low carbon steel cyclically deformed in 3% NaCl to 4% of total life showing crystallographic pitting (after Duquette and Uhlig[103]).

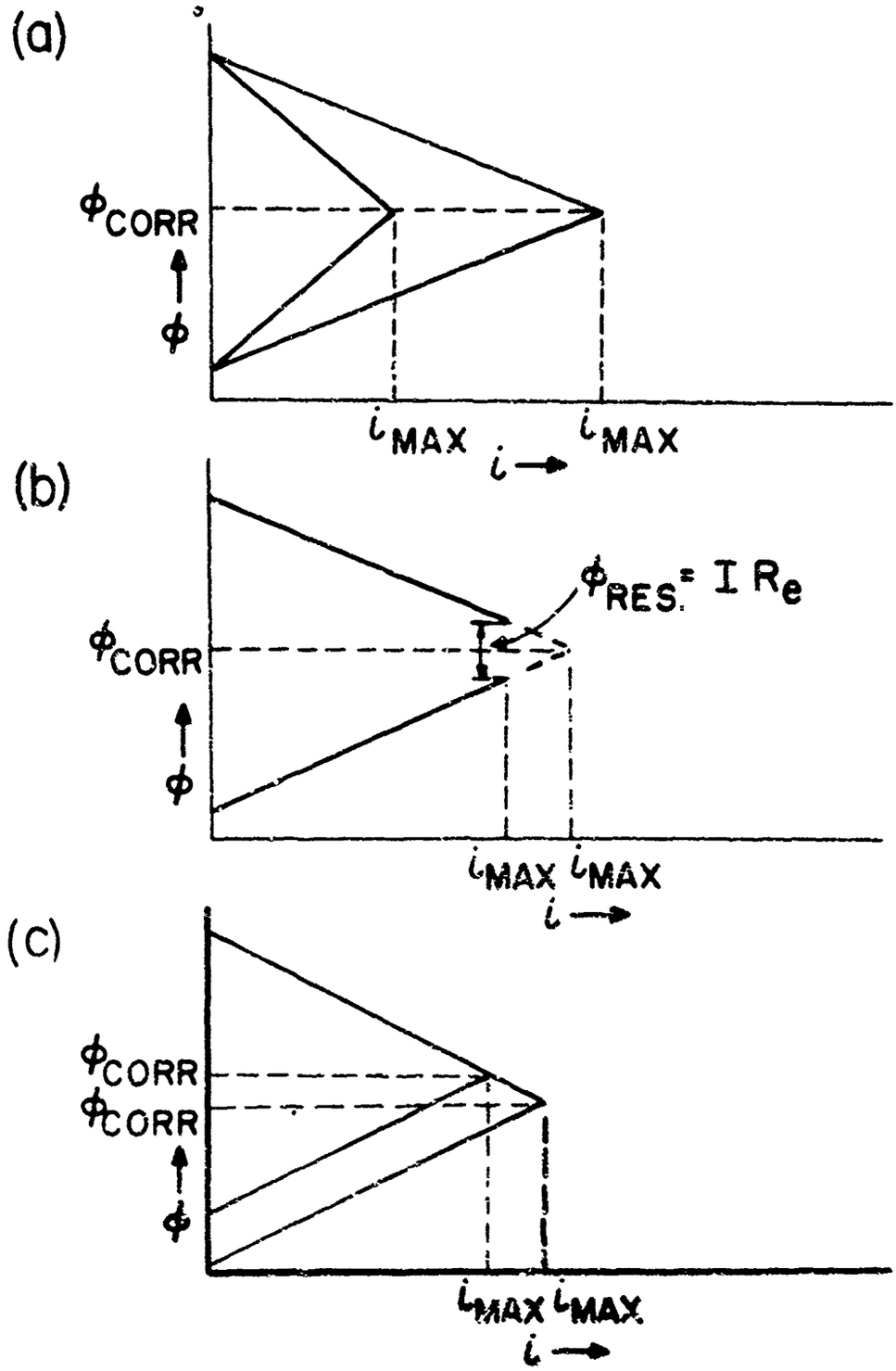

Fig. 43 Models for preferential dissolution of deformed regions in cyclically deformed metals, (a) depolarization of cathodic and anodic areas, anodic depolarization dominant, (b) reduction in resistance of electrolyte between local anodes and cathodes, (c) shift of open-circuit potential of local anodic sites at crack tip.

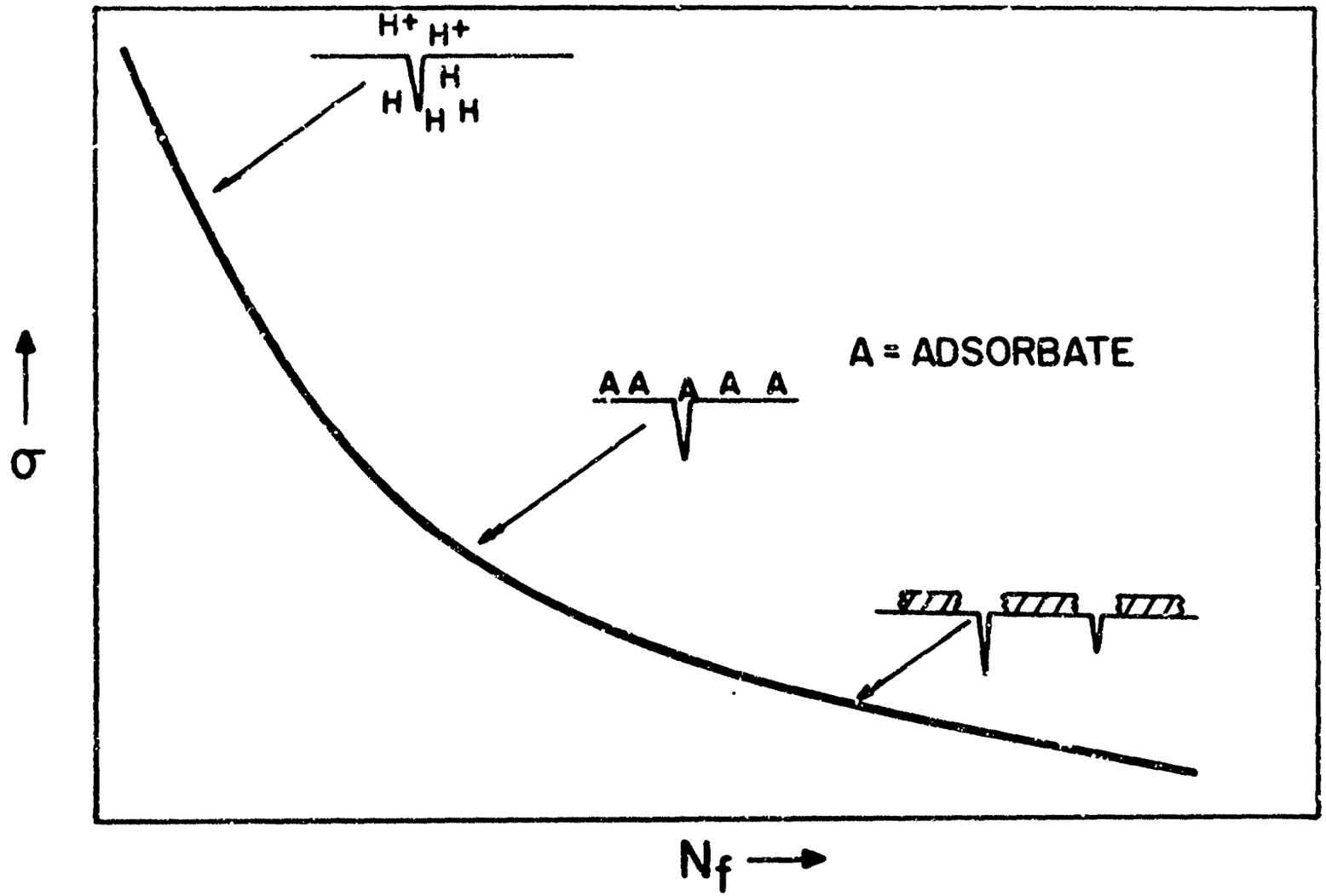

Fig. 44 Schematic diagram of Karpenko model of corrosion fatigue as a function of applied stress (after Karpenko[190]).

a

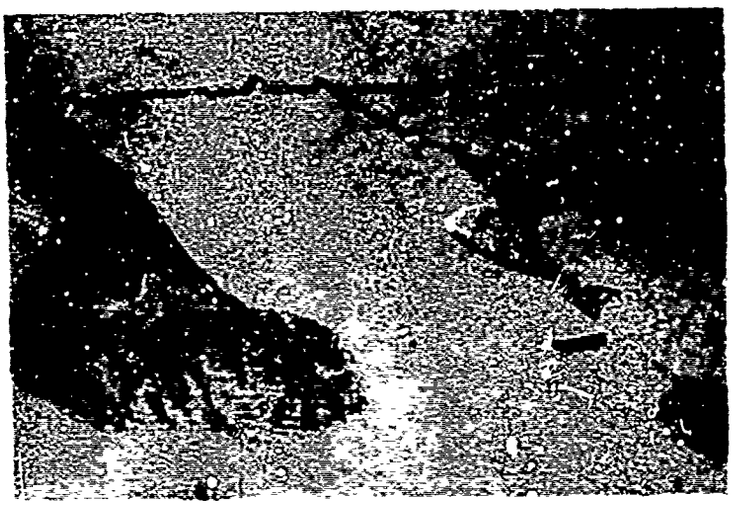

b

Fig. 45 Surface of low carbon steel cyclically stressed to ≈ 4% of total life in (a) air and (b) aerated 3% NaCl showing development of extrusions and intrusions (arrow in (a). Dark lines in air specimen are Stage I fatigue cracks (after Duquette and Uhlig[103]).

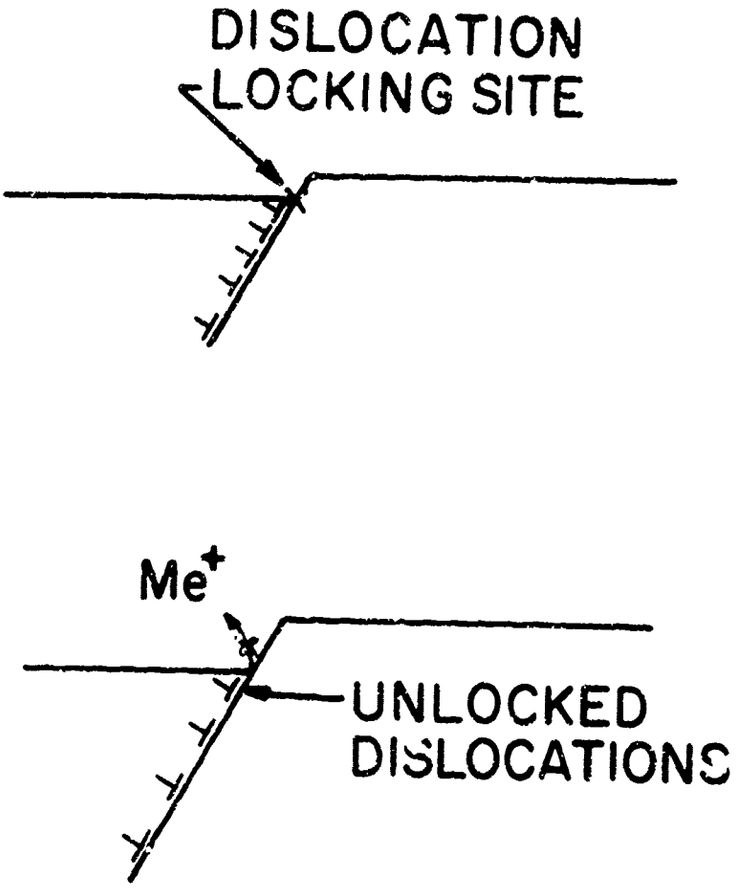

Fig. 46 Schematic diagram of model to explain accelerated slip and subsequent early crack nucleation in corrosion fatigue.